

NAVAL POSTGRADUATE SCHOOL

Monterey, California



THESIS

**LOW FREQUENCY ACTIVE SONAR (GENERIC UK)
PERFORMANCE ASSESSMENT IN THE
OPERATIONALLY SIGNIFICANT AREA OF THE
NORTHWEST APPROACHES TO THE UNITED
KINGDOM**

by
Charles J. Hunt

September 1998

Thesis Advisors:

Robert H. Bourke
James H. Wilson

19981117 024

Approved for public release; distribution is unlimited.

REPORT DOCUMENTATION PAGE

Form Approved
OMB No. 0704-0188

Public reporting burden for this collection of information is estimated to average 1 hour per response, including the time for reviewing instruction, searching existing data sources, gathering and maintaining the data needed, and completing and reviewing the collection of information. Send comments regarding this burden estimate or any other aspect of this collection of information, including suggestions for reducing this burden, to Washington headquarters Services, Directorate for Information Operations and Reports, 1215 Jefferson Davis Highway, Suite 1204, Arlington, VA 22202-4302, and to the Office of Management and Budget, Paperwork Reduction Project (0704-0188) Washington DC 20503.

1. AGENCY USE ONLY (Leave blank)

2. REPORT DATE
September 1998

3. REPORT TYPE AND DATES COVERED
Master's Thesis

4. TITLE AND SUBTITLE LOW FREQUENCY ACTIVE SONAR (GENERIC UK)
PERFORMANCE ASSESSMENT IN THE OPERATIONALLY SIGNIFICANT AREA OF
THE NORTHWEST APPROACHES TO THE UNITED KINGDOM

5. FUNDING NUMBERS

6. AUTHOR(S) Hunt Charles J.

7. PERFORMING ORGANIZATION NAME(S) AND ADDRESS(ES)
Naval Postgraduate School
Monterey, CA 93943-5000

8. PERFORMING
ORGANIZATION REPORT
NUMBER

9. SPONSORING / MONITORING AGENCY NAME(S) AND ADDRESS(ES)

10. SPONSORING /
MONITORING
AGENCY REPORT
NUMBER

11. SUPPLEMENTARY NOTES

The views expressed in this thesis are those of the author and do not reflect the official policy or position of the Department of Defense or the U.S. Government.

12a. DISTRIBUTION / AVAILABILITY STATEMENT

Approved for public release; distribution is unlimited.

12b. DISTRIBUTION CODE

13. ABSTRACT (maximum 200 words)

The goal of this research was to make a performance assessment for a generic UK Low Frequency Active Sonar (LFAS) operating in the northwest approaches to the UK. Five diverse and operationally significant sound speed and geoacoustic transects of the region in winter and summer were considered. The intention was to use an operational, ray theory based, acoustic propagation loss model for the performance assessment at 400 Hz and 800 Hz for various source/target depths. Prior to the assessment the ray model was compared with a finite element primitive equation transmission loss model (RAM) to, firstly, validate the propagation loss algorithms, and, secondly, to make any required corrections to the ray model propagation loss output as a result of variable geoacoustic conditions. Results show that the ray model compares favourably with RAM and only minor corrections were required. RAM was also used to evaluate the effect of the South East Icelandic Front in summer on acoustic propagation at the frequencies of interest. Results demonstrate that, depending upon source/receiver dispositions, the inclusion of range dependent sound speed profiles and geoacoustic parameters are a necessity. LFAS performance results demonstrate that the system is able to achieve good results with lower frequencies performing better than high frequencies. However, high reverberation levels are a severe limiting factor. Investigation into advanced signal processing techniques suggest that the utilisation of inverse beamforming techniques has the potential to improve detection opportunities by suppressing reverberation.

14. SUBJECT TERMS

Oceanography, Propagation Loss, Low Frequency Active Sonar, Performance Assessment, Northeast Atlantic, Inverse Beamforming.

15. NUMBER OF PAGES

145

16. PRICE CODE

17. SECURITY
CLASSIFICATION OF REPORT
Unclassified

18. SECURITY CLASSIFICATION OF
THIS PAGE
Unclassified

19. SECURITY CLASSIFI- CATION
OF ABSTRACT
Unclassified

20. LIMITATION OF
ABSTRACT
UL

NSN 7540-01-280-5500

Standard Form 298 (Rev. 2-89)
Prescribed by ANSI Std. Z39-18

Approved for public release; distribution is unlimited

**LOW FREQUENCY ACTIVE SONAR (GENERIC UK) PERFORMANCE
ASSESSMENT IN THE OPERATIONALLY SIGNIFICANT AREA OF THE
NORTHWEST APPROACHES TO THE UNITED KINGDOM**

Charles J. Hunt
Lieutenant Commander, Royal Navy
B.Eng., Bradford University, UK, 1988

Submitted in partial fulfillment of the
requirements for the degree of

MASTER OF SCIENCE IN PHYSICAL OCEANOGRAPHY

from the


NAVAL POSTGRADUATE SCHOOL

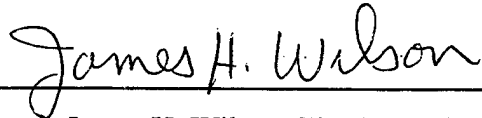
September 1998


Author: _____


Charles J. Hunt

Approved by: _____


Robert H. Bourke, Thesis Advisor


James H. Wilson, Thesis Advisor


Roland W. Garwood, Chairman
Department of Oceanography

ABSTRACT

The goal of this research was to make a performance assessment for a generic UK Low Frequency Active Sonar (LFAS) operating in the northwest approaches to the UK. Five diverse and operationally significant sound speed and geoacoustic transects of the region in winter and summer were considered. The intention was to use an operational, ray theory based, acoustic propagation loss model for the performance assessment at 400 Hz and 800 Hz for various source/target depths. Prior to the assessment the ray model was compared with a finite element primitive equation transmission loss model (RAM) to, firstly, validate the propagation loss algorithms, and, secondly, to make any required corrections to the ray model propagation loss output as a result of variable geoacoustic conditions. Results show that the ray model compares favourably with RAM and only minor corrections were required. RAM was also used to evaluate the effect of the South East Icelandic Front in summer on acoustic propagation at the frequencies of interest. Results demonstrate that, depending upon source/receiver dispositions, the inclusion of range dependent sound speed profiles and geoacoustic parameters are a necessity. LFAS performance results demonstrate that the system is able to achieve good results with lower frequencies performing better than high frequencies. However, high reverberation levels are a severe limiting factor. Investigation into advanced signal processing techniques suggest that the utilisation of inverse beamforming techniques has the potential to improve detection opportunities by suppressing reverberation.

TABLE OF CONTENTS

I.	INTRODUCTION	1
A.	BACKGROUND	2
1.	Ice Effects	4
a.	Area A	4
b.	Area B	4
c.	Area C and Area D	4
2.	Climatological Temperatures, Salinity and Sound Speed Profiles	4
a.	Area A	5
b.	Area B	6
c.	Area C	8
d.	Area D	10
3.	Ocean Fronts	12
a.	Area A and Area B	13
b.	Area C	15
c.	Area D	12
4.	Sediment Type and Low Frequency (LF) Bottom Loss	16
5.	Ambient Noise (AN)	17
a.	Area A	17
b.	Area B	18
c.	Area C	18
d.	Area D	18
6.	TASS Performance Assessment Versus a Modern SSN.....	19
a.	Area A	20
b.	Area B, Area C and Area D	18
B.	MOTIVATION	23
C.	AIM	26
II.	PROPAGATION LOSS MODELS	27
A.	THE FINITE ELEMENT PARABOLIC EQUATION (FEPE) MODEL AND THE RANGE DEPENDENT ACOUSTIC MODEL (RAM).	27
B.	THE HODGSON MODEL	29
1.	Range Dependency	29
2.	Sea Surface Loss	29
3.	Volume Absorption Loss	29
4.	Seabed Loss	30
5.	Propagation Loss	30
6.	Reverberation	31
C.	MIMIC (Multi-path Interference Model)	32

III.	METHODOLOGY AND PROPAGATION RESULTS	35
A.	AREA OF ASSESSMENT	35
1.	Weather	35
2.	Topography	36
3.	Oceanographic Conditions	36
4.	Data Acquisition	38
5.	Two Dimensional Environment Generation	38
B.	MODEL COMPARISON	41
1.	Propagation Loss Streamlining	41
2.	Range Independent Environment	42
a.	Sound Speed Profiles	42
b.	Geoacoustic Parameters	42
c.	Source and Receiver Dispositions	45
d.	Propagation Loss Results	47
(1)	Deep water	47
(2)	Shallow water	51
3.	Range Dependent, Cross Frontal Propagation	55
a.	Sound Speed Profiles	55
b.	Geoacoustic Parameters	60
c.	Source and Receiver Dispositions	60
d.	Propagation Loss Results	61
(1)	South East Icelandic Front, Winter	61
(2)	South East Icelandic Front, Summer	62
4.	Corrections to the HODGSON PL Model Output	67
a.	Transect Environments	68
(1)	Track A, SEIF in winter	68
(2)	Track B, SEIF in summer	68
(3)	Track C, upslope/downslope enhancement environment	69
(4)	Track D, Faeroes-Shetland Channel environment	71
(5)	Track E, Anton Dohrn Seamount environment	74
b.	Source and Receiver Dispositions	76
c.	Correction Method	76
d.	Propagation Loss Results	76
(1)	Track B, SEIF transect in summer, upslope propagation path	77
(2)	Track E, Anton Dohrn Seamount transect in summer, upslope propagation path	81
C.	LOW FREQUENCY ACTIVE SONAR PERFORMANCE ASSESSMENT	82
1.	Environmental Transects	82
2.	Source/Target Depths	82
3.	Acoustic Propagation Loss Models	83

4.	Results of the Investigation of Range Dependent(RD) vs. Range Independent (RI) Propagation of Acoustic Energy for the South East Icelandic Front (SEIF) in Summer	83
a.	Source Depth 50 m	84
b.	Source Depth 250 m	84
5.	Active Figure of Merit (AFOM)	90
a.	Active Sonar Equation	90
b.	Reverberation	92
6.	Low Frequency Active Sonar Performance Assessment Results	93
a.	Track A, South East Icelandic Front Transect in Winter	93
(1)	Upslope propagation	93
(2)	Downslope propagation	94
(3)	Reverberation	95
b.	Track B, South East Icelandic Front Transect in Summer	98
(1)	Upslope propagation	98
(2)	Downslope propagation	98
(3)	Reverberation	98
c.	Track C, Upslope/Downslope Propagation Comparison	101
(1)	Upslope/downslope propagation in winter ...	101
(2)	Upslope/downslope propagation in summer	101
(3)	Reverberation	102
d.	Track D, Faeroe-Shetland Channel	107
(1)	Winter	107
(2)	Summer	107
(3)	Reverberation	107
e.	Track E, Anton Dohrn Seamount	108
(1)	Winter	108
(2)	Summer	108
(3)	Reverberation	108
D.	ADVANCED SIGNAL PROCESSING TECHNIQUES	111
IV.	ADVANCED SIGNAL PROCESSING TECHNIQUES	113
A.	ADAPTIVE BEAMFORMING	114
1.	Beam-based ABF Algorithm	114
2.	Element-based ABF Algorithm	114
B.	INVERSE BEAMFORMING	115
1.	IBF Algorithms	115
2.	The IBF Performance Advantage	115
C.	MATCHED FIELD PROCESSING	116
1.	Passive Sonar MFP with IBF	116
2.	Active Sonar MFP	117
D.	TACTICAL DECISIONS	117

E.	SUPPRESSION OF REVERBERATION USING NEURAL NETS AND HIGHER ORDER STATISTICS	118
V.	OPERATIONAL ISSUES, CONCLUSIONS AND RECOMMENDATIONS	119
A.	OPERATIONAL ISSUES	119
1.	The HODGSON Propagation Loss Model	119
2.	Range Dependent SSP/Geoacoustic Data	119
3.	LFAS Performance	120
a.	Initial Detection Range Summary	120
b.	Frequency	121
c.	Seasonal Variability	121
d.	Upslope/Downslope Propagation	121
e.	Reverberation	122
B.	CONCLUSIONS	122
C.	RECOMMENDATIONS	125
	LIST OF REFERENCES	127
	INITIAL DISTRIBUTION LIST	131

ACKNOWLEDGEMENT

The author thanks Professors R H Bourke and J H Wilson for their guidance, encouragement, efforts and patience in preparing this study.

The author also thanks the personnel at the Directorate of Naval Surveying, Oceanography and Meteorology (DNSOM) for their assistance in acquiring the necessary environmental data used in this research, and the Physical Oceanography Branch of the Hydrographic Office, UK for providing the data.

My thanks to John and Diane Hodgson for providing the WADER/HODGSON/MIMIC Global Ocean Information System and Propagation Loss Models and the HODGSON Propagation Loss Model engine. All of these systems were used extensively throughout this investigation. I also thank them for their guidance and prompt answers to many questions pertaining to the attributes of the various models.

Lastly, and most importantly, I thank my wife Lisa for her encouragement, support and endurance during this educational adventure.

I. INTRODUCTION

Throughout the 1970's and early 1980's the problem of detecting and tracking nuclear submarines was relatively simple, indeed the greatest difficulty was with the location phase rather than the detection phase. With high source levels (SL's) at a number of tonal frequencies conventional towed array sonar systems (TASS) were able to detect and track targets, in some instances at ranges in excess of 100 km. The interest in shallow water TASS operations, which dominates today's Anti-Submarine Warfare (ASW) practice, was minimal during the Cold War because the primary threat was the Russian nuclear submarine operating in deep water.

Acoustic modeling systems were used to predict the detection ranges of submarines not only to give an indication of sonar performance but also to assist the Command in location assessment. However, the requirement for timely advice and the limitations of existing computer technology resulted in the operational acoustic models of preference being range independent. Sound speed variations, such as ocean fronts, appeared to be of little significance at the low frequencies of interest because the inherently high SL's of threat submarines produced large ranges regardless of environmental variations along the acoustic path.

Submarine noise quieting techniques made major advances in the late 1980's and 1990's. The result was a reduction in SL's of 20-30 dB with some high frequency tonals (>150 Hz) disappearing altogether. Coupled with this massive reduction in SL, the end of the Cold War produced a sudden change in operational emphasis from 'blue water' to 'brown water' - the littoral zone. In these littoral areas a proliferation of modern, quiet diesel submarines are now operating. This instigated the requirement for accurate range dependent acoustic propagation modeling systems to provide the Command with much more than a 'range of the day', but still in an operationally timely manner. Range dependent ray models are now widespread (HODGSON, ASTRAL, GRASS); range dependent models that are an approximate or exact solution to the wave equation (FEPE, FEPE-CM, RAM, ASTRAL, PAREQ, SNAP) are less widely available to the operational community due to long runtimes. However, they are used extensively in the research community and with advances in computer technology runtimes are decreasing significantly.

Many tactics employed by the Undersea Warfare (USW) professional were developed from experience based upon deep water operations and resulted in a somewhat stochastic approach to the exploitation of the ocean environment. Such an approach is inherently unavoidable due to the dynamic nature of both the ocean and tactical environment. In order to gain and maintain a tactical advantage an appreciation of the effects of the environment and its variations on USW sensors is essential.

A. BACKGROUND

Historically the Northeast Atlantic Ocean has been a predominant area for nuclear submarine activity. An assessment of TASS performance in this area is undertaken in this study in order to highlight the requirement for advances in signal processing techniques and the development of advanced sonar systems such as Low Frequency Active Sonar (LFAS).

Based upon similarities in water properties (temperature, salinity and sound speed), ice coverage and temporal variability the Northeast Atlantic has been delineated into four broad areas (NAVO, 1992), as shown in Figure 1.

Area A lies along the east coast of Greenland seaward to the 1000 m contour. In the north the boundary with area B crosses Fram Strait to follow the 1000 m contour associated with the Yermak Plateau. The bathymetry of the area is dominated by the broad continental shelf off Greenland that extends, at its widest, to 230 km off shore whilst gradually deepening to 400 m. In the north of area A the depth of the Fram Strait is in excess of 2500 m.

Area B is bound to the west by the 1000 m contour off the Greenland continental shelf and to the east by the Jan Mayen and Mohn Ridges, which shoal to sea level and 1800 m, respectively. In the south the area extends around the north and west coasts of Iceland to the Reykjanes Ridge. To the north the area extends to Fram Strait then south along the 1000 m contour to the west of Spitzbergen, thence into the Barents Sea. The bathymetry is varied; the centre of the area consists of the Greenland basin at depths greater than 3000 m. Fracture zones and ridges to the south of the basin shoal to around 1000 m. The relatively narrow Denmark Strait is orientated northeast to southwest in the south of the area.

Area C consists primarily of the Norwegian Sea. It is bound to the south by the United Kingdom (UK) and the Iceland-Faeroes Rise, to the east by Norway and the Barents Sea and to the west by the Jan Mayen and Mohn Ridges. The bathymetry is dominated by two basins, the Norwegian Basin and the Lofoten Basin both reaching depths in excess of 3000 m. In the west the Jan Mayen Ridge shoals to the surface at the island of Jan Mayen whilst the Mohn Ridge shoals to 1800m. The east and south consist primarily of continental shelf with the relatively gradual shoal of the Iceland-Faeroes Rise to 400 m in the southwest.

Area D lies to the south of Iceland, southeast of Reykjanes Ridge, southwest of the Iceland-Faeroes Rise and is bound to the west by the UK. The region of area D under consideration shown in Figure 1 consists of the Iceland Basin at depths of 2000-3000 m.

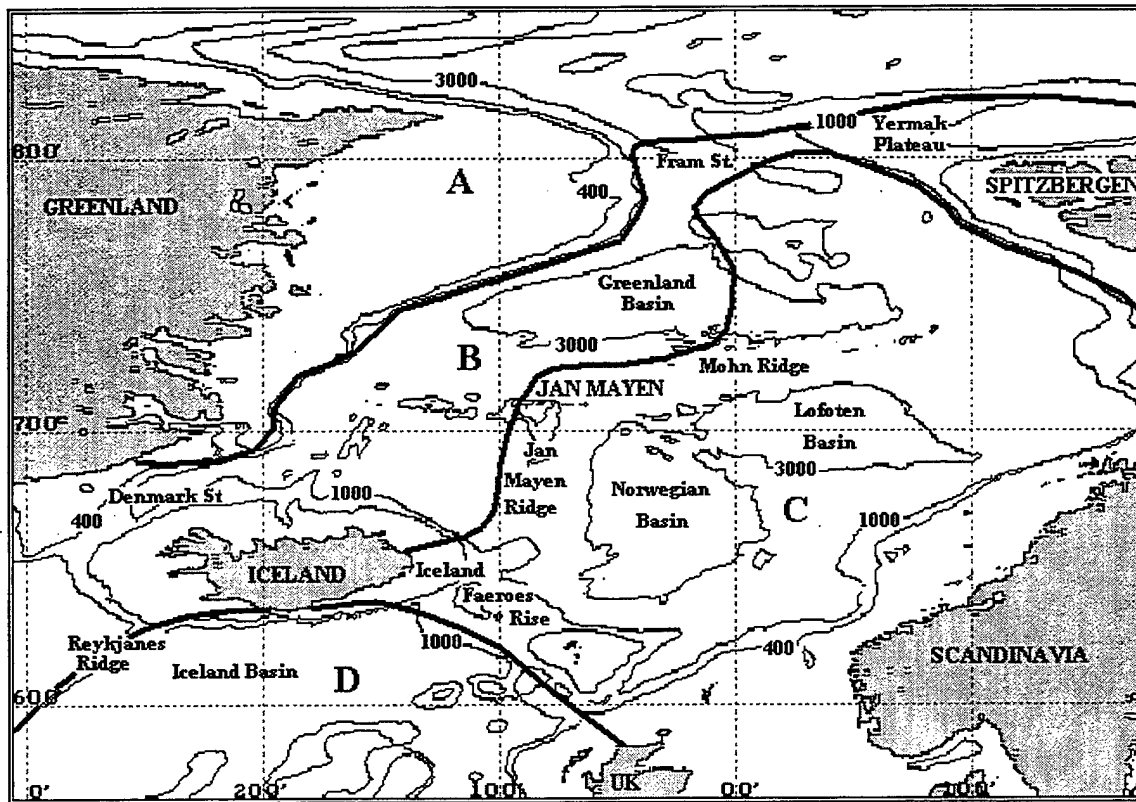


Figure 1. Northeast Atlantic Ocean delineated into areas of similar water properties, ice coverage and temporal variability. Topographically significant features and the 400 m, 1000 m and 3000 m contours are shown. (Adapted from NAVO, 1992 and Hopkins, 1988)

In the following sub-sections environmental parameters that typically affect sonar performance are discussed. These are the presence and location of sea ice, temporal and spatial variability of ocean temperature, salinity, sound speed and ocean fronts, transmission loss due to sediment interaction and ambient noise. The impact of these parameters on TASS performance versus a modern SSN with source frequency of 50 Hz is summarised based upon typical Figures of Merit (FOM's) and a deep-water assessment of transmission loss.

1. Ice Effects

a. Area A

This area is primarily ice covered year round (Hopkins, 1988), thus the only viable asset for target search and tracking is a passive sonar array from another submarine. The area is not feasible for LFAS operations unless submarine mounted, which will not be considered in this report.

b. Area B

During winter months this area is partially ice covered and may be exploited by surface ships. However, the course and orientation of the ship, in terms of being able to position the TASS to best exploit ambient noise directionality and acoustic features such as upslope or downslope enhancement, may be influenced by the location and concentration of sea ice. This can severely limit the operational effectiveness of a surface TASS unit. For these reasons it is considered that submarine or air assets are the most capable units for operations in this area. In summer spotty regions of relatively high ice concentration can be found, especially towards high latitudes. Although surface TASS ships can be used effectively, it is still considered that submarine or air assets are the most capable operational units.

c. Area C and Area D

Both areas are unaffected by ice coverage.

2. Climatological Temperature, Salinity and Sound Speed Profiles

All water property profiles shown in this section are associated with the deep water regions within each climatological area. Shallow water profiles are available but have not been considered due to a lack of data and high spatial variability in some areas.

This makes it difficult to describe mean conditions, which is the emphasis of this section. The plots were extracted from the WADER Global Information System (Hodgson and Hodgson, 1998a) which is based upon the Levitus 94SE (spatially enhanced) database.

a. Area A

Figures 2 and 3 show deep water climatological temperature, salinity and sound speed profiles (SSP) for area A in winter and summer, respectively.

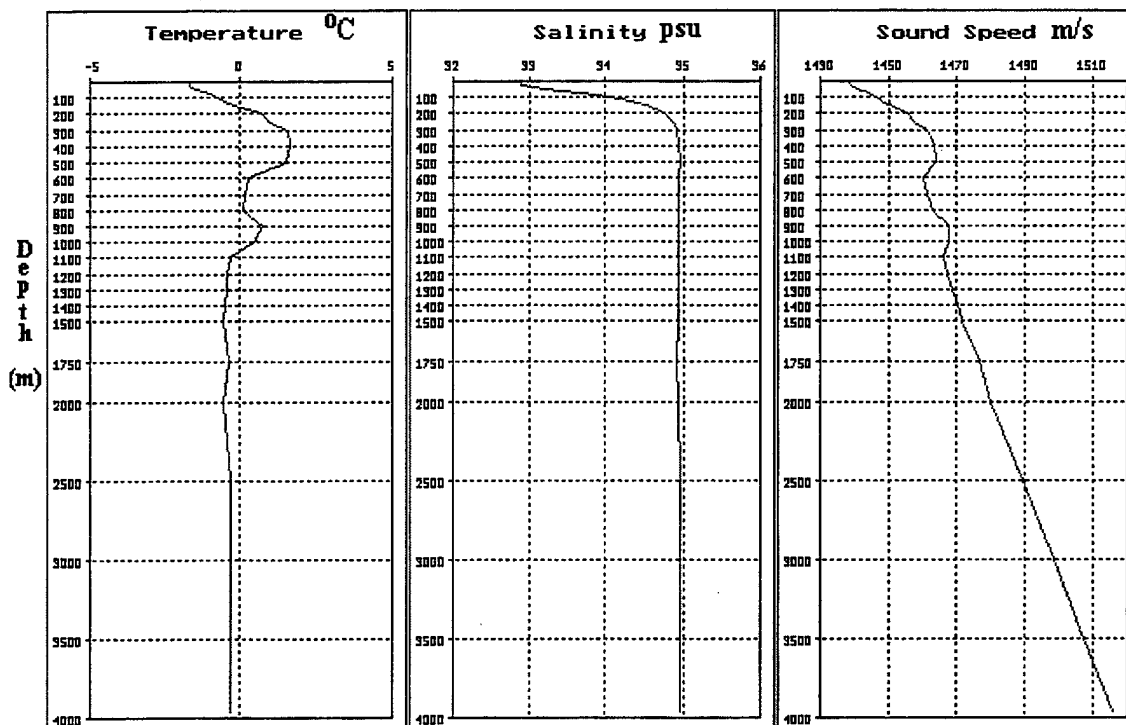


Figure 2. Deep water climatological temperature, salinity and sound speed profiles for area A in winter. In the near surface layer cold, relatively fresh water overlies warm, saline water; this results in a strong positive sound speed gradient to 300 m (WADER, OAD Ltd., 1998).

Due to the presence of cold, relatively fresh water in the near surface layers the sound speed profile in Figure 2 demonstrates a strong surface duct to 300 m with a cut-off frequency of ~16 Hz. Two relatively weak sound channels centred at 600 m and 1100 m are present, but due to the overall positive gradient of the entire profile they are of little tactical significance. The SSP has an inherently positive sound speed gradient to the seabed providing upward refraction of acoustic energy with limited bottom interaction. One can anticipate very good acoustic propagation conditions at very low frequencies (VLF) where under ice scattering losses are relatively low. At

frequencies above 100Hz ice scattering losses degrade propagation conditions as a result of the strong upward refraction increasing interaction with the rough underice surface (Urlick, 1983).

The SSP in Figure 3 is similar to the winter profile but exhibits a weaker near-surface gradient due to summer insolation of the water column. The near surface duct extends to 300 m with a cut-off frequency of ~16 Hz providing for excellent acoustic propagation, particularly at VLF. There is evidence of a near-surface, shallow, weak negative gradient but this has little or no tactical significance to TASS operations.

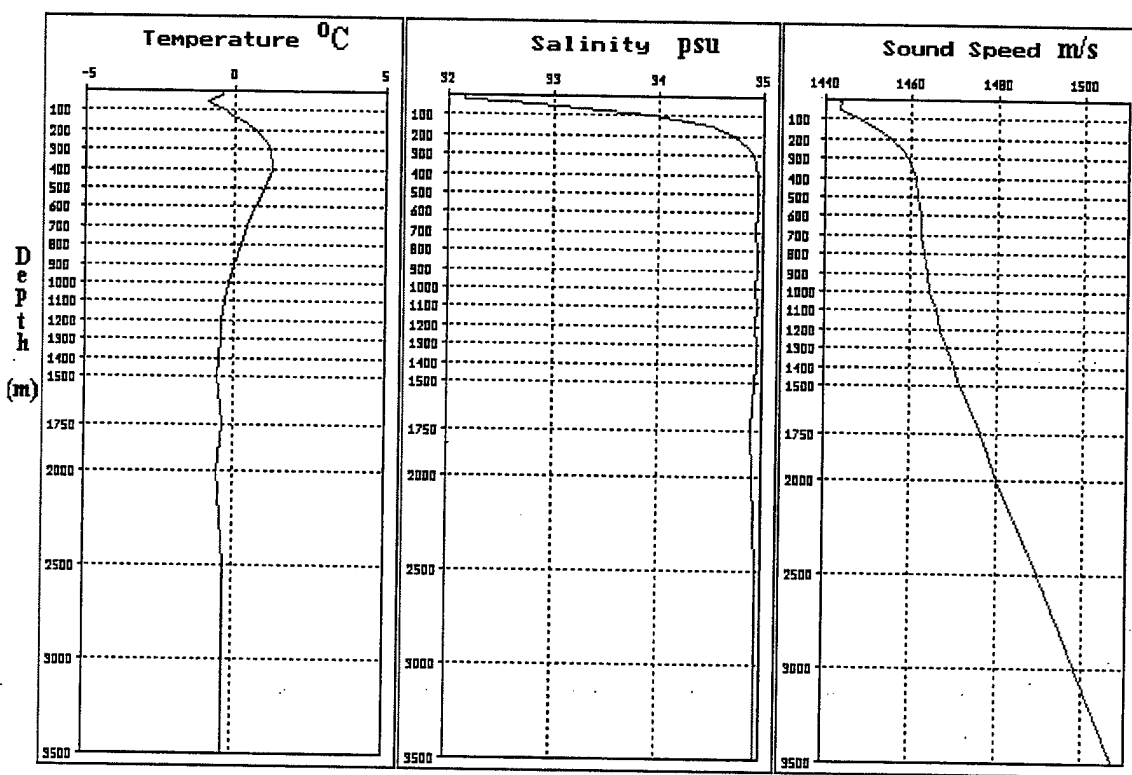


Figure 3. Deep water climatological temperature, salinity and sound speed profiles for area A in summer. Slight heating near the surface due to summer insolation creates a shallow sound channel; this has little effect on acoustic propagation (WADER, OAD Ltd., 1998).

b. Area B

Figures 4 and 5 show deep water climatological temperature, salinity and sound speed profiles for area B in winter and summer, respectively.

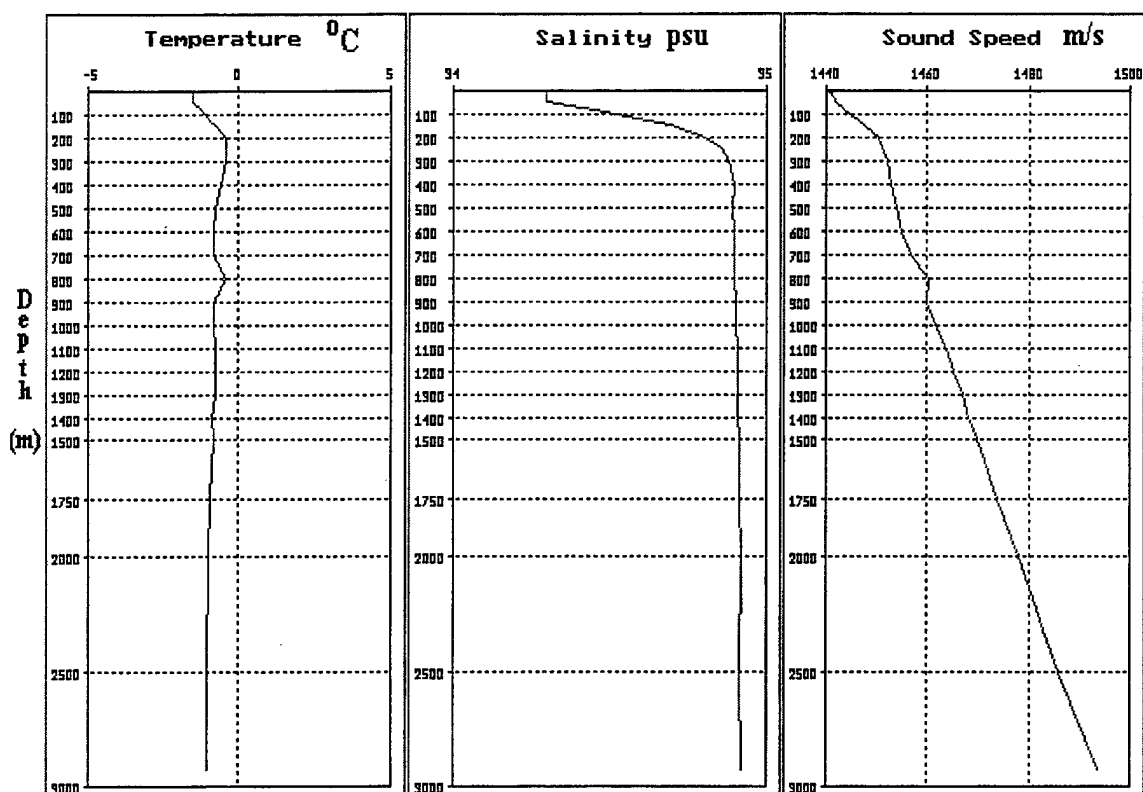


Figure 4. Deep water climatological temperature, salinity and sound speed profiles for area B in winter. The sound speed gradient is inherently positive throughout the water column resulting in good acoustic propagation conditions (WADER, OAD Ltd., 1998).

As would be expected, the winter profile is similar to that for area A, essentially a positive sound speed gradient to the seabed. Because area B is generally seaward of the ice edge or only infrequently ice-covered, the near surface waters are slightly warmer and more saline. The upper sound speed gradient is not quite as strong but acoustic propagation can be expected to be similar to that of area A.

In summer insolation of the near surface water results in a negative sound speed gradient to 50 m developing a very shallow sound channel with its axis at 50 m. The channel width is ~230 m resulting in a cut-off frequency of ~85 Hz. The gradient is inherently positive below the surface sound channel; the general acoustic propagation conditions are very good.

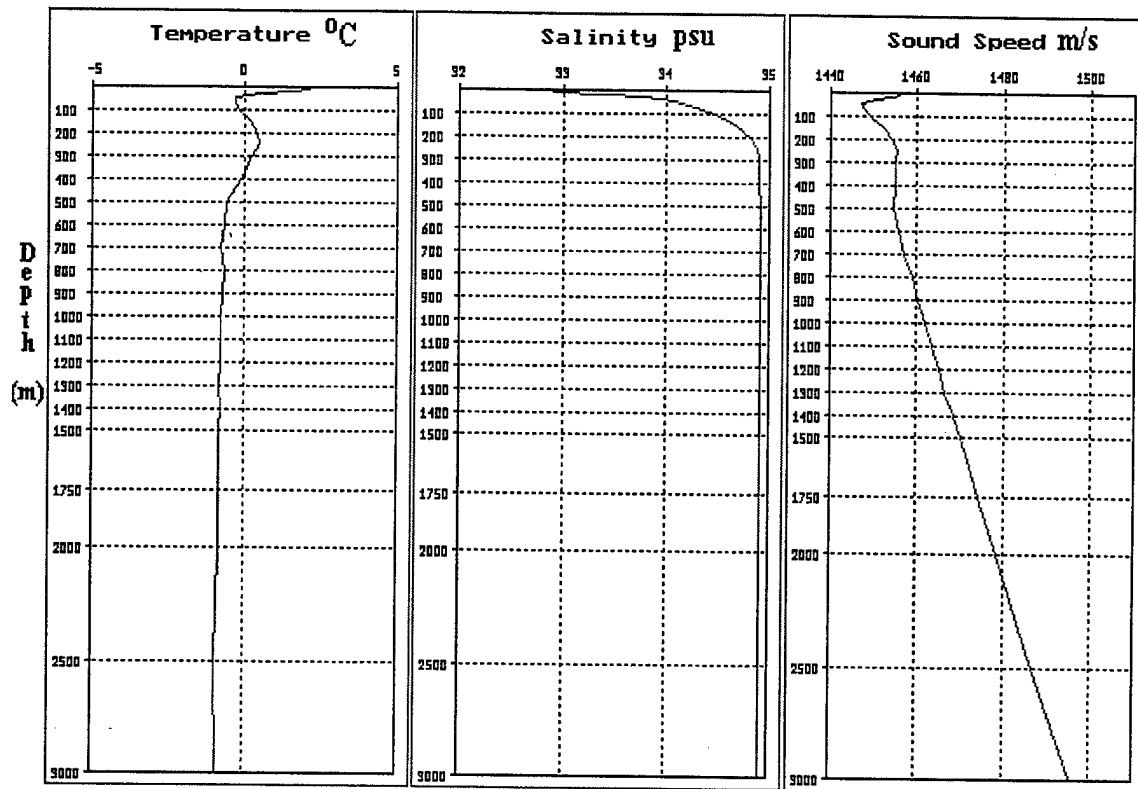


Figure 5. Deep water climatological temperature, salinity and sound speed profiles for area B in summer. Strong summer heating in the near surface layers has caused the development of the shallow sound channel centred at 50 m (WADER, OAD Ltd., 1998).

c. Area C

Figures 6 and 7 show the climatological temperature, salinity and sound speed profiles for area C in winter and summer, respectively.

The winter SSP has a surface duct to 150 m with a cut-off frequency of ~ 100 Hz. Of more significance for passive operations is the deep sound channel with an axis at 700 m and width of 1100 m having a cut-off frequency of ~ 7 Hz. Where the water depth is sufficiently deep (greater than 1300 m), the potential for convergence zone (CZ) propagation is good.

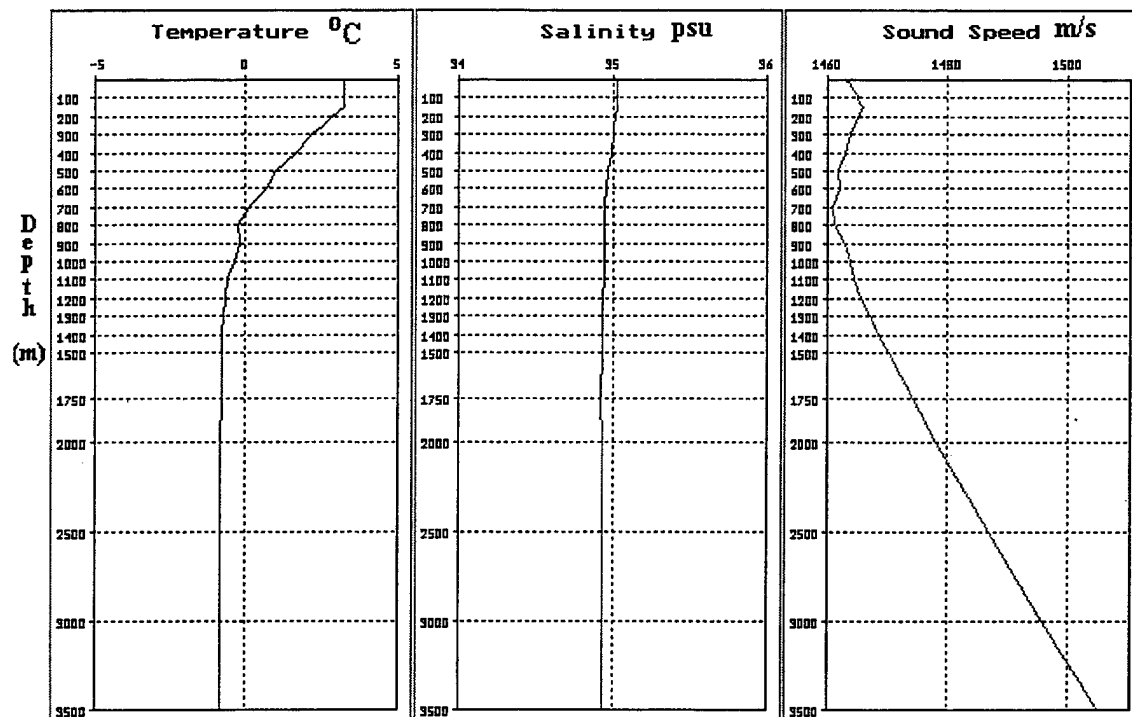


Figure 6. Deep water climatological temperature, salinity and sound speed profiles for area C in winter. These profiles are markedly different from the profiles for areas A and B. The salinity is almost constant whilst the surface layers have warmed considerably. The negative thermocline is now clearly evident (WADER, OAD Ltd., 1998).

The summer SSP is greatly affected by insolation with a shallow, weak surface layer of little tactical significance but a strong negative, downward refracting, gradient below. The channel axis has shoaled to 600 m and the channel width has increased to 2500 m, sufficient to trap all frequencies of tactical significance.

In summer the strong thermocline can be exploited by the submariner for evasion by making the submarine depth as shallow as possible. The effect of the strong thermocline is to create propagation paths, at small source angles, that are either surface reflecting (RSR) or surface/bottom reflecting (RSR/RBR). This results in high attenuation and large transmission loss. It should be noted that this area is susceptible to low-pressure systems traversing the area throughout the summer, in which instance the surface layer will deepen and the thermocline weaken altering the acoustic conditions.

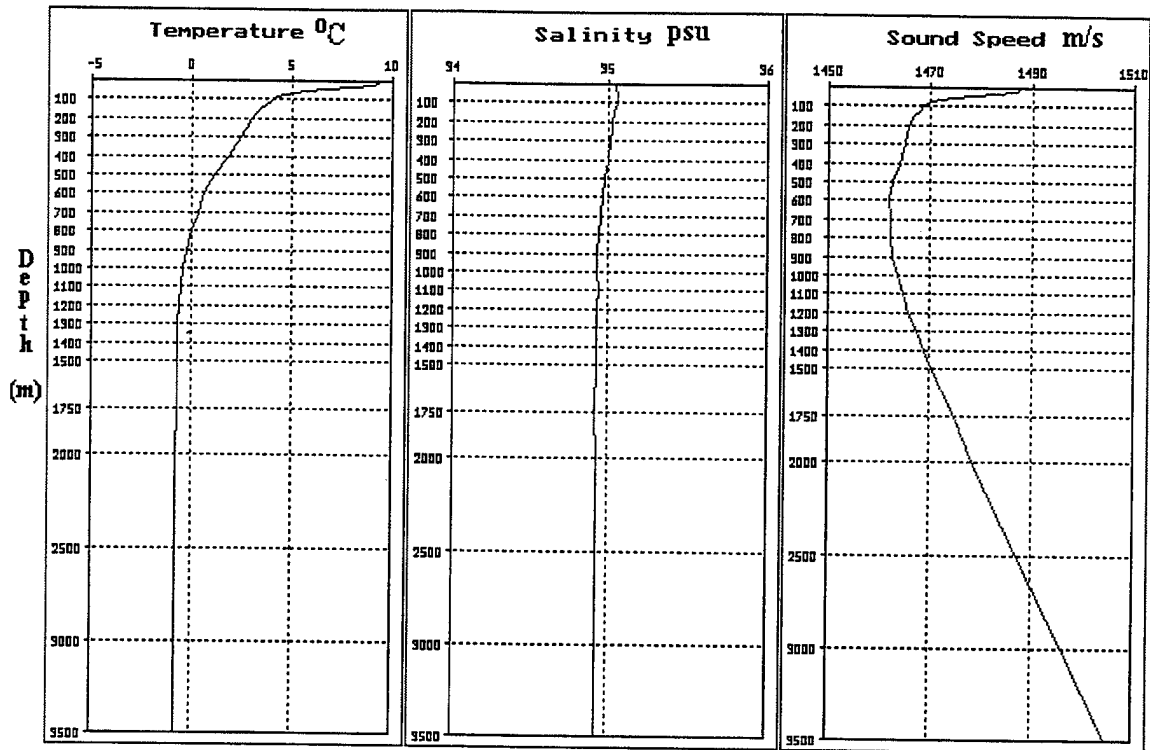


Figure 7. Deep water climatological temperature, salinity and sound speed profiles for area C in summer. Strong summer heating has strengthened the thermocline creating a wide, deep sound channel (WADER, OAD Ltd., 1998).

d. Area D

Figures 8 and 9 show the climatological temperature, salinity and sound speed profiles for area D in winter and summer, respectively.

The temperature and salinity profiles for winter are constant to 400 m, clear evidence of the deep well-mixed nature of the surface layer. The resulting SSP has a surface duct to 500 m with a cut-off frequency of ~16 Hz, thus low frequency sonar conditions are excellent. Convergence zone potential is good for water depths greater than 1700 m. This area is susceptible to extreme sea conditions on occasion during the winter, but nominally seas are generally in excess of 3 m.

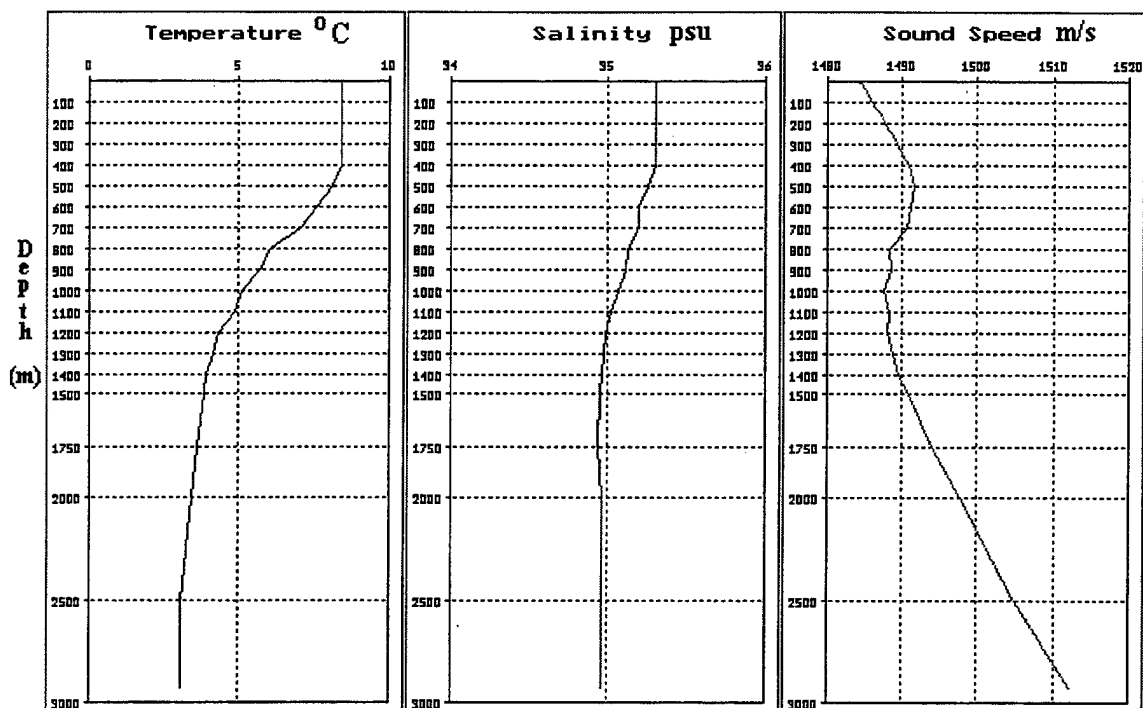


Figure 8. Deep water climatological temperature, salinity and sound speed profiles for area D in winter. Notice the isothermal temperature profile and isohaline salinity profile to a depth of 400 m. This results in a deep half channel and excellent acoustic conditions (WADER, OAD Ltd., 1998).

The SSP in summer is strongly influenced by insolation. The generation of a relatively weak shallow sound channel, axis at 150 m, width 500 m, cut-off frequency ~145 Hz, results in highly complex and tactically troublesome acoustic conditions. An evading submarine is likely to remain shallow within the thermocline to exploit downward refraction and the inherently poor detection ranges associated with high acoustic attenuation from seabed interacting propagation paths. However, at depths greater than ~2200 m CZ propagation is likely, giving the opportunity for long range initial detection. As described for area C, area D is susceptible to mobile low-pressure systems throughout the summer. These features cause abrupt changes to the acoustic propagation conditions.

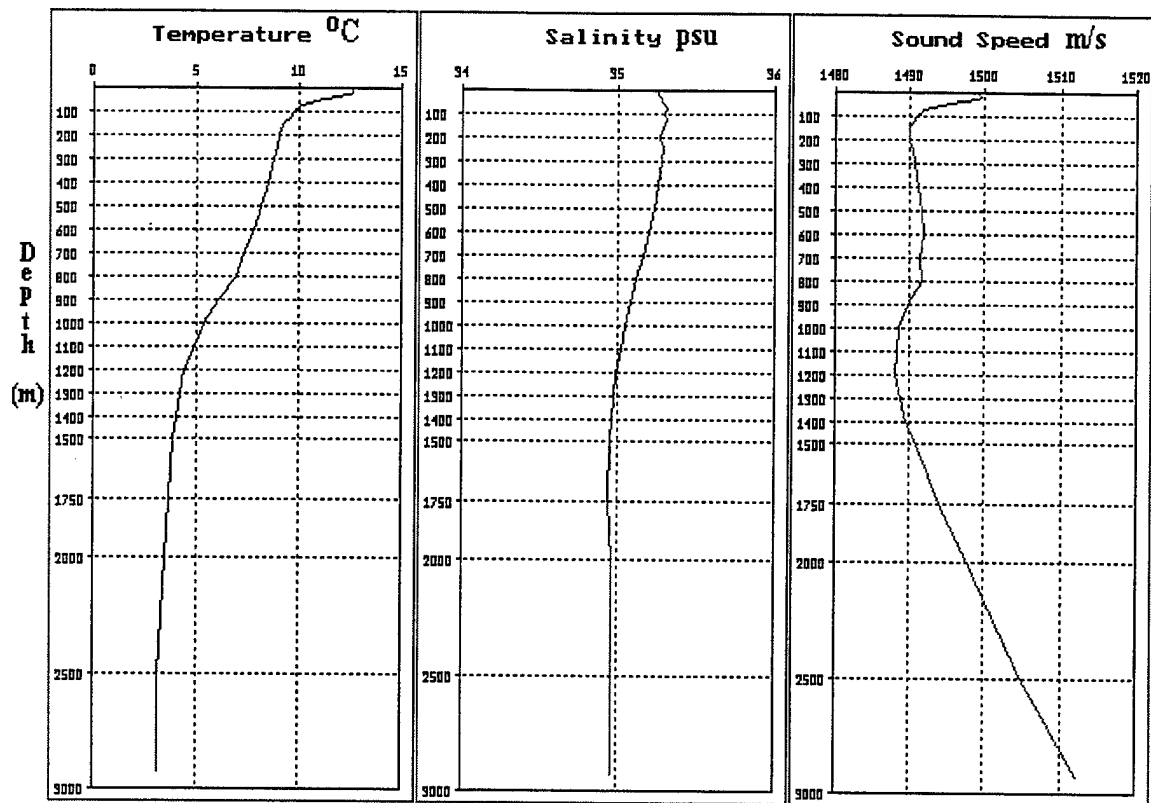


Figure 9. Deep water climatological temperature, salinity and sound speed profiles for area D in summer. Strong summer insolation has developed a shallow thermocline and shallow sound channel. CZ potential is good in water deeper than 2200 m (WADER, OAD Ltd., 1998).

3. Ocean Fronts

Several significant fronts are present as permanent features in the Greenland-Iceland-Norwegian (GIN) Sea. Figure 10 gives their approximate location. These fronts are a result of convergence of water types with differing characteristics of, amongst other properties, temperature and salinity.

The circulation in the GIN Sea, Figure 11, and its various water masses has been described in detail by Hopkins (1988). Warm, saline Atlantic Water enters the GIN Sea from the south; on proceeding north a portion of the flow branches into the Barents Sea. The majority of the flow continues northward passing west of Spitzbergen into the Arctic Ocean. Concurrently, cool, less saline Polar Water enters from the northwest and proceeds south along the Greenland Shelf. These current systems are often separated by cyclonic gyres centred in the Greenland and Norwegian Seas.

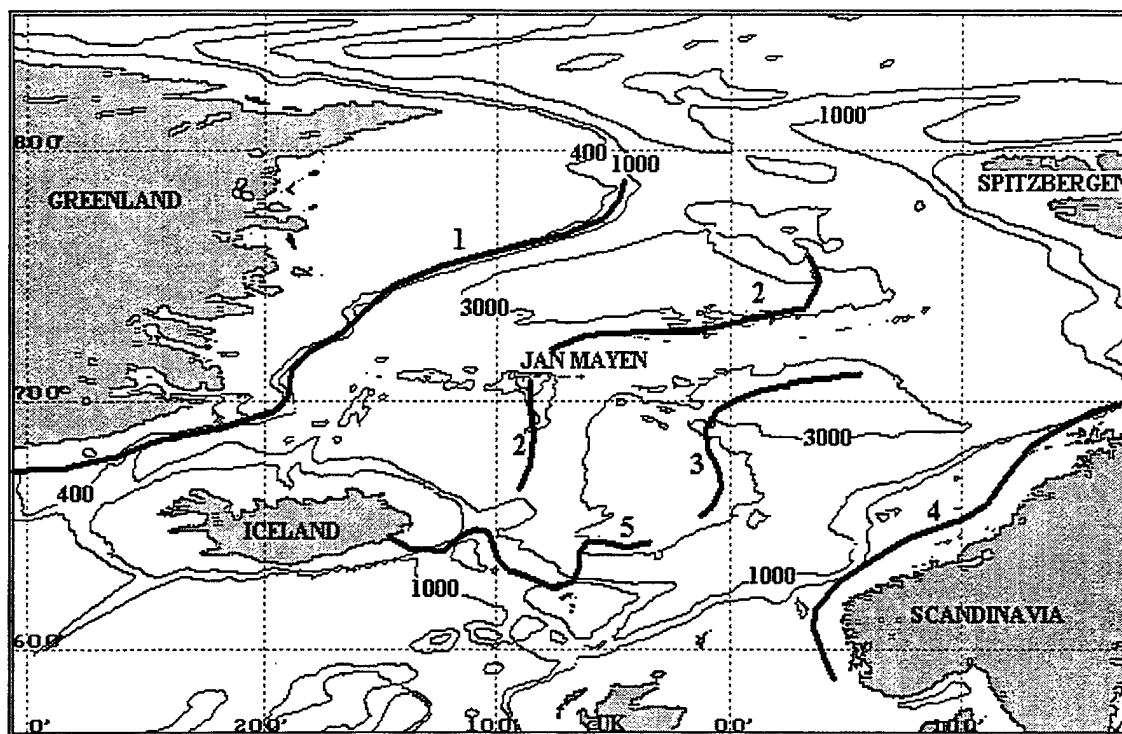


Figure 10. Approximate location of significant fronts in the northeast Atlantic.

1) East Greenland Polar Front (EGPF), 2) Jan Mayen Ridge Front/Polar Ocean Front (Johannessen, 1986), 3) Norwegian Sea Front, 4) Norwegian Coastal Front, 5) South East Icelandic Front. (adapted from NAVO, 1992 and Johannessen, 1986).

a. Area A and Area B

The East Greenland Polar Front (EGPF) is the only front of significance in areas A and B. The EGPF is associated with the boundary between cold, relatively fresh Greenland Polar Water (GPW) flowing southward along the Greenland continental shelf and the warmer, more saline Atlantic Water flowing southward as the Return Atlantic Current on a parallel path seaward of the Greenland continental slope (Hopkins, 1988). The EGPF is geostrophically constrained to remain along the Greenland continental margin by a combination of less dense waters and conservation of potential vorticity (Hopkins, 1988). The author has observed satellite imagery of cold eddies of 20-70 km diameter in the northern Denmark Strait. These eddies are a potential evasion tool for transiting submarines.

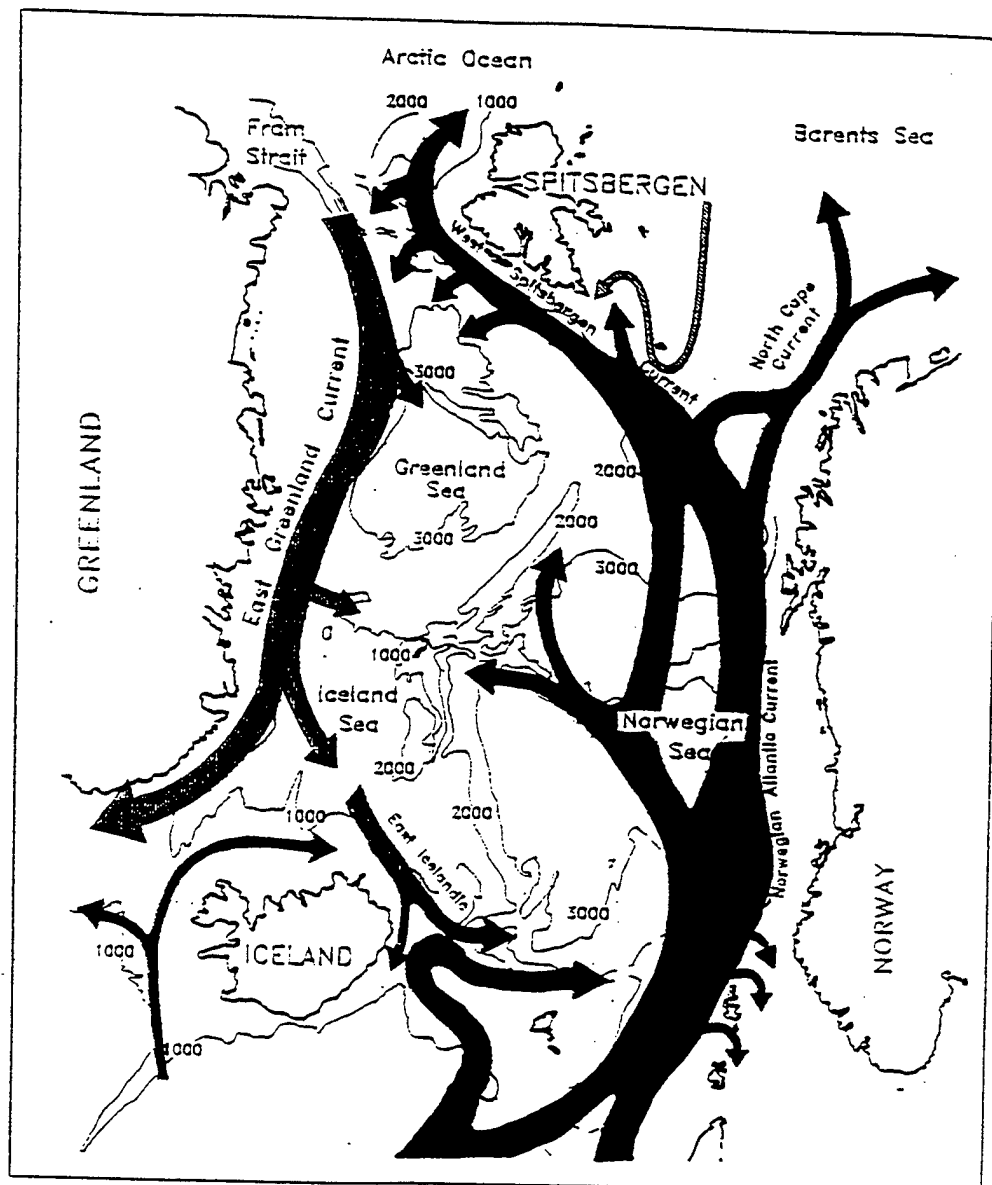


Figure 11. Schematic representation of the major surface currents in the GIN Sea. The Norwegian Current transports relatively warm, saline water northward into the eastern GIN Sea whilst the East Greenland Current transports cold, relatively fresh water southward along the Greenland Shelf. (Adapted from Osterhus, Pers comm.).

b. Area C

The remaining four fronts in Figure 10 are all located in area C.

The Jan Mayen Ridge Front, which becomes the Polar Ocean Front north of Jan Mayen (Johannessen, 1986), is strongly aligned with the Jan Mayen and Mohn Ridges. It is the boundary between the cold, relatively fresh eastern limb of the cyclonic Greenland gyre and a relatively warm, saline branch of the Norwegian Atlantic Current (NwAtC) (Hopkins, 1988). The Jan Mayen Ridge Front is historically significant as a navigation and evasion aid for submariners. However, as with many frontal features, the SSP's in the frontal zone can be highly spatially variable. In some cases, to the east of the Jan Mayen Ridge Front, a shallow sound channel can exist making acoustic evasion techniques for the submariner difficult without regular environmental assessments.

The Norwegian Sea Front (NSF) lies roughly north to south in the centre of the Norwegian Sea. The NSF forms the boundary between the northward setting NwAtC and embedded cyclonic gyres within the main flow of the same current (Saelen, 1963 and Dickson, 1972). It is suggested that such gyres are generated by variations in cross-stream shear, which is generated by barotropic interactions with topography (Kislyakov, 1960). The amplitude of the gyres has considerable temporal variation (Dickson, 1972). In addition, the surface expression of the front may be masked by wind mixing effects (NAVO, 1992). Because of the high temporal variability of the NSF, it is perceived to be useful to the submariner for evasion.

The Norwegian Coastal Current consists of cold, fresh water from the Baltic Sea and Norwegian Fjords. The current sets northward on the continental margin and follows the Norwegian coast. The Norwegian Coastal Front (NCF) is the boundary between the cold, relatively fresh Norwegian Coastal Water and the warmer, more saline Norwegian Atlantic Water transported by the NwAtC (Johannessen, 1986). This front is exploitable by submariners for evasion.

The Iceland Current (IC) is an extension of the Irminger Current that has passed through the Denmark Strait and along the northern coast of Iceland. During this track the relatively warm and saline water is cooled and freshened through advective mixing with Arctic and Polar Waters. On passing the northeast coast of Iceland, the IC is steered along the northern flank of the Iceland-Faeroes Rise where it re-encounters water

of the same north Atlantic origin (Hopkins, 1988). However, the Atlantic water has maintained its warm, saline characteristics and the water mass boundary constitutes the South East Icelandic Front (SEIF). The SEIF is complex in structure and is strongly prograde to the north (Hopkins, 1988). The surface manifestation of the front is often displaced up to 50 km from the front at 200 m (UKHO, 1997). Historically submariners have exploited the SEIF for navigation and evasion purposes.

c. Area D

There are no tactically significant fronts in this area.

4. Sediment Type and Low Frequency (LF) Bottom Loss

The Norwegian and Lofoten Basins consist of foraminiferal clay, marl and ooze interspersed with pockets of sand and mud (Vogt, 1986). There is no existing evidence of glacial marine detritus. The sediment composition in the Greenland Basin is clay and foraminiferal clay which merges with sandy clay, marl and oozes towards the Mohn Ridge and Greenland continental rise (Vogt, 1986). The sediment thickness in all three basins is of the order of hundreds of metres (NAVO, 1992). These sediment types constitute a poorly reflective, highly refractive medium to low frequency sound (less than 1000 Hz). Typical bottom loss (BL) values in this frequency range are -4 to 4 dB per bounce at low grazing angles (0 °-20 °) rising to 6 to 12 dB per bounce at higher grazing angles (Urlick, 1983).

The sediment types of the Greenland continental shelf, and large areas surrounding the Jan Mayen and Mohn Ridges and the Voering Plateau to the east are composed of sandy clay, marl and ooze. As in the basins there are relatively small areas of mud and sand-mud mixes. The sediment thickness is of the order 100 m or greater (Vogt, 1986). Due to the increase in sand content this sediment type is more reflective than that of the basins. However, typical BL values are similar to those given for the basin regions (adapted from NAVO, 1992).

Mid-ocean ridges such as the Jan Mayen Ridge, Mohn Ridge and Reykjanes Ridge are characterised by a lack of sedimentary deposits. Ridges frequently contain outcrops of crystalline bedrock (Vogt, 1986). Consequently, the bedrock is highly reflective but, due to its uneven nature, BL is relatively high at 8-12 dB (adapted from NAVO, 1992).

The Iceland-Faeroes Rise and continental shelf regions around Iceland, the Faeroe Islands and Norway have a more spatially variable sedimentary composition. Over relatively short distances the predominant seabed constituent can change from sand to sand-gravel mixes, sand-mud mixes or gravel-mud mixes (Vogt, 1986). Such variability will result in considerable BL fluctuations. For low grazing angles (0° - 20°) the BL associated with highly reflective sand is low at 0-2 dB increasing to 4-7 dB at higher angles, whilst more refractive sand-mud mixes have BL values typically 3 dB higher (adapted from NAVO, 1992). Because of this high spatial variability, the sedimentary composition is an extremely important parameter for sonar performance and tactical assessments.

5 Ambient Noise (AN)

Ambient noise is the total noise background in the sea measured using a non-directional hydrophone (Urick, 1983). Despite the implication of AN being non-directional, in ASW operations the directional nature of AN is an important consideration and will be discussed in this sub-section.

At the low frequencies of interest in this section (~ 50 Hz) the dominant sources of ambient noise in the northeast Atlantic Ocean are shipping traffic, drilling operations, distant storms, ice, biological sources such as whales, and seismic activity.

a. Area A

AN levels in ice covered areas, whether partially or full covered, is highly variable. The noise level and signal characteristics are dependent upon many environmental parameters: whether ice is forming or melting, rising or falling air temperatures, ice composition and density, wind speed and direction, sea conditions, snow cover and precipitation (Urick, 1983).

In winter area A is almost entirely covered by sea ice varying in thickness from <2 m near the ice margin to >5 m near the Greenland coast (Bourke, Pers. Comm.). AN levels at the frequency of interest are high in the vicinity of the MIZ at 85-90 dB and gradually reduce away from the marginal ice zone (MIZ), both seaward and under the ice, to 75-85 dB (Johannessen *et al*, 1988). This may fluctuate depending upon prevailing weather conditions, for example, with decreasing air temperatures tensile cracks in the ice are formed and increase noise levels (Milne and Ganton, 1964). In summer, the ice pack

retreats landward and the ice concentration at the boundary of area A and within the Fram Strait becomes highly variable (Hopkins, 1988). If the ice is influenced by relatively strong winds and/or increased sea states, the incidence of bumping and scraping increases, resulting in higher AN levels (Urlick, 1983). Although highly variable and weather-dependent, typical AN levels for area A in the marginal ice zone during summer are in the region 85-90 dB (Johannessen *et al*, 1988). However, if the conditions are calm, levels may be reduced by 10-15 dB (Urlick, 1983). Another distinctive source of AN in area A is that associated with biological activity – seals and whales. The acoustic signature associated with these marine mammals is transient in nature and may even appear as a false target in passive sonars (Urlick, 1983).

b. Area B

In this area AN is high close to the ice edge, as described above, and gradually decreases away from the ice (Johannessen *et al*, 1988 and Urlick, 1983). During the winter a large extent of this area is within, or in close proximity to, the marginal ice zone. Therefore, noise levels in winter are high at 85-90 dB (Johannessen *et al*, 1988). In summer, with the retreat of the MIZ into area A, noise levels become more varied and directional. AN is relatively high to the west and north towards the MIZ. To the south and east noise levels are dominated by shipping, biological noise and weather conditions and are in the range 72-77 dB (NAVO, 1992).

c. Area C

In the centre of the region AN can be as low as 72-77 dB but tends to increase to 82-87dB towards coastal regions associated with ice and shipping and drilling operations. Such activity is more concentrated along the Norwegian coast and in the North Sea (NAVO, 1992). AN directionality is affected by variations in the seabed shape causing topographic noise stripping, for example, the Jan Mayen Ridge area. In addition, frontal features, described in sub-section 3, may cause downward refraction of sound and noise stripping.

d. Area D

Towards Iceland, the Faeroes and the United Kingdom AN is in the range 82-87 dB associated with shipping and drilling operations. In the centre of the region levels reduce to 77-82 dB (NAVO, 1992). Topography plays a large role in directionality,

a good example being the northeast to southwest directionality of AN in the Rockall Trough. This is caused by the trough being bound to the northwest and east-southeast by shallow water, resulting in high attenuation of sound from distant sources in these directions. To the southwest high concentrations of merchant traffic transit towards Europe. The sound associated with this merchant traffic propagates through the deep water, experiencing little attenuation, into the Rockall Trough.

It should be noted that all areas have a moderate to high incidence of migrating sonic animals, such as whales, which not only increase ambient noise levels in a transient nature, but potentially acting as false targets. In addition, all areas are susceptible to transient noise sources from seismic activity, more especially near the Reykjanes, Jan Mayen and Mohn Ridges (Urick, 1983).

6 TASS Performance Assessment Versus a Modern SSN

The scenario presented is that of a typical TASS towed by either a surface ship or submarine (no distinction has been made between TASS performance capability on these units) deployed to detect a modern SSN operating in deep water within each of the climatological areas shown in Figure 1. The target submarine is considered to be operating at 100 m, TASS performance is assessed for deployment depths of 100 m and 300 m. The performance assessment is made using acoustic models to generate a propagation loss (PL) curve with initial detection ranges (IDR's) assessed by applying a generic but realistic passive figure of merit (FOM) based upon an ambient noise limited situation. The propagation loss models used to generate the appropriate PL curves are HODGSON and MIMIC; a description of HODGSON and MIMIC is given in chapter II.

Typical FOM's for a 50 % probability of detection at 50 Hz using the full passive sonar equation for an non-enhanced TASS versus a modern generic SSN operating at patrol speeds are given in Table 1. It is assumed that the tracking unit has been positioned such that the search is made utilising beams in a direction of relatively low ambient noise, i.e., an optimal performance situation.

	Operating Area			
	A	B	C	D
Winter FOM	54	54	56	53
Summer FOM	62	65	58	54

Table 1. Typical Passive FOM's for TASS v Modern SSN at 50 Hz.

The environment for each area and season is considered to be range independent in that the sound speed profile, bottom topography and geoacoustic parameters remain constant with range.

a. Area A

PL curves for winter and summer scenarios for a 50 Hz single modern SSN source at 100 m and TASS receiver towed at either 100 m or 300 m depth are shown in Figures 12 and 13, respectively.

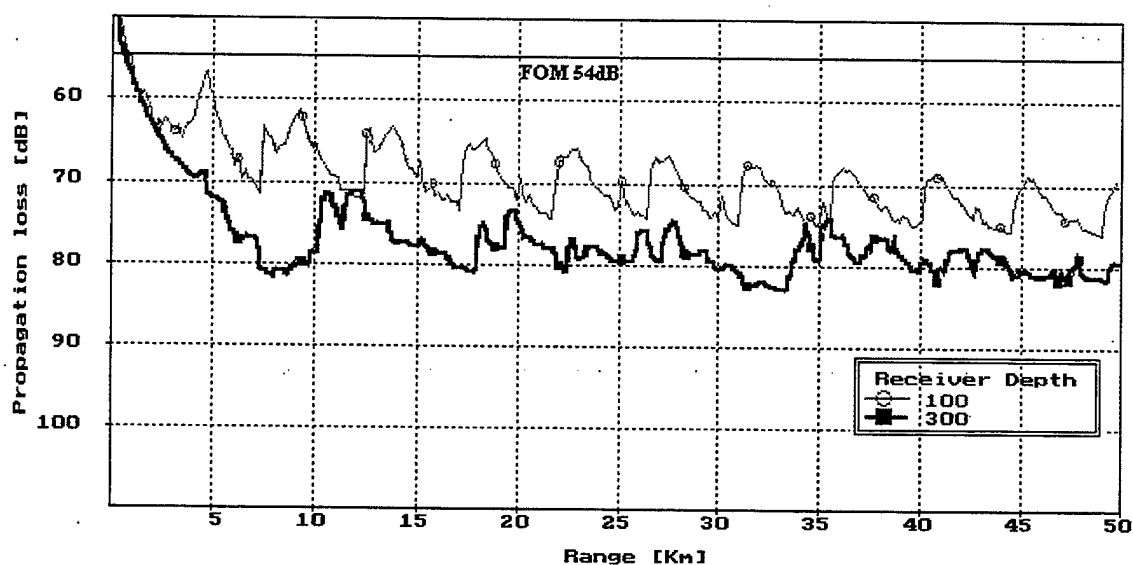


Figure 12. Propagation loss curve from the HODGSON model for a 50 Hz source at 100 m with a TASS receiver towed at 100 m (thin line) and 300 m (thick line). Climatological area A in winter.

The shape of the PL curve for the receiver at 100 m in Figure 12 clearly shows the influence of propagation in the strong surface duct, having a skip distance of about 4 km. In this case a typical IDR for the receiver at both 100 m and 300m is 1.5 km.

Although the shape of the PL curve in Figure 13 is essentially the same as Figure 12, the skip distance has increased to 5.5 km. This is caused by the decrease in sound speed gradient in the surface layer from winter to summer. Because of the reduced AN in summer, IDR's are better than in winter. For a receiver at a depth of 100 m the detection is intermittent with initial detection at 11km, with the receiver at 300 m the IDR is 2 km.

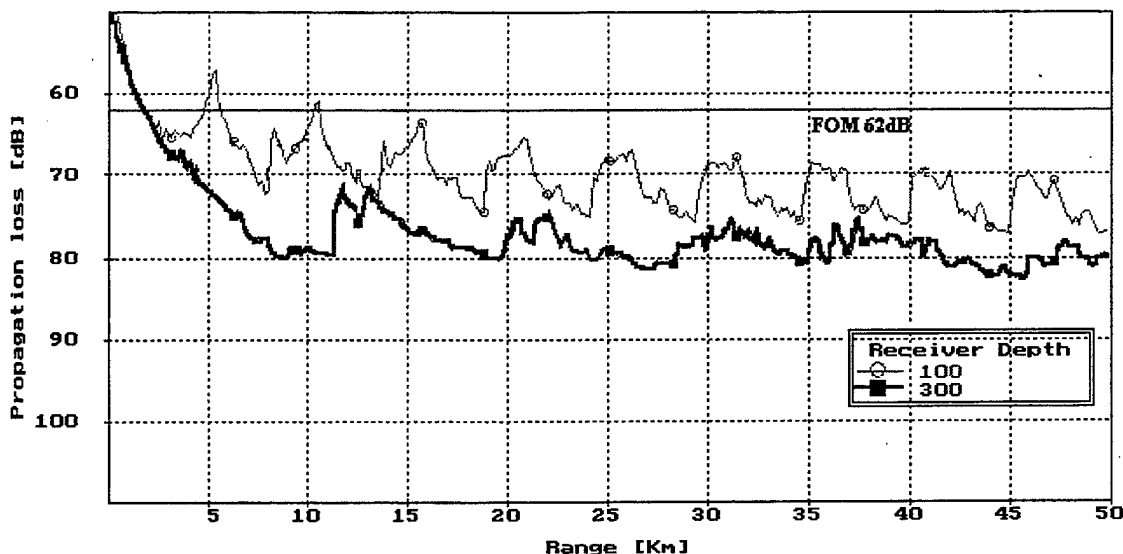


Figure 13. Propagation loss curve from the HODGSON model for a 50 Hz source at 100 m with a TASS receiver towed at 100 m (thin line) and 300 m (thick line). Climatological area A in summer.

b. Area B, Area C and Area D

The PL curve for this area in winter, Figure 14, indicates that ranges are now extremely poor. This is a result of the high AN due to ice-ice interaction and the weather conditions. Consequently, the short IDR's have been re-assessed using MIMIC as opposed to HODGSON to provide a more detailed PL curve (Figure 15).

IDR's are approximately 600-800 m. It is also evident that changes in tow depth at these short ranges exhibit little effect on predicted ranges.

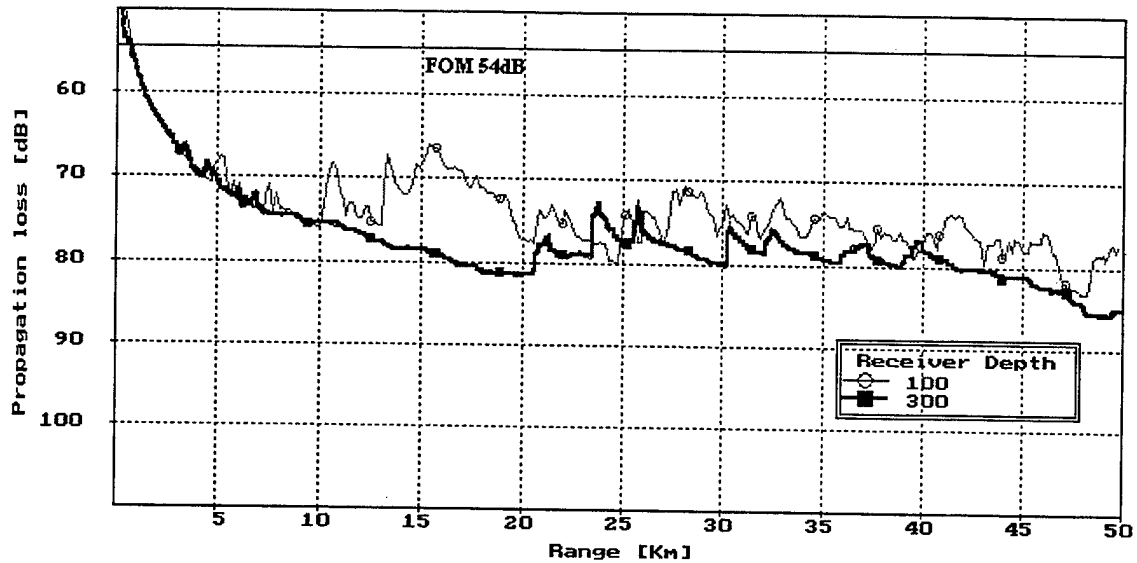


Figure 14. Propagation loss curve from the HODGSON model for a 50 Hz source at 100 m with a TASS receiver towed at 100 m (thin line) and 300 m (thick line). Climatological area B in winter.

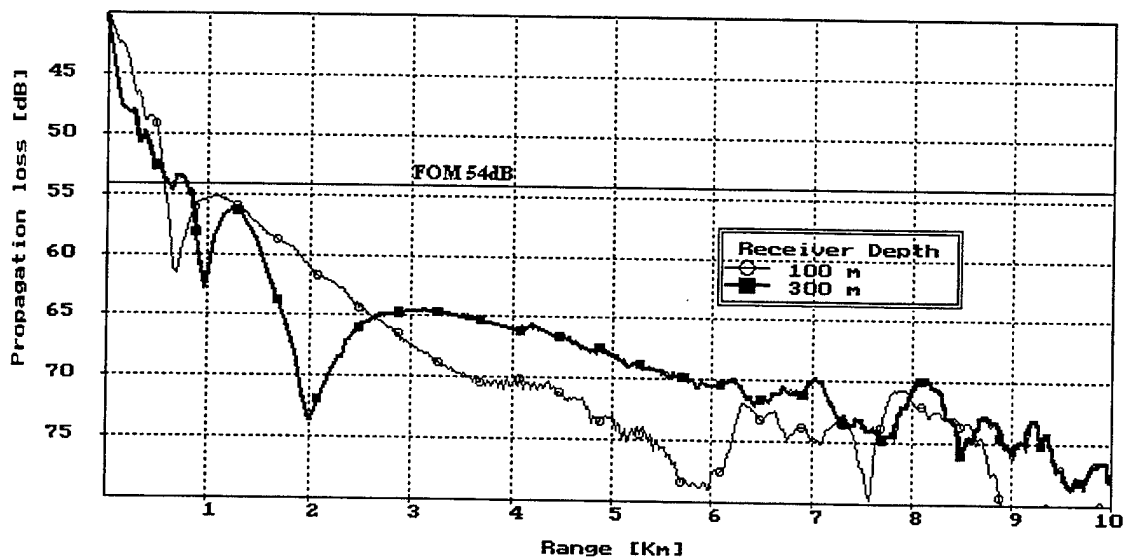


Figure 15. Propagation loss curve from the MIMIC model for a 50 Hz source at 100 m with a TASS receiver towed at 100 m (thin line) and 300 m (thick line). Climatological area B in winter.

The IDR's experienced throughout areas B, C and D are all less than 4 km and, as in Figure 15, exhibit little influence on TASS tow depth. The PL curves for these areas are omitted but Table 2 provides a full assessment of IDR's.

		Initial Detection Ranges (km)			
	Receiver Depth (m)	Area A	Area B	Area C	Area D
WINTER	100	2	0.6	1.5	0.6
	300	2	0.8	1.4	0.75
SUMMER	100	2 int 11	2.2	1.4	0.6
	300	2	3.4	1.6	0.8

Table 2. IDR's for TASS versus Modern SSN, 50Hz. The abbreviation 'int' signifies that the contact is likely to be intermittent to the longer range specified, for example, 2 km intermittent detection to 11 km.

From the results given in Table 2 it is clearly evident that today, against modern SSN's, ASW is now a close quarters affair. Passive detection ranges are expected to decrease even further as noise quieting technology advances. In order to alleviate the tactical problem that this poor performance assessment indicates several options are available for improvement of USW detection opportunities. The development of Low Frequency Active Sonar (LFAS) and improved signal processing are two options that are investigated in this study.

B. MOTIVATION

With the advent of LFAS the effect of the environment on frequencies in the range 200-1500 Hz has become an important issue. For purposes of interest to the Royal Navy (RN) this research will concentrate on the effects of the environment in operationally significant areas of the North West approaches (NWAPPS) to the United Kingdom. System performance will be modeled for a generic LFAS system under development for use by the RN. The frequencies considered throughout are 400 Hz and 800 Hz. All parameters used in modeling the acoustic energy associated with the sonar system are considered to be typical and not specific to a particular system.

The environmental area of interest is detailed in Chapter III-B. The area has been selected for a number of reasons:

1. Historically the RN has conducted many operations in this area, both as exercises in peacetime and for real in wartime.

2. The area is acoustically complex. The topography varies markedly over relatively short distances. Associated with these changes are ocean fronts, changes in geoacoustic conditions, changes in bottom depth with propagation over complex bathymetry including upslope and downslope conditions and variability in ambient noise levels and directionality. All these spatially and temporally varying parameters contribute to a highly variable sonar performance making this a good test bed area to study.
3. A considerable amount of environmental data exists for the area.

Although the NWAPPS has been the subject of much research, particularly in the region of the South East Icelandic Front (SEIF) (Hopkins, 1988), the majority of these studies have concentrated on the physical oceanography of the region rather than acoustic performance. A study of low frequency acoustic propagation through the SEIF by Carman and Robinson (1994) highlighted that the complex bathymetry and geoacoustics of the frontal region dominate any anticipated variation in sound speed profile. In their study it was clear that the SEIF did influence the acoustic propagation but was minor in comparison to the effects of the seabed. It should be noted that Carman and Robinson concentrated on frequencies of 25 Hz and 50 Hz. As previously stated, this research will concentrate on frequencies of 400 Hz and 800 Hz. At such frequencies the surface mixed layer and any sound channels are more likely to act as a wave-guide, thus variations in these features associated with an ocean front can be expected to exert a significant affect on acoustic propagation. A precursor to the research by Carman and Robinson was that undertaken by Jensen *et al.* (1991) who conclude, on modeling the acoustic propagation through the front, that the correct topographic input for modeling purposes had a greater influence on PL than sound speed variability. The intention in this research of the environmental assessment of LFAS performance is to include accurate two-dimensional topography and realistic geoacoustic parameters. The precise method of integration of the geoacoustic parameters is discussed in Section III.B.

The goal of this research is to highlight operational aspects of the environmental parameters influencing LFAS performance. As such, it is desirable to use an operational propagation loss model, namely the Royal Navy's HODGSON Propagation Loss model.

This is a range dependent model that allows for variations in water depth and SSP with range. However, the seabed loss algorithms, which are based on the Bottom Loss Upgrade (BLUG) parameters, are range independent. Because in shallow water geoacoustic conditions can change rapidly over relatively short distances, this research compares the HODGSON model to a parabolic equation model which allows for sedimentary range dependence, i.e., the Range Dependent Acoustic Model (RAM), and, if required, a correction will be applied to the HODGSON model for the performance assessment. The advantage of using the HODGSON model is that it allows for volume absorption, sea surface losses and provides reverberation data, all of which are not present in RAM. The models used are more fully described in chapter II. The ideal situation would be to compare the HODGSON propagation loss to measured data, unfortunately, such data is not available. Therefore, propagation loss from RAM is used as the control run. In the past there have been two types of significant model error, inaccurate input and inaccurate solutions to the wave equation. RAM gives a realistic solution to the wave equation and is, therefore, a suitable model for defining control propagation loss curves in this research. Highly accurate model input is difficult to achieve in terms of the environmental parameters, however, the input parameters used in providing an accurate model solution have been made as realistic as possible.

Additional to the effects of the front are the implications on target detection of upslope and downslope enhancement. This is a subject of much debate. Urick (1983) provides insight into the upslope effect whilst in the operational community downslope enhancement has been generally advocated over upslope propagation. This research will briefly broach this issue for LFAS operations at 400 Hz and 800 Hz in the NWAPPS.

It is a well-documented characteristic of shallow water operations that ambient noise levels are highly variable (Urick, 1983). Indeed, the presence of a single merchant ship can increase LF background noise by as much as 40dB. This effectively renders any LF sonar useless. For active sonar operations the limiting factor to performance is generally reverberation. It then behooves us to investigate signal processing techniques that may suppress the noise background and/or reverberation or permit enhancement of a signal embedded in a noisy background. The CST 1996 Final Report (Raff, 1996) considers enhancement to detection resulting from improvements in signal processing,

more specifically advances in beamforming techniques such as adaptive beamforming (ABF). These methods increase array gain, therefore, enhancing the signal to noise ratio, which results in improved detection opportunities. Inverse Beamforming (IBF) is a proven method of reducing the masking effect of ambient noise and, presently in development, reverberation effects at the sonar by advanced signal processing techniques. The basic methodology and results associated with this method are discussed in chapter IV.

C. AIM

There are two main aims for this research:

1. To assess the expected performance capability and the effects of the ocean environment on a generic UK LFAS system operating in a monostatic scenario against a modern target in the operationally significant area of the North West Approaches to the UK.
2. To briefly describe the basic principles of the Inverse Beamforming (IBF) method of signal processing for passive sonar and state how this method can be adapted for active sonar use to improve sonar performance.

II. PROPAGATION LOSS MODELS

The models used in this research are described below. The references are stated but those for the HODGSON and MIMIC models may be difficult to locate.¹

A. THE FINITE ELEMENT PARABOLIC EQUATION (FEPE) MODEL AND THE RANGE DEPENDENT ACOUSTIC MODEL (RAM).

The parabolic equation (PE) has proven to be an effective method for solving range dependent, one way propagation, ocean acoustic problems (Collins, 1995). The Finite Element Parabolic Equation (FEPE) model (Collins, 1988) and the Range dependent Acoustic Model (RAM) (Collins, 1995) employ the latest techniques in PE modeling.

The FEPE model produces a fully coherent solution to the acoustic pressure field in an ocean overlying a sediment that supports only propagation of compressional waves (Collins, 1988). The FEPE model includes high accuracy for wide propagation angles, large depth variations in the acoustic parameters, high accuracy for range dependent environments (including steep slopes), a highly accurate self starter and an algorithm for solving tridiagonal systems that are efficient for problems involving variable ocean depth (Collins, 1988). FEPE is a powerful tool due to its ability to deal with nearly all practical two-dimensional problems where the geology and water column are functions of both depth and range (Collins, 1988).

RAM² is a variant of FEPE; it is based upon the most recent improvements to PE modeling techniques. The method for obtaining a solution from RAM is based on the split-step Padé solution (Collins 1993a and 1993c), which allows large range and depth steps to be employed. This reduces model run time while still providing an accurate and timely solution (Collins, 1995). The FEPE model provides a numerical solution to the parabolic wave equation by repeatedly solving tridiagonal systems of equations. In RAM

¹ The HODGSON references may be requested from: OAD Ltd., 'Pendower', Leverlake Rd., Widemouth Bay, Bude, Cornwall, EX23 0AF, UK.

² RAM was updated in Apr 1998 by an amendment to the self-starter, which improved stability, and to the solve sub-routine to reduce run-time on some computer systems (from www.oalib.njit.edu).

this process is optimised by minimising the number of operations by employing an elimination scheme that is efficient for solving problems involving variable ocean depth (Collins, 1995). This method is the split-step Padé algorithm. It is based upon solving rational function approximations, using tridiagonal systems of equations, in parallel to achieve significant gains in efficiency (Collins, 1995).

In both RAM and FEPE range dependence of the acoustic parameters within the water column and sediment is handled by approximating the medium as a sequence of range independent regions with acoustic parameters making a step change at the range they are introduced (Collins, 1995 and Fabre, 1998). In order to maintain an accurate solution both models conserve energy flux at the vertical boundary (Collins, 1993b). Despite the acoustic parameters being stepped, both models account for variation in bottom depth with range. This is done by discretising the depth operator using Galerkin's method (Collins and Westwood, 1991) and allows piecewise continuous depth variations in the acoustic parameters at the sediment/water column interface (Collins, 1995).

The input parameter requirements for RAM are shown in Table 3.

RAM Input Values/Structure	Description
Example	Title
400.0 100.0 100.0	Frequency (Hz) Source Depth (m) Receiver Depth (m)
53000.0 4.0 5	Range of Plot (m) Range Step (m) Range Skip Factor
4132.0 2.0 2 500	Max. Depth (m) Depth Step (m) Depth Skip Factor Max. Plot Depth (m)
1500.3 3 1 0	Ref. Sound Speed (m/s) Padé Terms Stability Constraints Max. Range of Stability Constraints
0.00 2130.00	Bathymetry: Range (m) Depth (m)
52972.0 600.00	
-1.000 -1.000	Data Separator
0.000 1487.4	SSP at Range 0 m: Depth (m) Sound Speed (m/s)
2130.0 1499.8	
-1.000 -1.000	Data Separator
2130.0 1441.0	Sediment Sound Speed: Depth (m) [from sea surface] Sound Speed (m/s)
4130.0 2003.0	
-1.000 -1.000	Data Separator
2130.0 1.354	Sediment Density: Depth (m) [from sea surface] density (g/cm ³)
4130.0 1.676	
-1.000 -1.000	Data Separator
2130.0 0.021	Sediment Attenuation: Depth (m) [from sea surface] Attenuation (db/λ)
4130.0 0.015	
4132.0 20	
-1.000 -1.000	Data Separator
53000.0	Starting range for next environment, followed by new environment

Table 3. Input Parameters for Range Dependent Acoustic Model, RAM.
(Adapted from Fabre, 1997).

B. THE HODGSON MODEL

The HODGSON model is a range dependent acoustic ray trace propagation loss model owned by the UK Ministry of Defence (MOD). It is used by the Royal Navy as the standard PL model for use at frequencies above 150 Hz, but is able to give a representative solution at lower frequencies in deep water environments. The model has undergone formal validation by the UK MOD (Hodgson and Hodgson, 1988a).

1. Range Dependency

The model will accept up to 20 sound speed profiles or depth definitions in generating a two dimensional ocean environment, which is divided into 50 depth steps and 320 range steps effectively creating a 50 x 320 grid. The user selected range and depth limits are matched to the 50 x 320 dimension. Range dependency is achieved by interpolating between successive sound speed profiles or bottom depth points at the grid points. The source and receiver can be placed by the user at any range and depth within the defined environment (Hodgson and Hodgson, Pers. Comm.).

2. Sea Surface Loss

Losses associated with scattering from the sea surface are calculated as a loss per bounce using either the Beckmann and Spizzichino algorithm (Beckmann and Spizzichino, 1963) or the AMOS algorithm (based upon Schulkin, 1968). The model evaluates the loss from both algorithms and uses the highest value. The logic behind this process is that the Beckmann and Spizzichino algorithm gives more realistic results at low frequency x wave height ($f \times H$) values whilst the AMOS algorithm is more realistic at high $f \times H$ values (Hodgson and Hodgson, 1998b). The loss is a function of wave height, frequency and grazing angle.

3. Volume Absorption Loss

The model applies the full version of the Francois and Garrison algorithm (Francois and Garrison, 1982) fully range dependently, applying the method described for sound speed range dependency in subsection 1. The default value for pH is 8.1 and, at present, it is fixed. The model uses inputs of frequency, depth, temperature and salinity to calculate the loss with range (Hodgson and Hodgson, 1998b). It is likely that on many occasions the salinity data is not available; in this case the WADER system provides climatological data from Levitus 94SE (Hodgson and Hodgson, Pers. Comm.).

4. Seabed Loss

The model uses the Navy standard Interim Bottom Loss Upgrade (IBLUG) high frequency and low frequency curves (Naval Oceanography Office, 1990) or, for frequencies below 2kHz, can accept standard Bottom Loss Upgrade (BLUG) parameters and applies BLUG algorithms (Naval Oceanography Office, 1990). The model generates a loss versus grazing angle curve using the BLUG parameters as follows:

1. A sound speed profile in the sediment is created.
2. A simple ray trace program 'fires' rays at the sediment layer with grazing angles from 0° to 90° at ray angle steps of 0.1° .
3. If the grazing angle is below the critical angle for the ocean-sediment interaction then it is reflected and attenuated. If the grazing angle is above the critical angle then it is refracted through the sediment layer and attenuated. The total attenuation is the sum of the reflected and refracted components.
4. If a refracted ray reflects at the rock sub-bottom, it is reflected and attenuated as prescribed by the defined sub-bottom attenuation.

The BLUG algorithms do not allow for the possibility of the refracted ray re-emerging into the water column at some distance downrange, instead the acoustic energy from this source is added to the reflected ray of the same source. Additionally, the HODGSON model includes a loss at low grazing angles, below the critical angle, which is not allowed for in the BLUG algorithms at low frequency with a highly reflective seabed. The seabed loss is not range dependent.

5. Propagation Loss

Two separate PL modules are present in the HODGSON model, coherent (below 150Hz only) and incoherent. Additionally, the model can be set up to calculate passive one-way loss or active two-way loss (Hodgson and Hodgson, 1998a). The loss algorithm applied is that defined by Urick(1983) as a function of range and ray separation at the source and receiver, loss being evaluated at the specific grid points that define the environment. The model, in essence, creates a ray tube with adjacent rays defining the tube dimensions and applies range dependent ray theory where the radius of curvature of

each ray is recalculated at each range and depth step. Caustics are dealt with by limiting the ray spacing to a minimum of 10m unless this is greater than the ray spacing for standard spherical spreading at the prescribed location. This is a fix that is intended to remove spikes in the PL curve prior to the PL curve construction. It is not intended to model caustics although it does attempt to remove the problem of PL assessment caused by them. Earlier versions of HODGSON used Weston Fat Ray theory (Weston and Focke, 1985). The Weston method essentially performs the same task as the present HODGSON model but applies a variable ray spacing limit that is based on ray curvature and frequency. The Weston algorithm can produce a 'Fat Ray' width that is very large; this proved impossible to accommodate within the standard HODGSON code (Hodgson and Hodgson, Pers. Comm.).

6. Reverberation

The model applies reciprocal and non-reciprocal path methods to calculate reverberation from the sea surface and seabed. The environment is dealt with as in the majority of reverberation models; the reverberating surfaces are treated as a series of equally spaced concentric rings. Each individual ring is treated as a target with the target strength calculated as a function of the reverberating area and scattering strength (Hodgson and Hodgson, 1998b). The HODGSON model applies the ARL:UT scattering algorithms for sea surface scatter, seabed scatter algorithms developed by ARL:UT from work by McKinney and Anderson (1964) and, for a very rough seabed, applies Lambert's Law as treated by Urlick (1983). At present the inclusion of volumetric scatter and reverberation is under investigation (Hodgson and Hodgson, Pers. Comm.).

The multipath method plots all ray tubes to the target area and stores the arrival data for each beam, the travel time, propagation loss and backscatter coefficient. In many cases, but more especially in shallow water over a low loss seabed, the number of returns from a single reverberating ring may be very large (>40000). However, many of these returns will have suffered multiple attenuation at the seabed and sea surface and can be ignored. In order to limit processing time and computer memory requirements the model applies a simple filtering technique to remove highly attenuated returns and use only the loudest 200 returns. The arrival data is summed for display purposes based upon the pulse length for a Carrier Wave (CW) pulse or the resolved pulse length for a Frequency

Modulated (FM) pulse (Hodgson and Hodgson, 1998b and Hodgson and Hodgson, 1997-98). This model compares well with benchmark curves in development at Defence Establishment Research Agency (DERA) Winfrith, UK (Hodgson and Hodgson, 1998b).

An example of some of the pertinent input parameters for the HODGSON propagation loss model are shown in Table 4.

RUN PARAMETERS		RUN OPTIONS		SEDIMENT PARAMETERS	
Max. Range (km)	100	Plot Left	OFF	Speed Ratio	1.100
Source Depth (m)	40	Plot Right	ON	Density Ratio	1.962
Source Range (km)	0.0	Spike Filter	ON	Curvature Factor	0.86
Max. Ray Angle	15	Shadow Detector	ON	Sed. Gradient	1.8
Min. Ray Angle	-15	Variable Ray Step	OFF	Sed. Thickness	100.0
Ray Angle Step	0.05	Coherent Mode	OFF	(m)	
Frequency (Hz)	400	Calculate Reverbs	ON	Sed. Attenuation	0.25
Wind Speed (kts)	0.0	Calculate Proploss	ON	(dB/m/KHz)	
Wave Height (m)	0.0	Range Scale	KM	Base Loss	6.02
Sea State	0.0	SSP Smoothing	OFF	(dB/bounce)	
Display Depth (m)	250				
Range Step (m)	313				
Pulse Length (s)	2.00				
Beam Width (Deg)	360				
Target Strength (dB)	10				
Bottom Type	Sand				

Table 4. Typical input parameters for the HODGSON propagation loss model.
(Adapted from Hodgson and Hodgson, 1998a)

C. MIMIC (Multi-path Interference Model)

MIMIC is a range independent, short range (<10km), low frequency (<150Hz) propagation loss model owned and developed by Ocean Acoustic Developments (OAD) Ltd. The model has undergone formal validation by the UK MOD and has been accepted by the Royal Navy for use at frequencies below 150Hz in both deep and shallow water. The MIMIC model is intended for use against quiet, therefore, short range, low frequency noise sources. It is applicable for TASS and sonobuoy performance assessments against modern targets (Hodgson and Hodgson, 1998a).

MIMIC calculates PL and phase for eigenrays between the source and receiver and coherently sums the acoustic energy from a variety of propagation paths. The paths accounted for are as follows; direct path, sea surface reflected path, sediment-reflected

path, sediment refracted path and sediment refracted rock sub-bottom reflected path. The sediment data is based upon the BLUG algorithms (Hodgson and Hodgson, 1998a and Pers. Comm.).

III. METHODOLOGY AND PROPAGATION RESULTS

The aims of this chapter are:

1. To briefly describe the geographical area for the LFAS performance assessment phase, including environmental data acquisition and processing.
2. To describe the modeling methods employed and results for the model to model comparison and the LFAS performance assessment.
3. To state the approach used in this study for the consideration of advanced signal processing techniques.

A. AREA OF ASSESSMENT

The underlying reasons for selecting the NWAPPS to the UK have been outlined in Section I.B. This section gives a brief physical and environmental description of the area selected for the LFAS performance assessment phase. The source of environmental data and how the data was manipulated for use in the acoustic propagation loss models is outlined. The emphasis of each sub-section is directed at the parameters required for the LFAS performance assessment and the acoustic propagation models. Figure 16 shows the area under consideration in this study.

1. Weather

For the operational assessment phase, this study focuses on the extreme environmental regimes of winter and summer. The Polar Front and the Icelandic Low dominate the weather patterns of the region and low pressure systems traverse through, or in close proximity to, the area of interest in a generally northeasterly track throughout the year (Hopkins, 1988). Associated with the deepening of the Icelandic low, the number of occurrences of such an event increases from 10-12 during July to September (summer) to 17-20 during the winter months (January to March) (Hopkins, 1988). Typical wave heights in the area during summer are nominally 1-2 m. These increase to 2-4 m in winter, although extreme conditions with wave heights in excess of 7 m may occur in periods of sustained high winds (Gathman, 1986). The percentage of observations that include precipitation is at its lowest, 10-15%, during the summer months, increasing to 25-30% during the winter months (Gathman, 1986). The climatological wave height and

precipitation levels described are applied in the LFAS performance assessment phase described in Section III.C.

2. Topography

The topography of the NWAPPS is complex and varied (Figure 16). The Norwegian Basin and Iceland Basin extend to depths in excess of 3000 m and are separated by the Iceland-Faeroes Rise. This rise shoals to a relatively flat-topped bank averaging 400 m in depth. Between the Faeroe Islands and the UK mainland lies the relatively steep sided Faeroes-Shetland Channel. This channel extends from the southern Norwegian Basin southwestward towards the Rockall Trough. The Faeroes-Shetland Channel is separated from the Rockall Trough by the north-to-south-orientated, relatively narrow, Wyville-Thomson Ridge, which shoals to ~600 m. The Rockall Trough and Iceland Basin are separated by a broad region of undulating topography interspersed with broad banks, such as Rosemary Bank and Bill Bailey's Bank. In addition to the multitude of islands, rises, banks and channels is the presence of several seamounts. Most notable of these is Anton Dohrn. Located in the northern Rockall Trough, Anton Dohrn rises steeply from 2000 m to 700 m with a summit at a depth of ~570 m.

Due to the tactical significance of topography for submarine navigation, the topography of the region is the dominant factor in the selection of tracks for the LFAS performance assessment phase of this study. The precise reasons for track selection, as shown in Figure 16, are stated in Section III.A.5.

3. Oceanographic Conditions

The predominant influence on the oceanographic conditions of the NWAPPS is the warm, saline surface flow of the North Atlantic Drift. However, on the northern flank of the Iceland-Faeroes Rise the Iceland Current introduces cold, relatively fresh water to the north of the region. As described in chapter I, section A.3.b, the boundary between these water types forms the South East Icelandic Front (SEIF). The frontal structure is very complex and highly spatially variable; typical widths of the surface or near surface expression of the front are of the order 30 km (Willebrandt and Meincke, 1980). Additionally, the frontal location at the surface and at 300 m may be displaced by over 100 km (Smart, 1994). With a lateral change in temperature of the order 5-7 °C across the front (Hopkins, 1988) and because of the large vertical shift in horizontal

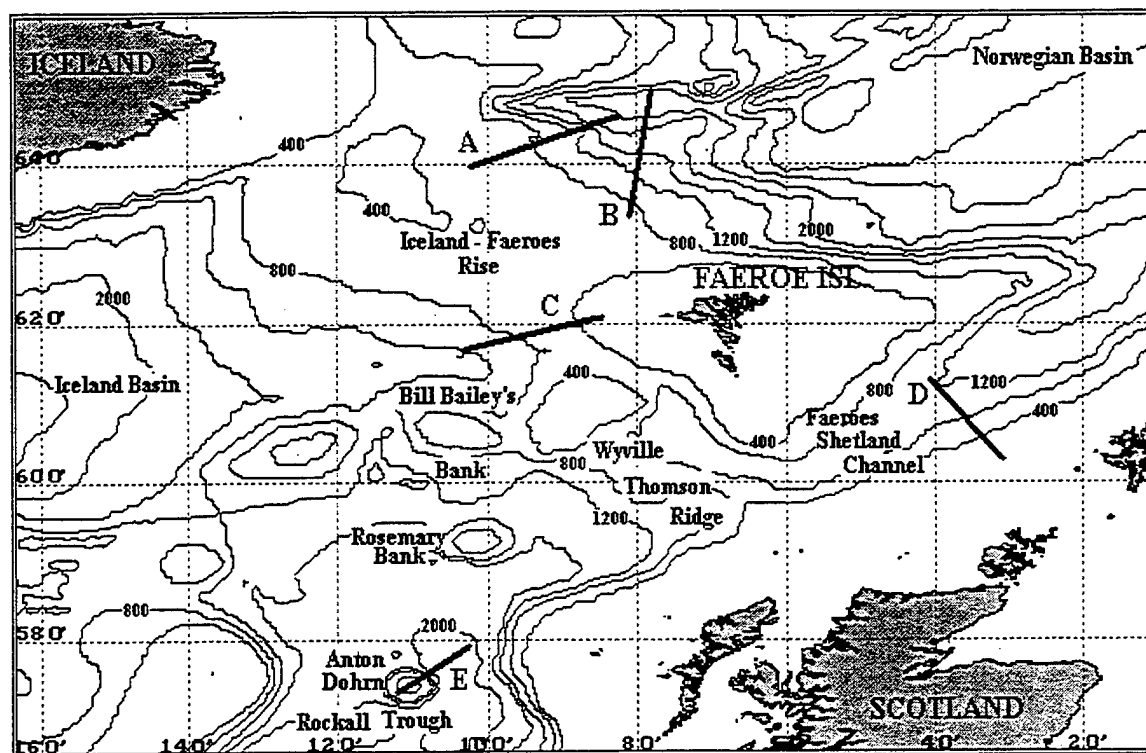


Figure 16. Bathymetric chart of the North West Approaches (NWAPPS) to the UK (depth contours in metres). Shown are the environmental sections used in the model to model comparison and LFAS performance assessment; A – South East Icelandic Front transect in winter, B – South East Icelandic Front transect in summer, C – Upslope/Downslope transect, D – Faeroes-Shetland Channel transect, E – Anton Dohrn transect. (Adapted from WADER Global Information System, OAD Ltd.)

location of the boundary, the influence of the front on acoustic propagation paths at 400 Hz and 800 Hz (the frequencies of interest) is likely to be considerable. For this reason the effect of the front on acoustic propagation is investigated as part of the LFAS performance assessment phase of this study. The sound speed profile generation through the front is described in Section III.A.5.

The typical temperature, salinity and sound speed profiles for the NWAPPS in winter and summer are shown in Figures 8 and 9, respectively. However, for the propagation modeling phases of this study the sound speed profiles used are more spatially refined, depending more specifically on location. The procedures for environment generation are outlined in Section III.A.5.

4. Data Acquisition

The data requested from, and provided by, the UK Hydrographic Office (UKHO) for the NWAPPS during winter and summer, as applicable, was as follows:

1. Climatological and synoptic temperature, salinity and sound speed profiles.
2. Geoacoustic properties at 400 Hz and 800 Hz, to include vertical profiles of density, compressional wave sound speed and compressional wave attenuation.
3. South East Icelandic Front description, climatological location and any existing survey information/data.
4. Bathymetry charts with 100 m depth contours.

The WADER Global Information System provides climatological temperature, salinity and sound speed profiles based upon the Levitus 94(SE) database (Hodgson and Hodgson, 1998a).

5. Two Dimensional Environment Generation

This sub-section describes the methods applied in generating two-dimensional (2D) representations of the environment for acoustic propagation modeling. There are two important facets to generating a 2D range dependent environment; 1) representative seabed shape and associated geoacoustic parameters, and 2) representative sound speed profiles.

In all range-dependent cases the 2D seabed depth with range profiles are generated using the UKHO charts C7813, C7814 and C7816 along the tracks shown in Figure 16. Data entry points for the model are generated at 100 m contour intervals or

across a region considered to be of constant gradient seabed slope. The transects have a length in excess of 100 km allowing selection of the most representative 60-100 km section of the track for entry into the acoustic propagation model. An example of a range dependent seabed shape (bathymetry vs. range) used for input model parameters is shown in Table 5.

Range(km)	Depth(m)
0	1000
5.7	1300
11.4	1500
17.1	1800
25.9	1900
37.6	2000
49.8	2100
63.8	2130
77.8	2100
83.5	2120
88.7	2100
90.5	2000
96.4	1000
99.5	800
103.9	700
111.1	600
113.9	560
116.8	600
124.5	700
132.0	800
135.3	1000
139.7	1500
143.6	2100

Table 5. Data entry points for the seabed transect across Anton Dohrn.
(Track E in Figure 16)

Tracks A and B have been selected to give a representative sound speed cross-section across the SEIF in winter and summer, respectively. The exact orientation of the track is such that the propagation transects are perpendicular to the plane of the front in order to minimise three-dimensional propagation effects.

Track C is representative of a relatively gentle gradient slope from shallow to relatively deep water that characterises much of the NWAPPS. This track is selected in order to compare upslope and downslope enhancement.

The Faeroes-Shetland Channel is an area that has historically been exploited for navigation by transiting submarines, hence the selection of track D.

Track E transects another historically important navigational feature, Anton Dohrn Seamount.

In the ideal world sound speed profiles would be available to a very high resolution, scales of kilometre's or less. The data would then encompass high frequency variations and highlight features such as internal wave motions and synoptic scale variability. This is not a reasonable or viable option for this study. For the tracks of interest, away from frontal zones, climatological SSP's are used. This data has a spatial resolution of $\frac{1}{2}^{\circ} \times \frac{1}{2}^{\circ}$ and a half-month temporal resolution and is extracted from the UKHO Gridded Physical Properties Database (Version 2.0) (GPPDB) (UKHO, 1997). The SSP is linked to a specific range/depth location according to its proximity to the nearest climatology grid point. It should be noted this method of environmental generation cannot represent small scale features, e.g., internal wave fields.

As climatological data is too large scale to accurately depict the SEIF, the SSP's are generated using results from surveys taken in the respective winter and summer periods of interest. Data provided by the UKHO includes horizontal temperature contours at specified depth levels with contour intervals of 0.5 °C; the depth levels are surface, 100 m, 200 m, 300 m and 400 m. The temperature section through the front is created using the UKHO survey temperature contour plots to adjust climatological temperature profiles. By linear interpolation, both horizontally and vertically, along the frontal transect representative temperature profiles are generated. Using climatological salinity values and the Chen and Millero (1977) algorithm for sound speed embedded within the HODGSON model, a SSP for each data point is calculated. As with the use of climatological data, small scale features are not depicted, but this method gives a more realistic frontal cross-section than pure climatology.

Unfortunately, not all tracks selected have geoacoustic parameters available from the UKHO Geophysical database. In order to standardise the method of geoacoustic parameter calculation all data is generated from the following sources; typical values for various sediment types are as suggested by Hamilton and Bachman (1982), algorithms for sediment sound speed, density and compressional wave attenuation are taken from

Bachman (1994) and the BLUG algorithms and typical BLUG parameters summarised by Bourke (Pers. Comm.) are used to calculate the geoacoustic input parameters for the propagation loss models.

B. MODEL COMPARISON

The aim of the model comparison section of this study is to further verify the accuracy of the HODGSON propagation loss model for use at frequencies associated with LFAS operation. Additionally, the PL model output from HODGSON and RAM are compared to assess the applicability of the BLUG algorithms (Naval Oceanography Office, 1990) in a range dependent environment; bottom loss parameters are range independent in the HODGSON model. This section describes the methods used to compare HODGSON and RAM in both range independent and range dependent environments and details the propagation loss comparison results.

1. Propagation Loss Streamlining

As stated in chapter II, RAM does not account for sea surface scattering loss or volume absorption. In order for model to model comparison to be consistent both of these sources of loss must be either applied to the RAM propagation loss output or removed from the HODGSON model PL output. The latter option is the most simple to apply. Sea surface scattering loss is removed from the HODGSON model calculations by setting the sea surface wave height to zero. The absorption loss discrepancy is more difficult to remove. By applying a basic correction factor to the HODGSON model PL output using values adapted from Francois and Garrison (1982), as shown in Table 6, the HODGSON model PL output is altered. Throughout the range of the PL calculation the absorption loss correction is subtracted from the HODGSON-calculated PL.

Frequency (Hz)	Absorption Loss (dB/km)
400	0.015
800	0.045

Table 6. Absorption Loss at 400 Hz and 800 Hz for 10°C, 35psu, pH 8.
(Adapted from Francois and Garrison, 1982).

Although this method is not absolutely precise, the error introduced by this approach is minimal.

2. Range Independent Environment

The HODGSON model and RAM are run over a range of 100 km in both deep (2000 m) and shallow (200 m) water using a climatological SSP from NWAPPS area in winter and summer. The sediment type is range independent; both sand and silty clay are considered. This approach is applied in order to confirm the accuracy of the propagation loss algorithms in the HODGSON ray theory model compared to the wave theory model RAM.

a. Sound Speed Profiles

The winter and summer SSP's for the deep water environments are shown in Figures 17 and 18, respectively. The profiles are extracted from the UKHO GPPDB and displayed using the WADER Global Information System (OAD Ltd.). Winter and summer SSP's for the shallow water environments are simply the top 200 m of the deep water SSP's; the shallow water profiles are shown in Figures 19 and 20, respectively.

In this phase of the research SSP's for winter and summer are used in order to compare model output in the two regimes that are studied in the LFAS performance assessment phase. In shallow water the incidence of interaction of acoustic energy with the seabed is increased. Hence, the shallow water regimes are studied in order to test the BLUG algorithms within the HODGSON model.

b. Geoacoustic Parameters

RAM and HODGSON apply different algorithms for seabed loss and, thus, treat the seabed in a different way; this is described in chapter II. For a comparison of the propagation algorithms to be worthwhile it is imperative that the input seabed parameters specific to each model are equivalent. The seabed loss parameters used are derived from typical values suggested by Hamilton and Bachman (1982) for silty clay and fine sand. These are sediment surface values and are used in conjunction with typical BLUG parameters, suggested by Bourke (Pers. Comm.), to provide input parameters for

Profile Analysis				
Layer Depth 900m		Cut-off Freq 7Hz		
Sound Channels				
Axis	Top	Base	Strength	Cut-off Freq
1500m	900m	1964m	Strong	9Hz

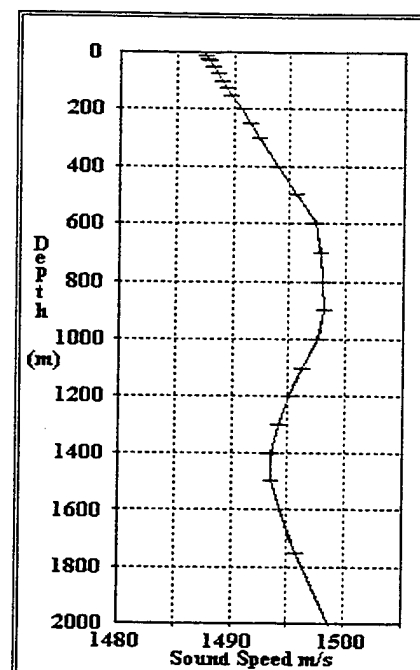


Figure 17. Model comparison range independent deep water environment, winter sound speed profile. The wide half channel makes for excellent acoustic propagation conditions. (UKHO, 1997 and WADER, OAD Ltd).

Profile Analysis				
Layer Depth 30m			Cut-off Freq 1072Hz	
Sound Channels				
Axis	Top	Base	Strength	Cut-off Freq
100m	40m	900m	Strong	191Hz
1500m	900m	1864m	Moderate	13Hz

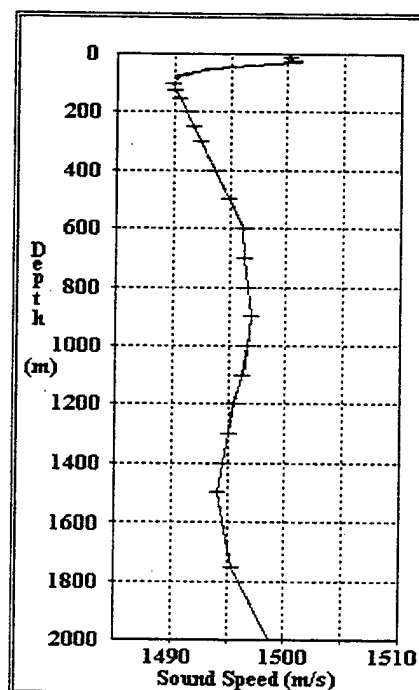


Figure 18. Model comparison range independent deep water environment, summer sound speed profile. Summer insolation has resulted in the formation of a shallow sound channel, which is sufficiently strong to trap both 400 Hz and 800 Hz. (UKHO, 1997 and WADER, OAD Ltd).

Profile Analysis		
Layer Depth	200m	Half Channel
Cut-off Freq	62Hz	

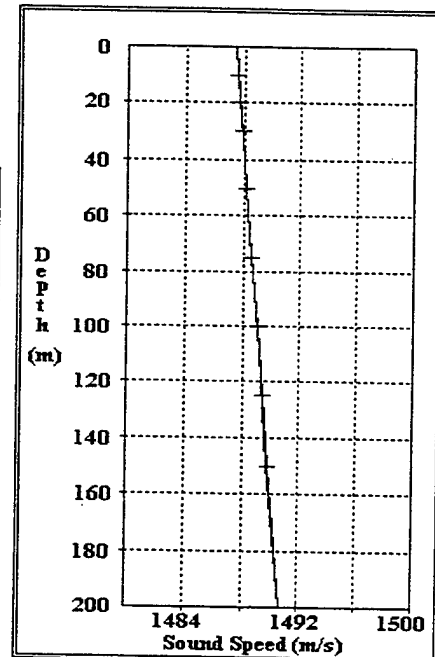


Figure 19. Model comparison range independent shallow water environment, winter sound speed profile. The positive sound speed gradient to the seabed provides excellent acoustic propagation conditions. (UKHO, 1997 and WADER, OAD Ltd).

Profile Analysis				
Layer Depth 30m		Cut-off Freq 1072Hz		
Sound Channels				
Axis	Top	Base	Strength	Cut-off Freq
100m	71m	200m	Weak	548Hz

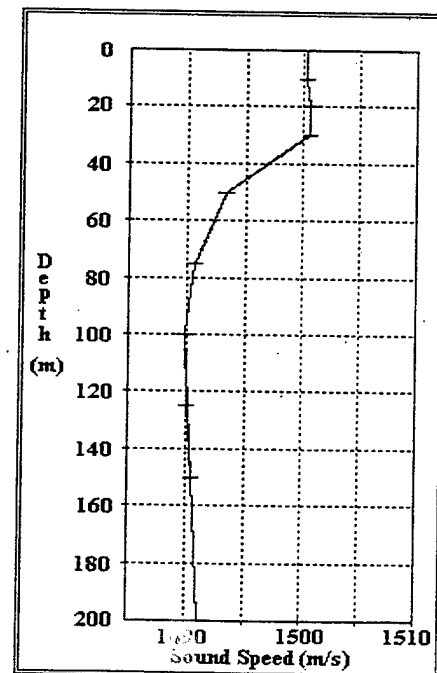


Figure 20. Model comparison range independent shallow water environment, summer sound speed profile. Despite the sound channel being weak it is sufficient to trap 800 Hz, however the profile is inherently downward refracting and will result in a high incidence of seabed interaction. (UKHO, 1997 and WADER, OAD Ltd).

the HODGSON model and to calculate equivalent input parameters for RAM. The parameters suggested by Bourke (Pers. Comm.) are selected in order to fit Hamilton and Bachman's (1982) sediment data. The geoacoustic input parameters for HODGSON and RAM are shown in Tables 7 and 8, respectively.

The BLUG-derived bottom loss curves associated with fine sand and silty clay seabed, as calculated by the HODGSON model, are shown in Figures 21 and 22, respectively.

BLUG Parameters	Sand	Silty clay
Speed Ratio	1.152	0.991
Density Ratio	1.962	1.356
Curvature Factor	0.86	-0.5
Sediment Gradient	1.7	1.3
Sediment Thickness (m)	500	500
Sediment Attenuation (dB/m/KHz)	0.314	0.0146
Base Loss (dB/bounce)	6.021	6.021

Table 7. Geoacoustic input parameters for the HODGSON propagation loss model.

Sediment Parameters	Depth (m)	Sand		Silty Clay	
		Deep	Shallow	Deep	Shallow
Sound Speed (m/s)	0	1726.4	1717.5	1485.1	1477.3
	500	2486.4	2477.0	1974.1	1965.8
	502	3140	3140	3140	3140
Density Ratio	0	1.962	1.962	1.356	1.356
	500	1.962	1.962	1.899	1.899
	502	2.25	2.25	2.25	2.25
Attenuation (dB/λ)	0	0.468	0.468	0.022	0.022
	500	0.617	0.617	0.025	0.025
	502	20	20	20	20

Table 8. Geoacoustic input parameters for RAM.

c. Source and Receiver Dispositions

Both the HODGSON model and RAM calculate PL from a point source at a defined depth to a specified receiver depth that is constant with range. The source and receiver dispositions for PL curve generation are shown in Table 9.

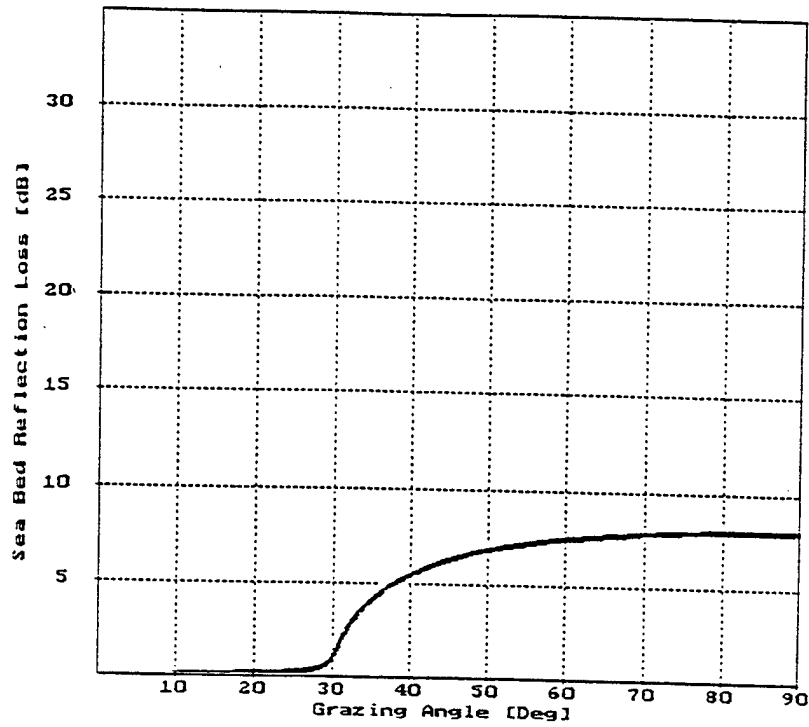


Figure 21. Seabed loss (dB/reflection) for a fine sand sediment from BLUG algorithms. (generated using the HODGSON propagation loss model).

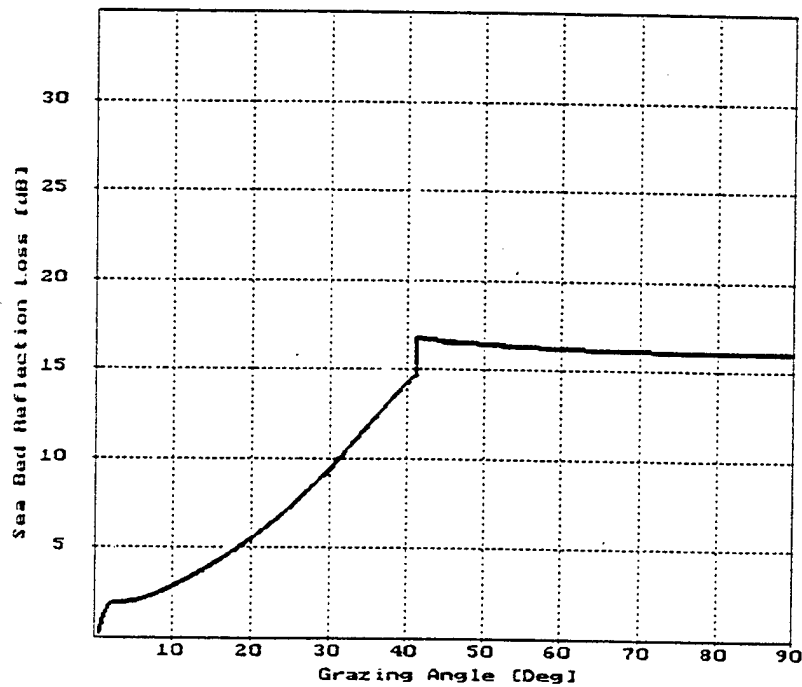


Figure 22. Seabed loss (dB/reflection) for a silty clay sediment from BLUG algorithms. (generated using the HODGSON propagation loss model).

Environment Depth	Winter		Summer	
	Source Depth (m)	Receiver Depth (m)	Source Depth (m)	Receiver Depth (m)
Shallow (200 m)	40	100	40	40
			40	100
Deep (2000 m)	40	125	40	40
			125	100

Table 9. Source and receiver depths for the range independent environments.

In winter, the disposition of the source and receiver are expected to have little impact on the propagation loss whether in shallow or deep water. In summer, the strongly downward refracting thermocline is an aid to evasion for the submariner. The effect of variation in receiver depth is expected to cause considerable variation in PL between source and receiver.

d. Propagation Loss Results

Propagation loss (PL) computed from the RAM and the HODGSON models are compared directly by qualitative analysis. The main concerns are propagation loss magnitude and phase variations. The RAM output is more akin to the real world in that it exhibits large fluctuations in PL magnitude, certainly more than that of a ray model. The underlying reason for these large fluctuations is that RAM, in applying wave theory, coherently sums acoustic energy. To achieve this the range and depth resolution must be high, hence, transmission loss can vary markedly over relatively short distances. In this comparison phase a good correlation between the models is when the HODGSON PL curve is within 5-7 dB of what can be considered the mean of the RAM PL curve. In order for a qualitative assessment to be made more easily the RAM PL curve has been averaged with range by application of a running mean function. This reduces the amplitude of fluctuation and also affects slight phase changes; the phase changes throughout are considered insignificant.

(1) Deep Water. In winter the SSP has a deep half channel which traps all frequencies above ~ 7 Hz. Strong upward refraction reduces seabed interaction and the sediment type can be expected to play little part on the transmission

loss when source and receiver are within the surface layer. As half channel propagation dominates the path of the acoustic energy the skip effect should be clearly evident in the PL curve from both models. Such is the case, shown in Figure 23. As a consequence of the differing model treatments of phase, the skip distance calculated by each model is not the same. HODGSON has an approximate skip distance of 10 km whilst RAM is approximately 11 km. Note, the skip effect becomes less noticeable in the RAM PL curve; this is a function of separation of propagation modes with range. The PL magnitude and phase correlation between HODGSON and RAM is good. The HODGSON PL curve appears optimistic compared to RAM, more so at 800 Hz than 400 Hz with a mean propagation loss 4-5 dB less than RAM. This is considered operationally acceptable as the HODGSON PL curve is within the bounds of the RAM fluctuations, which have been suppressed by application of a running mean.

In summer with the sound source in the shallow negative thermocline, the dominant refractive path is towards the seabed. There is no potential for convergence zone propagation. With both a sand and mud sediment type HODGSON and RAM correlate well. However, as expected, there is no evidence of modal propagation in the HODGSON PL curve although it is clearly evident in the RAM transmission loss curve, Figure 24. This may have operational significance as a receiver can fade in and out of the low loss regions at considerable range, such an event could not be anticipated from the HODGSON PL curve. On comparing the propagation loss at 400 Hz and 800 Hz it is evident that as frequency increases the incidence of transmission loss fluctuation increases (Figure 24). The operational significance of the fluctuation is an increase in target fading occurrence, however, the duration of the contact time is reduced, as is the duration of the no contact time. This result suggests that in certain environmental conditions coherent summation must be applied at low frequencies in order to achieve realistic initial detection range predictions.

The transmission loss curves in Figure 24(b), 800 Hz with a mud seabed type, show considerable difference between HODGSON and RAM at a range of 65-80 km. It is believed this is due to poor treatment by the BLUG algorithms of acoustic energy that refracts through the sediment from shallow grazing angles.

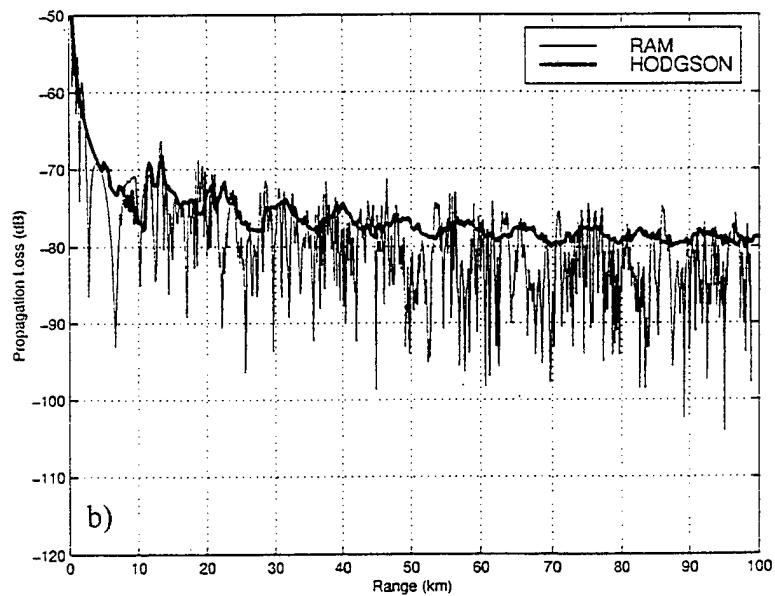
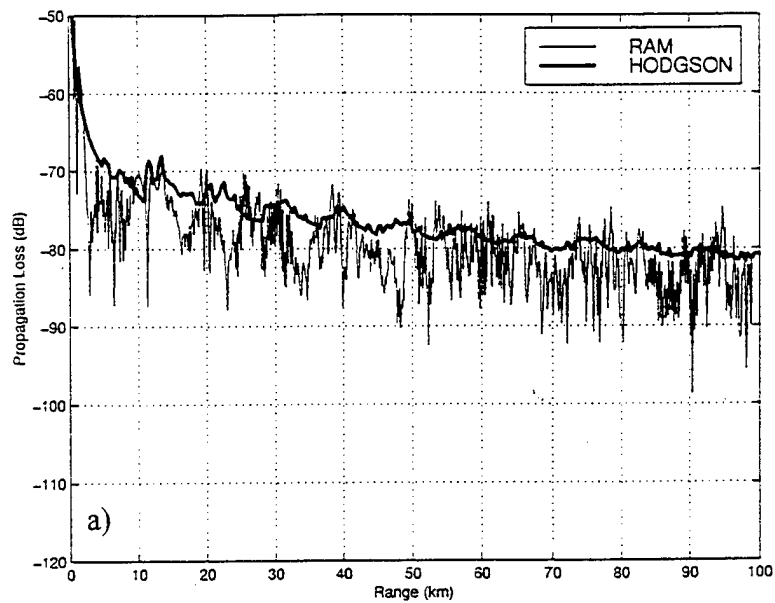


Figure 23. Comparison of propagation loss curves generated using RAM (thin line) and HODGSON (thick line) for a range independent deep water (2000 m) winter environment. a) 400 Hz, source depth 40 m, receiver depth 100 m, sand sediment. b) 800 Hz, source depth 40 m, receiver depth 100 m, mud sediment.

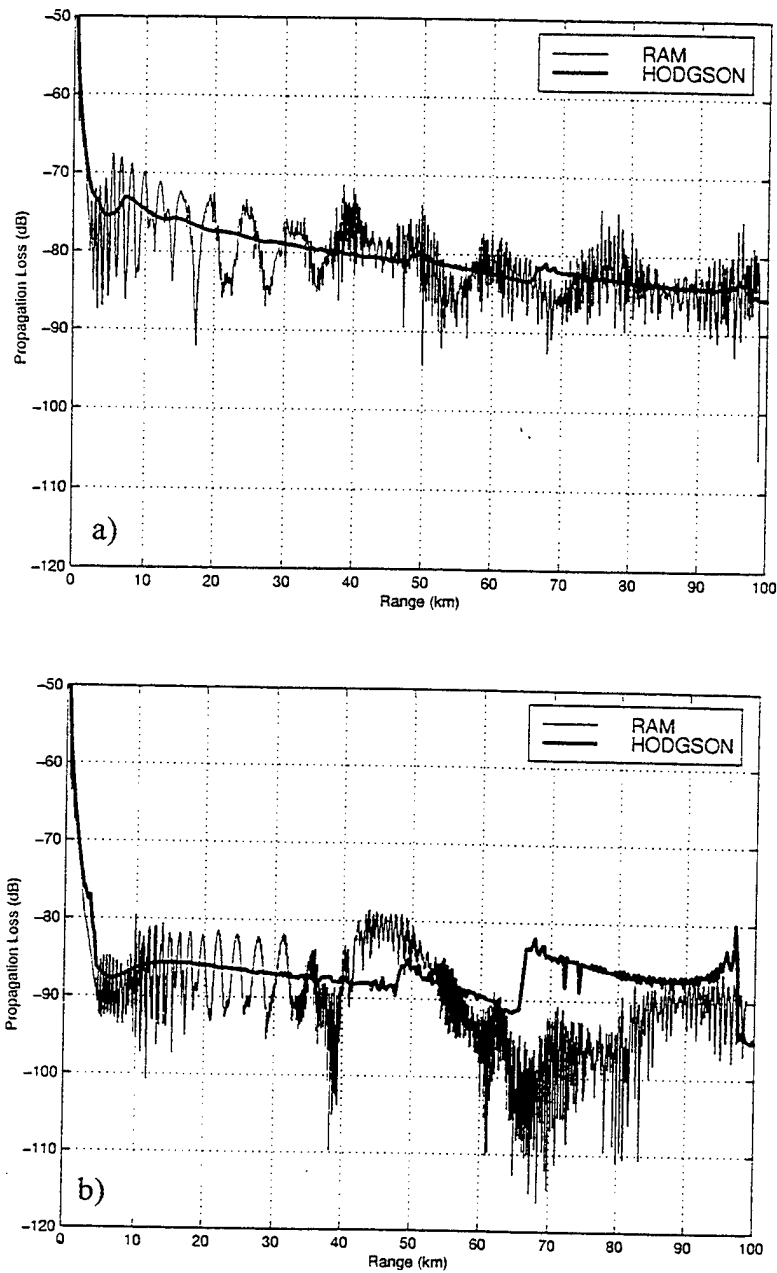


Figure 24. Comparison of propagation loss curves generated using RAM (thin line) and HODGSON (thick line) for a range independent deep water (2000 m) summer environment. a) 400 Hz, source and receiver depth 40 m, sand sediment. b) 800 Hz, source and receiver depth 40 m, mud sediment.

When the source and receiver are located at depths such that both are within the shallow sound channel (Figure 25), the similarity between the model outputs is good. As with a deep half channel, the effect of seabed interaction can be expected to be relatively insignificant compared to the acoustic energy trapped within the channel. The cut-off frequency of the sound channel is ~ 191 Hz, hence the frequencies of interest, 400 Hz and 800 Hz, are trapped within the channel.

(2) Shallow Water. In winter, the SSP is upward refracting hence seabed interaction may be considered to be a minimum. However, unlike the deep water environment, it is significant. As described for the deep water winter environment, the PL curve from HODGSON appears optimistic, however, the correlation with the RAM output is good. The propagation loss curves for shallow water in winter are shown in Figure 26.

In summer the sound speed profile is downward refracting making for a large incidence of seabed interaction. With both a highly reflective sand sediment and highly absorptive and refractive mud sediment the PL curve magnitude and phase correlation between RAM and HODGSON is good; indeed, the similarity is striking to a range of ~ 50 km. At ranges in excess of 50 km with a mud sediment type the PL curves diverge (Figure 27.a)). Once more, this is a result of the inability of the BLUG algorithms to adequately account for acoustic energy from shallow grazing angles that has refracted through the sediment. The BLUG algorithm incoherently sums the acoustic energy from the refractive path to the energy from the reflected path (Hodgson and Hodgson, Pers. Comm.). In addition, there is likely to be diffractive leakage into the sound channel as a result of normal mode propagation. These variations in PL occur when transmission loss is in excess of 100 dB and is thus of little operational significance.

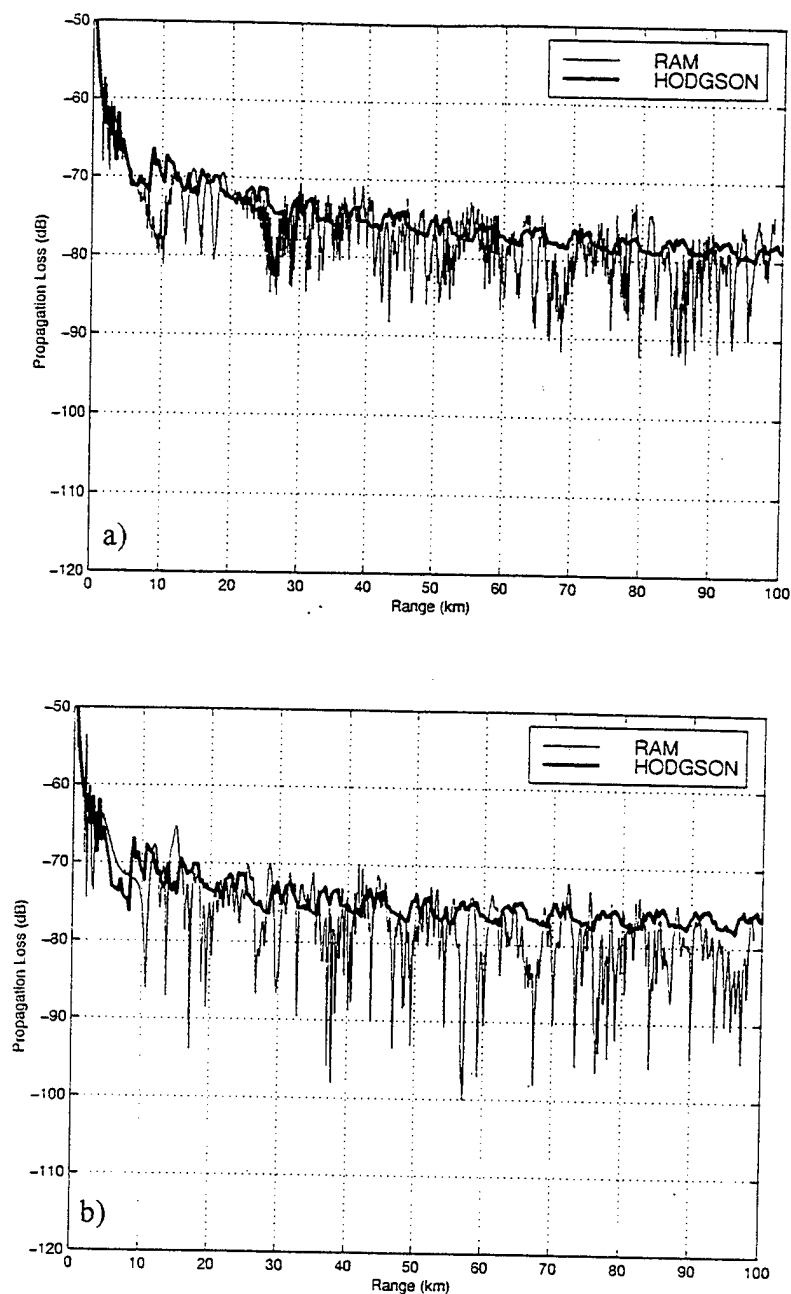


Figure 25. Comparison of propagation loss curves generated using RAM (thin line) and HODGSON (thick line) for a range independent deep water (2000 m) summer environment. a) 400 Hz, source depth 125 m, receiver depth 100 m (both in the shallow sound channel), sand sediment. b) 800 Hz, source depth 125 m, receiver depth 100 m, mud sediment.

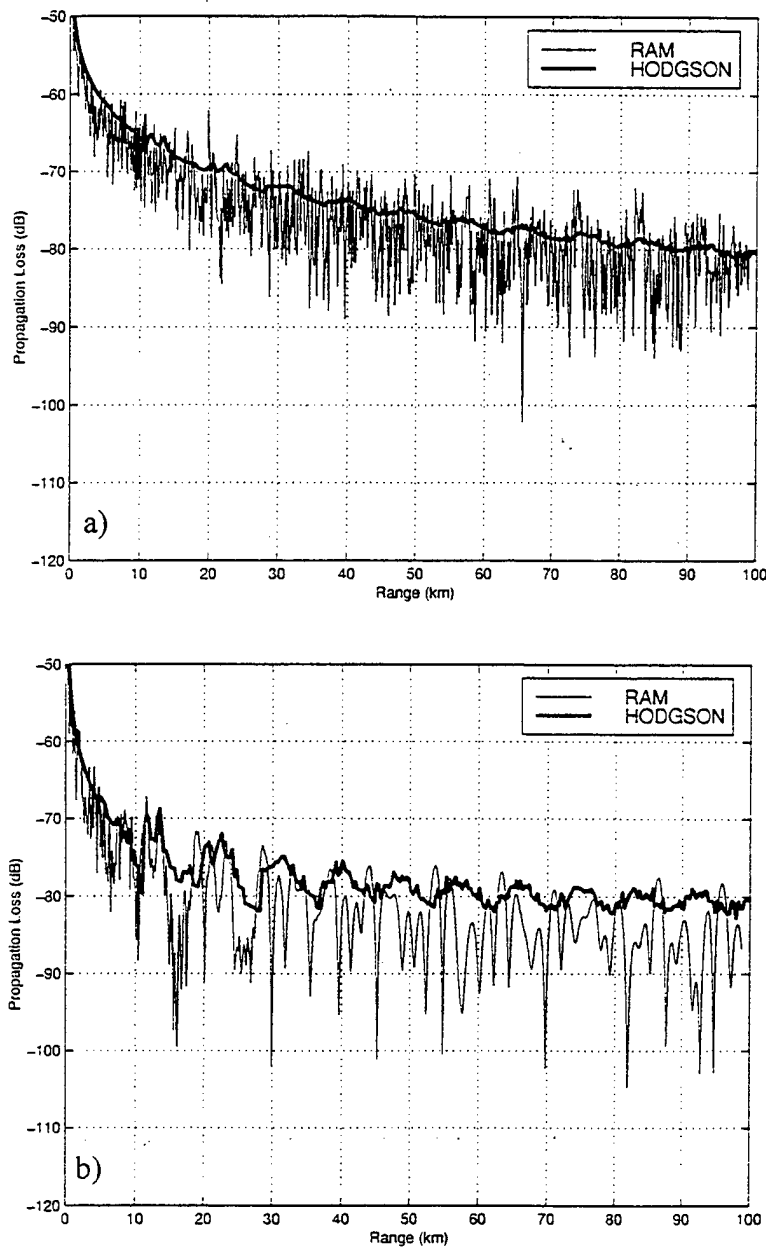


Figure 26. Comparison of propagation loss curves generated using RAM (thin line) and HODGSON (thick line) for a range independent shallow water (2000 m) winter environment. a) 400 Hz, source depth 40 m, receiver depth 100 m, sand sediment. b) 800 Hz, source depth 40 m, receiver depth 100 m, mud sediment.

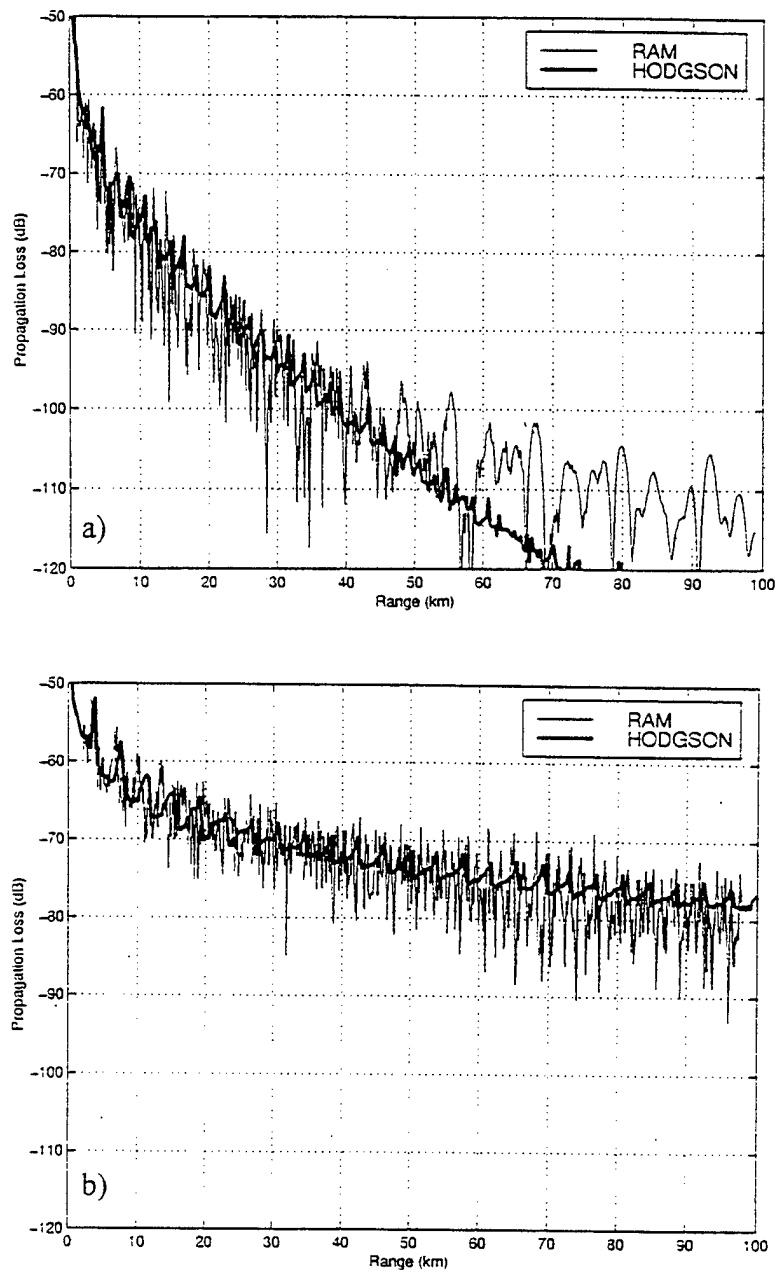


Figure 27. Comparison of propagation loss curves generated using RAM (thin line) and HODGSON (thick line) for a range independent shallow water (200 m) summer environment. a) 400 Hz, source depth 40 m, receiver depth 100 m, mud sediment. b) 800 Hz, source and receiver depth 40 m, sand sediment.

3. Range Dependent, Cross Frontal Propagation

A logical test of any range dependent acoustic propagation loss model is its ability to deal with complex range dependency. Some of the most complex range dependent environments are through frontal zones; not only is the sound speed profile variable but many fronts are coupled to topographic features. The South East Icelandic Front (SEIF) is in this category; the front lies along the Iceland-Faeroes Rise and is prograde to the north. The SEIF is of significant operational interest to the LFAS performance assessment phase of this research and will, therefore, be considered in this phase of the acoustic model comparison.

RAM and HODGSON are run in a range dependent environment comprising the frontal section through the South East Icelandic Front (SEIF) in winter and summer, transects A and B in Figure 16.

a. Sound Speed Profiles

Sound speed contour plots for the frontal section in winter and summer are shown in Figures 28 and 29, respectively. SSP's each side of the SEIF in winter and summer are shown in Figures 30 and 31, respectively.

In winter, the SSP's at both ends of the transect have a relatively deep surface layer at ~100 m, this layer shoals to ~80 m in the frontal zone. Below the surface layer, the SSP along the track is inherently downward refracting and occasions strong interaction of the acoustic energy with the Iceland-Faeroes Rise. This is likely to result in high transmission loss. It should be noted, there is the possibility of convergence zone propagation in the deeper water away from the main frontal zone in water depths greater than ~1000 m. The change in sound speed across the frontal zone is of the order 15-20 m/s and occurs over a range of approximately 60 km.

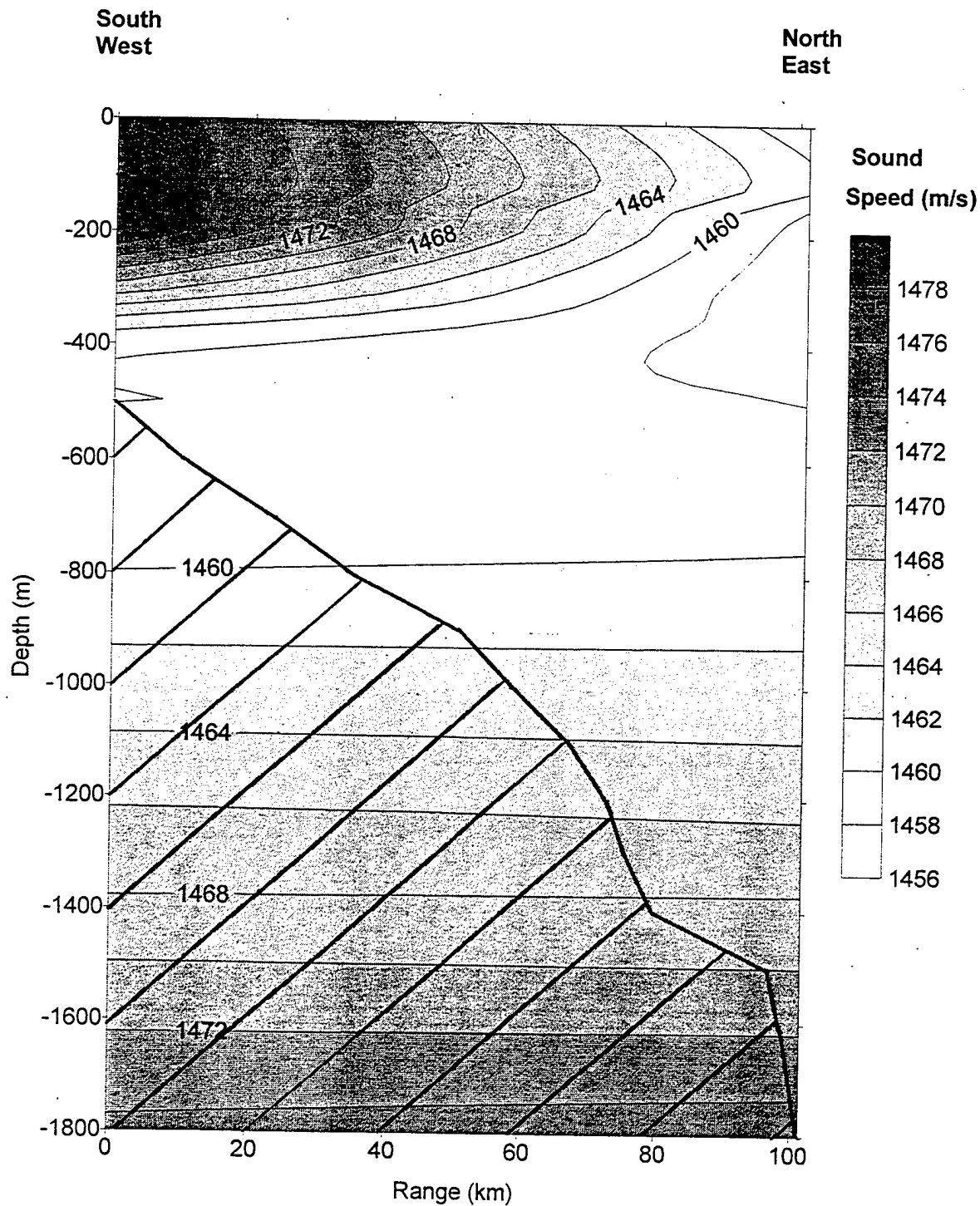


Figure 28. Sound speed contour plot from southwest to northeast through the South East Icelandic Front in winter. Below the surface layer, the negative sound speed gradient weakens towards the northeast. (adapted from UKHO GPPDB and UKHO, 1997).

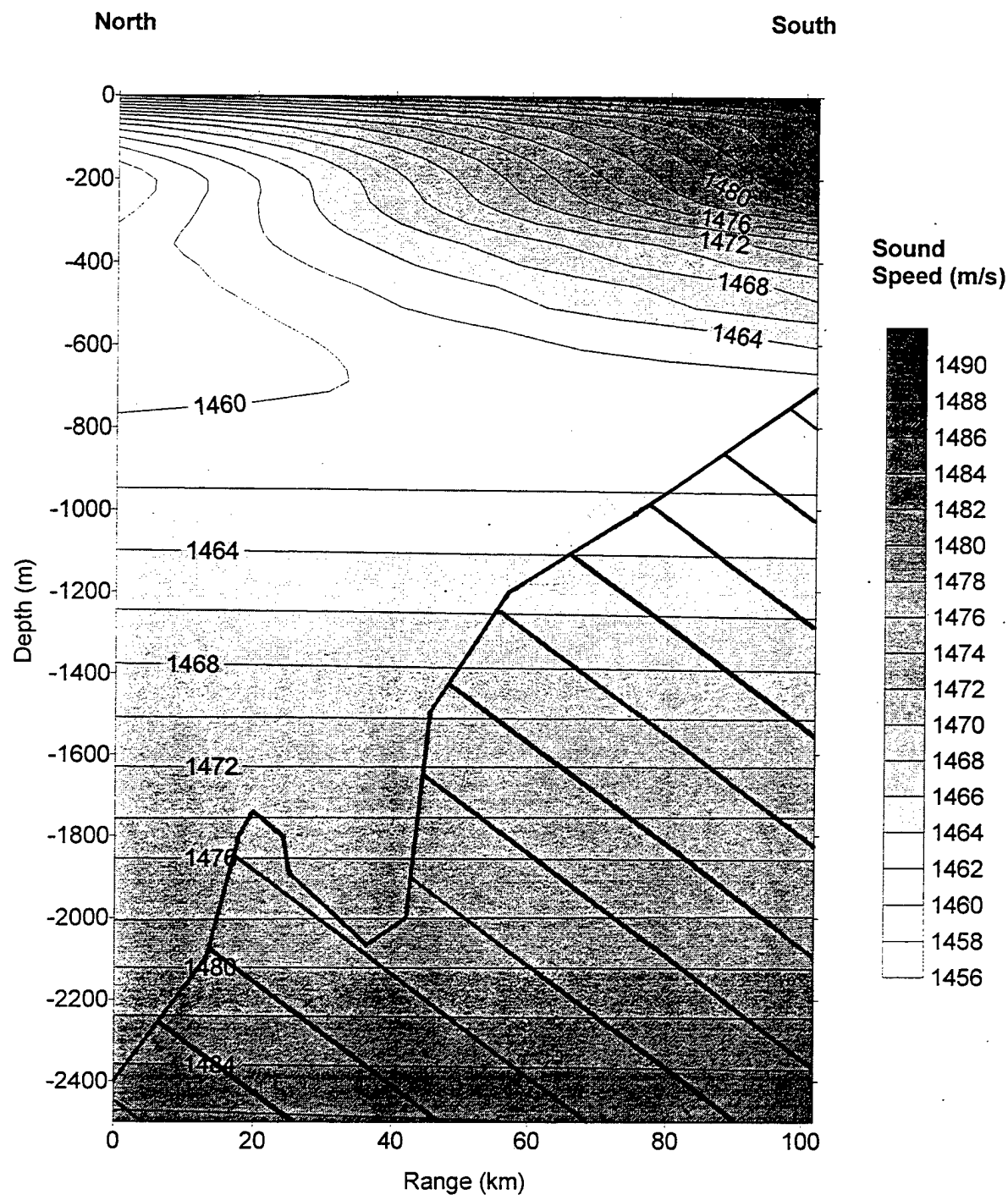
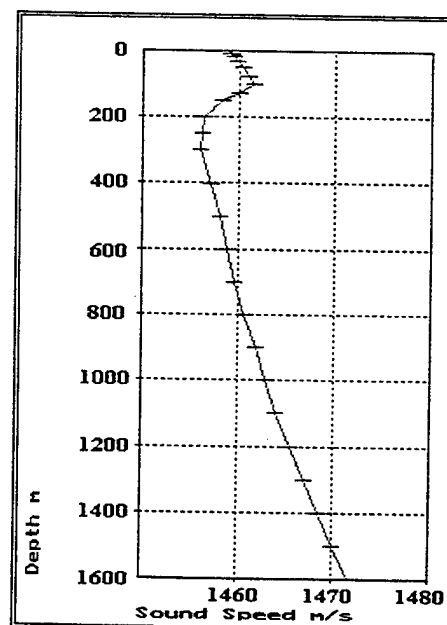


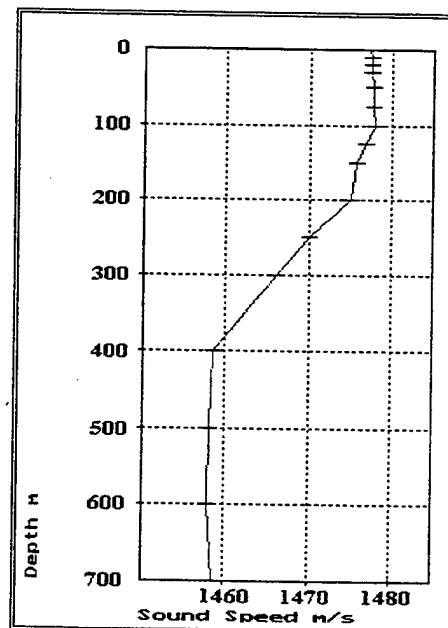
Figure 29. Sound speed contour plot from north to south through the South East Icelandic Front in summer. The near surface, negative sound speed gradient weakens to the south, however, it extends to the seabed in the shallow water. A shallow sound channel in the colder water to the north weakens and disappears in the frontal zone. (adapted from UKHO GPPDB and UKHO, 1997).

Profile Analysis to Depth 1600m				
Layer Depth 100m		Cut-off freq 176Hz		
Sound Channels				
Axis	Top	Base	Strength	Cut-off freq
300m	100m	878m	Strong	6Hz
Depth Excess 722m CZ Potential is GOOD				



a) Northeastern SSP.

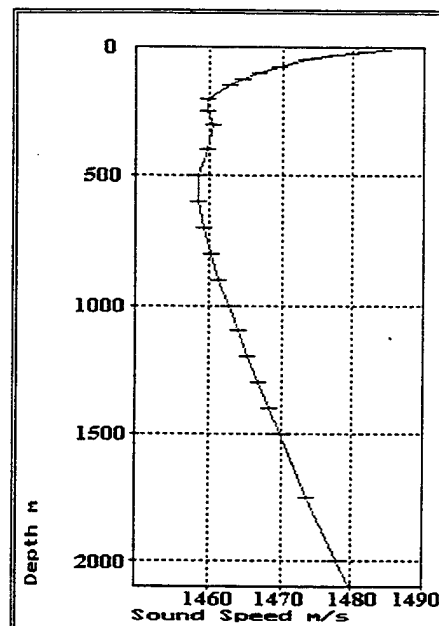
Profile Analysis to Depth 700m				
Layer Depth 100m		Cut-off freq 176Hz		
Sound Channels				
Axis	Top	Base	Strength	Cut-off freq
600m	399m	700m	Weak	30Hz
Zero Depth Excess No CZ possible				



b) Southwestern SSP.

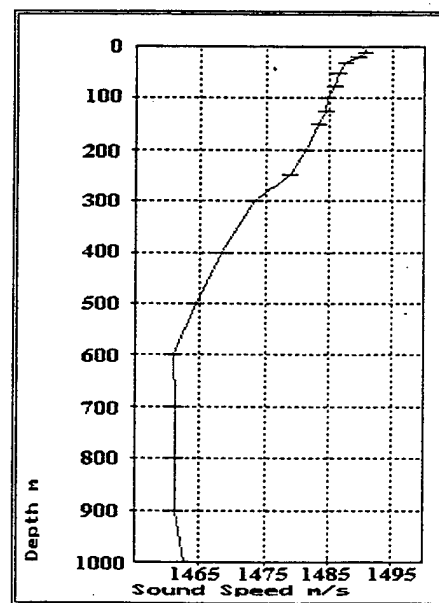
Figure 30. SSP's from a) the northeastern end and b) the southwestern end of the South East Icelandic Front cross-section in winter. Both SSP's have a mixed layer depth of 100 m with a strong negative thermocline below. The deeper water SSP in the northeast provides the possibility for convergence zone propagation in water depths greater than ~1000 m. (Adapted from GPPDB, UKHO, 1997).

Profile Analysis to Depth 2100m				
Layer Depth 10m			Cut-off freq 5572Hz	
Sound Channels				
Axis	Top	Base	Strength	Cut-off freq
250m	188m	300m	Weak	176Hz
600m	300m	815m	Moderate	27Hz
Zero Depth Excess No CZ possible				



a) Northern SSP.

Profile Analysis to Depth 1000m				
Layer Depth 10m			Cut-off freq 5572Hz	
Sound Channels				
Axis	Top	Base	Strength	Cut-off freq
600m	555m	1000m	Weak	281Hz
Zero Depth Excess No CZ possible				



b) Southern SSP.

Figure 31. SSP's from a) the northern end and b) the southern end of the South East Icelandic Front cross-section in summer. The SSP's are strongly downward refracting as a consequence of strong near surface heating during the summer months. (Adapted from GPPDB, UKHO, 1997).

In summer, strong insolation results in the development of a distinctive shallow thermocline and the surface manifestation of the front weakens compared to that of winter. The sound speed gradient in the frontal zone is strongly negative; it has a thickness of ~700 m in the south (shallow water) whilst the gradient strengthens in the north as a shallow sound channel develops. For a shallow noise source, interaction of acoustic energy with the seabed is the dominant mode of propagation. However, in the deeper water to the north with depths in excess of 2000 m and with the source deeper than 40 m there is potential for convergence zone-like propagation.

b. Geoacoustic Parameters

For initial model runs the geoacoustic parameters are range independent; this allows the propagation algorithms of the models to be compared. The parameters used are as shown in Section III.2.b. The major difference in the methodology for a range dependent run is that geoacoustic parameters are selected depending on the direction of propagation. When the propagation direction is from deep to shallow water the geoacoustic parameters used are for silty clay; conversely, from shallow to deep the parameters used are for fine sand. This is consistent with present operational acoustic modeling practices where range dependent geoacoustic parameters cannot be entered into most operational acoustic propagation models. In such an instance, the sediment expected in the vicinity of the source is used for modeling purposes.

c. Source and Receiver Dispositions

The source and receiver dispositions for propagation loss curve generation are shown in Table 10.

Propagation Direction (Sediment type)	Winter Front		Summer Front	
	Source Depth (m)	Receiver Depth (m)	Source Depth (m)	Receiver Depth (m)
Deep to Shallow (silty clay)	300	150	50	50
			250	40
Shallow to Deep (fine sand)	75	150	50	50

Table 10. Source and receiver depths for the range independent environments.

In winter, the source depth is near the sound channel axis whilst the receiver depth is in the negative thermocline for the deep water to shallow water propagation direction. The principal propagation path for any eigenrays is via seabed reflection. When the propagation direction is from shallow to deep, the source is within the surface layer and the receiver in the negative thermocline. These selections are made in order to compare the PL curves when there is considerable interaction of acoustic energy with an uneven seabed.

A similar principle is employed for the selection of the source and receiver dispositions in summer. When the source is at 50 m, it is in the main thermocline; when at 250 m it is 20 m below the sound channel axis as present in the SSP at zero range. The receiver remains in the thermocline throughout.

d. Propagation Loss Results

In essence, this phase of the comparison is a test of the propagation paths calculated by the acoustic models and the ability to model the effects of changing bathymetry on acoustic energy. Variation between the model's output is expected as a result of the different methods applied to deal with range dependent SSP's. It is reiterated that the HODGSON model applies a smoothing algorithm from one SSP to the next, whilst RAM applies the change in SSP as a step function. In consequence, when considering propagation loss across a frontal zone that is inherently downward refracting, such as the SEIF, it is anticipated that PL calculated by the HODGSON model will be slightly greater than that calculated by RAM. This is due to the increased downward refraction in the frontal zone being applied by HODGSON earlier in the propagation path, hence, seabed interaction is likely to occur earlier in range resulting in higher acoustic attenuation.

(1) South East Icelandic Front (SEIF), Winter (Track A, Figure 16). The upslope propagation path through the frontal zone is considered first. The bottom type is mud; a likely choice by an operational acoustic modeler as a mud sediment type is generally associated with deep water. Depicted in Figure 32(a), the HODGSON model and RAM PL curves compare well in both amplitude and phase. Bottom bounce (BB) propagation paths at 35-40 km and 50-55 km have been characterised well by HODGSON. The region of reduced propagation loss at 25-30 km is

associated with sound channel propagation. From approximately 60 km onwards the PL curves diverge. This is believed to be a function of increased seabed interaction and the poor ability of BLUG to deal with sound that has refracted through the sediment. Note, the transmission loss calculated by HODGSON is generally greater than that calculated by RAM, as anticipated.

With downslope propagation and a sand sediment type, i.e., a highly reflective seabed, the similarity between the HODGSON and RAM PL curves is striking (Figure 32(b)). The HODGSON model PL curve also shows evidence of downslope enhancement at ~80 km.

(2) South East Icelandic Front, Summer (Track B, Figure 16). As a consequence of surface insolation, the dominant refractive path through the front is downwards. Seabed interaction is high and attenuation of acoustic energy is likely to be high, particularly if the sediment type is mud.

Considering upslope propagation with a mud sediment type, the correlation between the HODGSON transmission loss curves and RAM PL curves is reasonable (Figure 33(a)). In the first 55 km the correlation is good, however, there are some variations. The raytrace images in Figure 34 depict a convergence zone (CZ) propagation path. This is evident as reduced PL at 38 km in the HODGSON PL curve and at 30-34 km in the RAM curve. This range disparity can be attributed to the different methods of accounting for range dependent SSP's by the two models. As the RAM applies these alterations as a step function, as opposed to the smoothed SSP variation in HODGSON, the CZ range given by HODGSON is likely to be most representative of the propagation path. At a range of 40-41 km in the HODGSON transmission loss curve there is a large increase in loss over a relatively short range. This can be explained by considering the raytrace in Figure 34(b); this figure depicts only the top 200 m of the water column to a range of 50 km. Only refracted-refracted (RR) and refracted-surface reflected (RSR) paths have been selected for display. In this manner the convergence zone propagation is clearly illustrated. It is clearly evident that the propagation loss associated with the CZ path is likely to be low, whilst outside this region the loss is relatively high. Further observations of raytrace images indicate that there is almost no incidence of acoustic rays from refracted-bottom reflected (RBR) or surface reflected-

bottom reflected (SRBR) paths in the spatial field from 41-42 km. At ranges greater than 55 km the PL output compares relatively poorly. Figure 33(a) shows strong upslope enhancement in the RAM PL curve and zones of convergence at 55-60 km, 72-76 km and 85-90 km. The HODGSON representation of the same phenomenon is pessimistic, by approximately 5-10 dB, and the phase correlation is poor. The spatial difference in PL magnitude may be attributed to the coherent summation of RAM propagation loss output. The difference of ~5 km in the transmission loss peaks can be attributed to the stepped treatment of the range dependent SSP's by RAM.

When the propagation path is downslope with a sand seabed; the transmission loss correlation is good. This is in keeping with all previous results and is further evidence that the ray model, HODGSON, copes well with reflective sediment types.

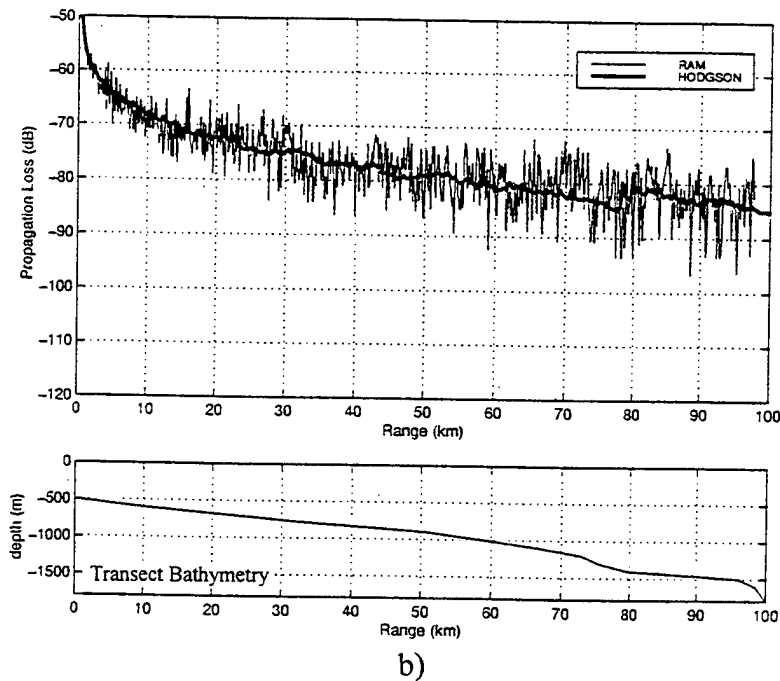
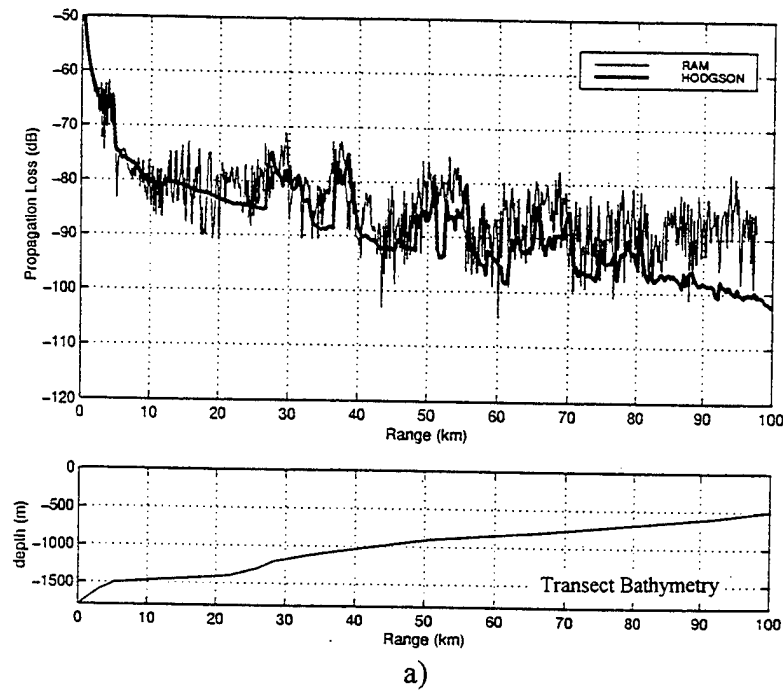


Figure 32. Comparison of propagation loss curves generated using RAM (thin line) and HODGSON (thick line) for the winter South East Icelandic Front transect. a) 400 Hz, source depth 300 m, receiver depth 150 m, range independent mud sediment. Propagation direction is from deep to shallow water as depicted in topography chart below the PL vs. Range plot. b) 800 Hz, source depth 75 m, receiver depth 150 m, range independent sand sediment. Propagation direction is from shallow to deep water.

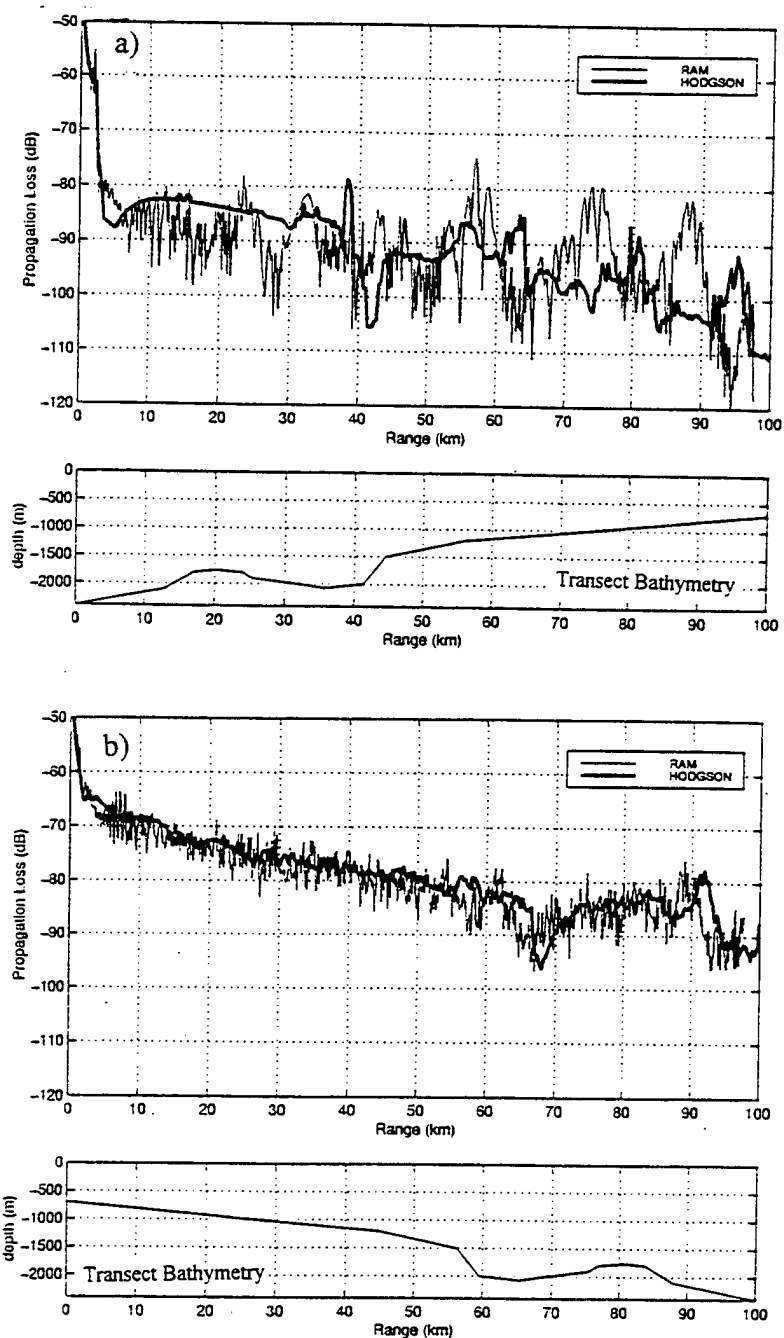
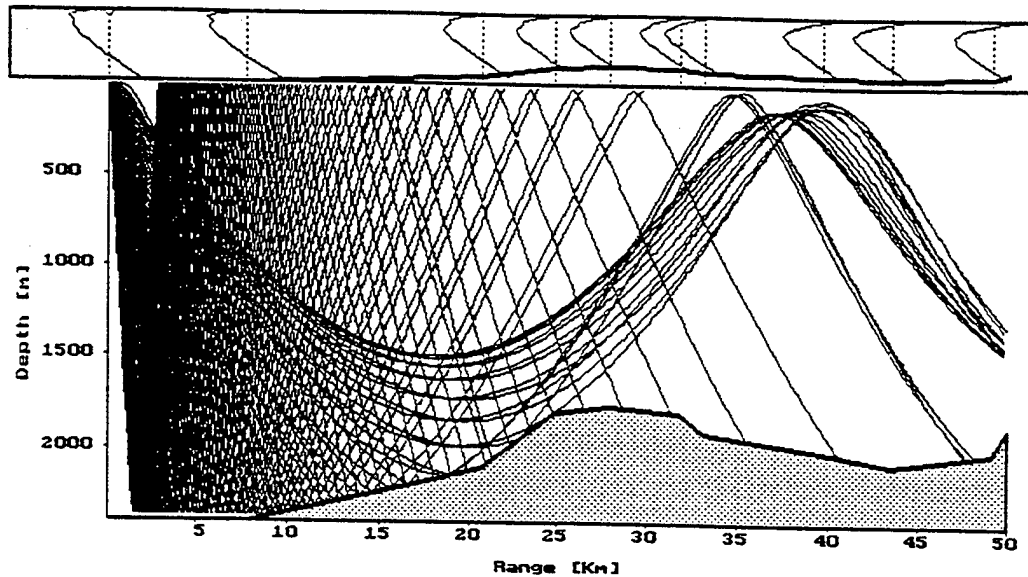
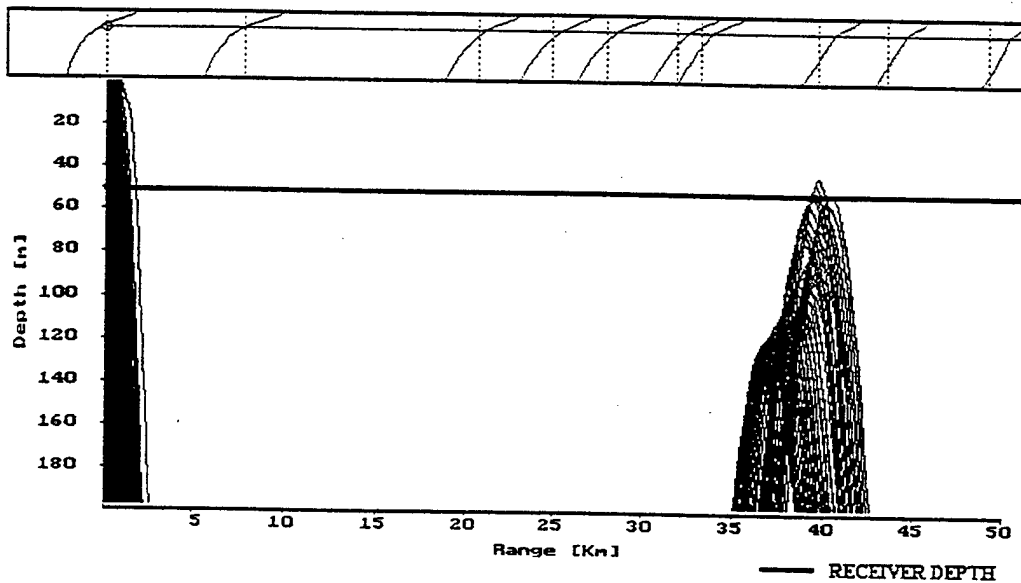


Figure 33. Comparison of propagation loss curves generated using RAM (thin line) and HODGSON (thick line) for the summer South East Icelandic Front transect. a) 400 Hz, source depth 250 m, receiver depth 40 m, range independent mud sediment. Propagation direction is from deep to shallow water as depicted in topography chart below the PL vs. Range plot. b) 800 Hz, source and receiver depth 50 m, range independent sand sediment. Propagation direction is from shallow to deep water.



a) Raytrace showing convergence zone propagation path.



b) Raytrace showing the top 200 m of the convergence zone path depicted in a).

Figure 34. Raytrace of propagation path through the first 50 km of the deep to shallow water, summer South East Icelandic Front environment. a) raytrace showing convergence zone path with source depth 50 m. b) raytrace of top 200 m of the convergence zone propagation path with the receiver depth of 50 m. The intersection of the receiver depth with the raytrace indicates that the propagation loss in this region is likely to be low whilst the area immediately either side will have a high propagation loss. (Adapted from the HODGSON model, OAD Ltd.)

4. Corrections to the HODGSON PL Model Output

The HODGSON model at present cannot account for changes in geoacoustic parameters with range. In shallow water changes in sediment composition and thickness can be marked and frequent. Thus, in a highly variable geoacoustic environment the HODGSON model will not provide accurate transmission loss estimates. In order to ensure realism in the LFAS performance assessment phase of this research the HODGSON model PL may require a correction to be applied when the sediment type is range dependent.

In the analysis that follows it is stipulated that the HODGSON model algorithms are not changed in any way. Corrections or adjustments are made as required only to the PL output of the model. The terms, 'correction', 'amendment' and 'adjustment' pertain only to actions upon the output of the HODGSON model, not the model algorithms.

The adjustments to be applied to the HODGSON PL curves are derived from comparison with RAM PL curves for a fully range-dependent environment. In this respect RAM fulfills the role of 'ground truth' or measured data, a necessity brought about by the lack of recorded exercise data containing complete acoustic and environmental information. As in previous model comparisons within this study, the sea surface loss is removed from the HODGSON model output and a correction for absorption loss is applied.

In this phase of the model comparison the methodology has changed from that described previously (Sections III.B.2 and III.B.3) to one directed towards LFAS operational assessment. As such, the HODGSON model input parameters apply a more realistic vertical beam width for the LFAS system. This makes direct comparison with HODGSON difficult because there is no control over the beam angle in RAM. This difficulty is negated somewhat because only the acoustic energy from shallow angles contribute to the acoustic energy at considerable range. The energy associated with higher beam angles is effectively stripped due to high attenuation from multiple seabed interactions. As the amendments to the HODGSON model transmission loss output is specifically for use in the operational assessment of LFAS, an adjustment is only applied if it is considered operationally significant. For example, if one-way transmission loss is greater than ~90 dB for both HODGSON and RAM, then no amendment to the PL output

is applied. The level of 90 dB is selected because the highest two-way figure of merit calculated in this area is 171 dB (this equates to 85.5 dB one-way loss). It should be noted that if passive intercept of active transmissions from the LFAS were to be considered, this constraint would not be applicable as typical FOM's are likely to exceed 100 dB.

a. Transect Environments

The method of SSP selection and creation of seabed bathymetry with range is described in previous sections within this chapter. Geoacoustic parameters for the LFAS assessment phase environments, tracks A-E, are derived from Hamilton and Bachman (1982), Bachman (1994) and Bourke (Pers. Comm.), as stated previously. In order to apply reasonably realistic parameters the sediment type and thickness for each environment is required. Generic values are available from unclassified publications, but the spatial resolution of such data is relatively coarse.

(1) Track A, SEIF in winter. The sound speed environment associated with this track is described in Section III.B.3. Attention is drawn to Figures 28 and 30 that depict the sound speed cross-section through the front and representative SSP's, respectively.

The sediment type along the entire length of the track is a sand, silt and clay mix (NAVO, 1986). The sediment thickness varies from ~200 m in the shallow bathymetry areas on top of the rise (southwestern end of the track) to ~1200 m in the deeper water of the continental slope (northeastern end of the track). The geoacoustic parameters associated with this sediment type are given in Table 11.

Sediment Type	Geoacoustic Parameter	Sediment Thickness (m)			
		Surface	200	500	1500
Sand-silt-clay mix	Velocity (m/s)	1523	1749	2018	2314
	Density (g/cm ³)	1.575	1.829	2.118	2.361
	Attenuation	dB/m/kHz	0.0146	0.025	0.02
		dB/λ	0.021	0.037	0.03

Table 11. Geoacoustic parameters along track A, frontal section in winter.
(Calculated from Hamilton and Bachman (1982) and Bachman (1994).

(2) Track B, SEIF in summer. The sound speed environment associated with this track is described in Section III.B.3. Attention is drawn to Figures 29 and 31 that depict the sound speed cross-section through the front and representative SSP's, respectively.

The sediment type along the track comprises of a sand, silt and clay mix in the shallow waters of the continental shelf and slope and of mud and ooze in the deeper waters (NAVO, 1986). The sediment thickness varies from ~200 m in the shallow bathymetry areas (southern end of the track) to ~1500 m in the deeper water (northern end of the track). The geoacoustic parameters for sand-silt-clay mix and for a mud-ooze mix are given in Tables 11 and 12, respectively.

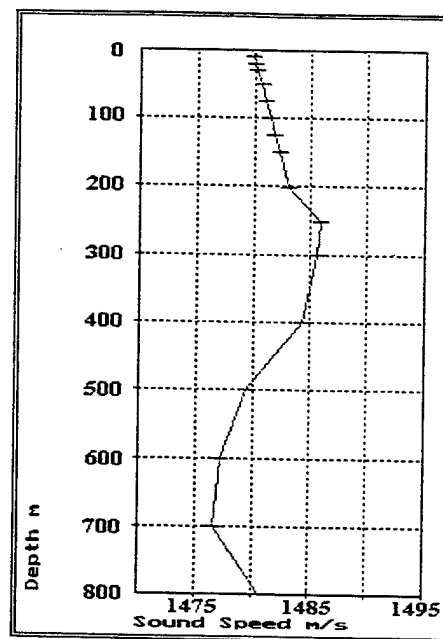
Sediment Type	Geoacoustic Parameter	Sediment Thickness (m)			
		Surface	200	500	1500
Mud-ooze mix	Velocity (m/s)	1467	1693	1962	1974
	Density (g/cm ³)	1.356	1.610	1.899	2.060
	Attenuation dB/m/kHz	0.0146	0.025	0.020	0.01
	dB/ λ	0.021	0.037	0.029	0.015

Table 12. Geoacoustic parameters along track B, frontal section in summer.
(Calculated from Hamilton and Bachman (1982) and Bachman (1994).

(3) Track C, upslope/downslope enhancement environment. Typical SSP's for this track in winter and summer are shown in Figure 35. In winter, a relatively deep surface layer to 250 m with a cut-off frequency of 45 Hz leads to good acoustic propagation conditions at the frequency of interest. In summer, surface insolation causes the development of a relatively weak shallow sound channel that is likely to be avoided by a submariner. The sound speed gradient is generally negative; downward refraction dominates the propagation paths and the attenuation of acoustic energy is likely to be high.

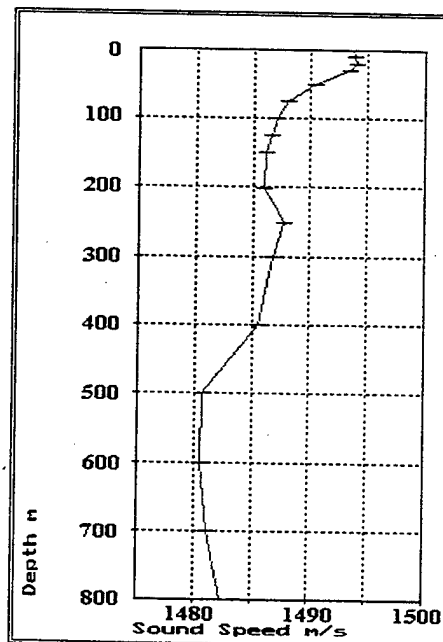
The bathymetry along the transect is a gradual slope from 200 m to 1300 m over a range of 100 km. The sediment type along the entire length of the track is sand (Nekritz, 1975). The sediment thickness varies from ~50 m to ~500 m from shallow water to deep water (NAVO, 1986).

Profile Analysis to Depth 800m				
Layer Depth 250m			Cut-off freq 45Hz	
Sound Channels				
Axis	Top	Base	Strength	Cut-off freq
700m	472m	800m	Strong	25Hz
Zero Depth Excess No CZ possible				



a) SSP in winter.

Profile Analysis to Depth 800m				
Layer Depth 20m			Cut-off freq 1970Hz	
Sound Channels				
Axis	Top	Base	Strength	Cut-off freq
200m	84m	250m	Weak	72Hz
600m	464m	800m	Weak	55Hz
Zero Depth Excess No CZ possible				



b) SSP in summer.

Figure 35. Sound speed profiles for track C, upslope/downslope environment in a) winter and b) summer. The deep surface layer in winter results in upward refraction trapping all frequencies above ~45 Hz, hence the acoustic propagation conditions are good. Strong insolation in the summer months results in a negative thermocline near the surface and the development of a weak shallow sound channel; the acoustic conditions are relatively poor. (Adapted from GPPDB, UKHO, 1997).

The geoacoustic parameters associated with this sediment type are given in Table 13.

Sediment Type	Geoacoustic Parameter	Sediment Thickness (m)			
		Surface	50	200	500
Sand	Velocity (m/s)	1693	1878	1917	1944
	Density (g/cm ³)	1.962	1.962	1.962	1.962
	Attenuation	dB/m/kHz	0.314	0.164	0.130
		dB/ λ	0.417	0.245	0.195

Table 13. Geoacoustic parameters along track C, upslope/downslope enhancement environment. (Calculated from Hamilton and Bachman (1982) and Bachman (1994)).

(4) Track D, Faeroes-Shetland Channel Environment. Typical SSP's for this track in winter and summer are shown in Figure 36. The winter SSP is characterised by a surface layer to ~200 m, thus acoustic propagation conditions are likely to be good. In summer, the SSP has a negative sound speed gradient from near the surface to ~600 m. The dominant propagation path is towards the seabed resulting in high attenuation of acoustic energy.

The bathymetry along the track is across the continental rise from deep to shallow water. Sediment types vary from a sand-silt-clay mix in deep water near the channel centre to gravel at the top of the continental rise (NAVO, 1986). The sand-silt-clay mix sediment thickness is near 2000 m in the centre of the channel reducing to 1000 m on the continental slope. The gravel sediment type in shallow water (southeastern end of the transect) is ~50 m thick or less (NAVO, 1986 and Nekritz, 1975). The geoacoustic parameters associated with these sediment types are given in Table 14(a) and (b).

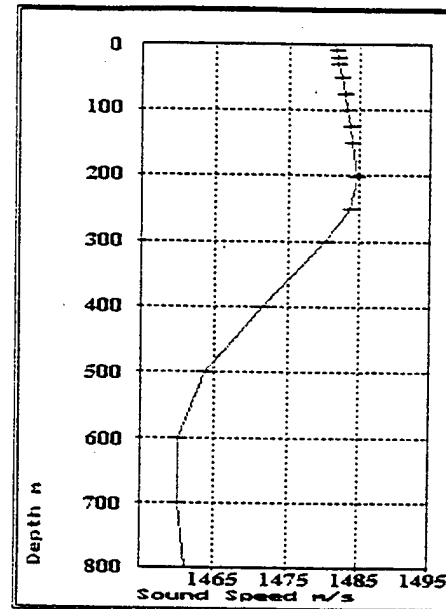
Sediment Type	Geoacoustic Parameter	Sediment Thickness (m)				
		Surface	200	500	1000	2000
Sand-silt-clay mix	Velocity (m/s)	1523	1749	2018	2277	2085
	Density (g/cm ³)	1.575	1.829	2.118	2.353	1.897
	Attenuation	dB/m/kHz	0.0146	0.025	0.02	0.01
		dB/ λ	0.021	0.037	0.03	0.015

Table 14.a) Sand-silt-clay mix geoacoustic parameters along track D, Faeroes-Shetland Channel environment. (Calculated from Hamilton and Bachman (1982) and Bachman (1994)).

Sediment Type	Geoacoustic Parameter	Sediment Thickness (m)			
		Surface	10	25	50
Gravel	Velocity (m/s)	1777	1924	1950	1958
	Density (g/cm ³)	2.228	2.228	2.228	2.228
	Attenuation				
	dB/m/kHz	0.254	0.173	0.148	0.132
	dB/ λ	0.373	0.254	0.218	0.194

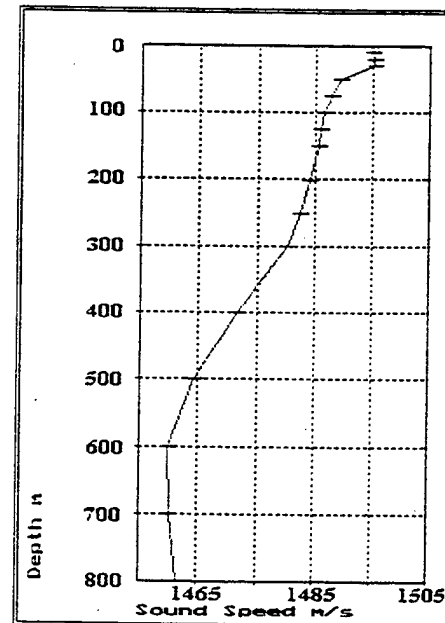
Table 14.b) Gravel geoacoustic parameters along track D, Faeroes-Shetland Channel environment. (Calculated from Hamilton and Bachman (1982) and Bachman (1994)).

Profile Analysis to Depth 800m				
Layer Depth 200m			Cut-off freq 62Hz	
Sound Channels				
Axis	Top	Base	Strength	Cut-off freq
600m	573m	800m	Weak	611Hz
Zero Depth Excess No CZ possible				



a) SSP in winter.

Profile Analysis to Depth 800m				
Layer Depth 30m		Cut-off freq 1072Hz		
Sound Channels				
Axis	Top	Base	Strength	Cut-off freq
600m	564m	800m	Weak	402Hz
Zero Depth Excess No CZ possible				



b) SSP in summer.

Figure 36. Sound speed profiles for track D, Faeroes-Shetland Channel environment in a) winter and b) summer. Strong vertical mixing in winter results in good acoustic propagation conditions associated with the relatively deep surface layer to ~ 200 m; cut-off frequency ~62 Hz. In summer, insolation generates a strong negative sound speed gradient from near the surface to 600 m, the acoustic propagation conditions are poor. (Adapted from GPPDB, UKHO, 1997).

(5) Track E, Anton Dohrn Seamount environment. Typical SSP's for this track in winter and summer are shown in Figure 37. A very deep mixed layer to ~900 m is a characteristic of the northern Rockall Trough region. As a result, acoustic propagation conditions are excellent. With the majority of the acoustic energy remaining in the surface layer, due to upward refraction, the effect of seabed interactions are minimal. In summer the development of a strong negative thermocline near the surface, coupled with the remnants of the deep surface layer from the winter months, results in a strong sound channel with a cut-off frequency of ~191 Hz. This feature is difficult for the submariner to avoid and may lead to long range propagation paths and long initial detection ranges.

The sediment type on top of Anton Dohrn is gravel, in the deep water the sediment type is mud and ooze (NAVO, 1986 and Nekritz, 1975). The thickness of the gravel sediment is from 50-100 m whilst the mud-ooze mix can be as thick as 2000 m. The geoacoustic parameters associated with these sediment types are given in Table 15(a) and (b).

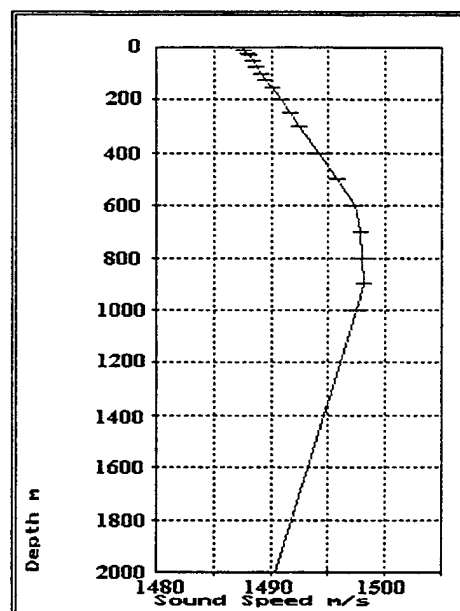
Sediment Type	Geoacoustic Parameter		Sediment Thickness (m)			
			Surface	200	500	2000
Mud-ooze mix	Velocity (m/s)		1467	1693	1962	2029
	Density (g/cm ³)		1.356	1.610	1.899	1.678
	Attenuation	dB/m/kHz	0.0146	0.025	0.020	0.01
		dB/λ	0.021	0.037	0.029	0.015

Table 15.a) Mud-ooze mix geoacoustic parameters along track E, Anton Dohrn Seamount environment. (Calculated from Hamilton and Bachman (1982) and Bachman (1994)).

Sediment Type	Geoacoustic Parameter		Sediment Thickness (m)			
			Surface	10	50	100
Gravel	Velocity (m/s)		1777	1924	1958	1992
	Density (g/cm ³)		2.228	2.228	2.228	2.228
	Attenuation	dB/m/kHz	0.253	0.173	0.132	0.118
		dB/λ	0.381	0.254	0.198	0.173

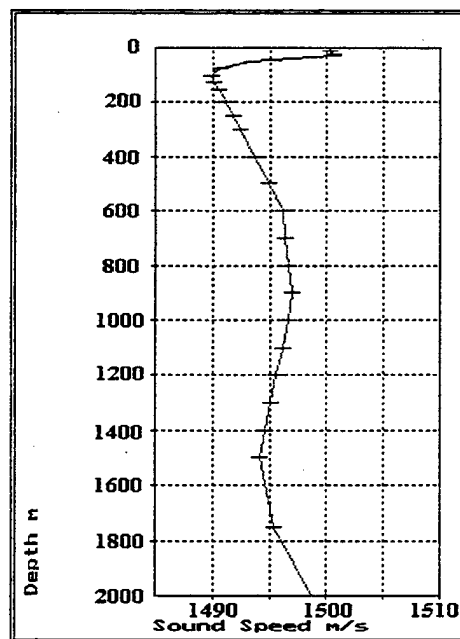
Table 15.b) Gravel geoacoustic parameters along track E, Anton Dohrn Seamount environment. (Calculated from Hamilton and Bachman (1982) and Bachman (1994)).

Profile Analysis to Depth 2000m
 Layer Depth 900m Cut-off freq 7Hz
 Sound Channels
 No Sound Channels Found
 Zero Depth Excess No CZ possible



a) SSP in winter.

Profile Analysis to Depth 2000m				
Layer Depth 30m			Cut-off freq 1072Hz	
Sound Channels				
Axis	Top	Base	Strength	Cut-off freq
100m	40m	900m	Strong	191Hz
1500m	900m	1864m	Moderate	13Hz
Zero Depth Excess No CZ possible				



b) SSP in summer.

Figure 37. Sound speed profiles for track E, Anton Dohrn Seamount environment in a) winter and b) summer. The acoustic propagation conditions are excellent in winter associated with the surface layer to ~900 m trapping all frequencies above ~7 Hz. The summer SSP exhibits a strong shallow sound channel caused by near surface heating. It is difficult for the submariner to avoid the sound channel, hence intermittent but long-range detections in the sound channel are possible. (Adapted from GPPDB, UKHO, 1997).

b. Source and Receiver Dispositions

The depth for both source and receiver is 40 m throughout this phase of the model comparison. The most stringent test of the model comparison is when the acoustic energy is refracted downwards to interact with the seabed. This is more likely to occur in the summer associated with the shallow negative thermocline; hence, the sound source and receiver are placed within the thermocline for all summer environments.

c. Correction Method

The approach for adjusting propagation loss output from the HODGSON model, in order to account for its lack of range dependent geoacoustic parameters, is qualitative. A direct transmission loss correction is applied (or calculated) at the appropriate range as governed by the difference in the HODGSON and RAM transmission loss output. The requirement for correction is anticipated to be in a region where the geoacoustic parameters change, typically from absorptive/refractive to reflective or vice versa. A major difference between the two propagation loss curves is most likely to occur in summer when downward refraction of near surface acoustic energy is dominant.

d. Propagation Loss Results

Corrections are applied to the HODGSON output only when they are of operational significance. It is reiterated that the HODGSON model algorithms are not changed in any way; if an adjustment is made it is merely to the output data from the model.

The Hodgson model PL output compares well with the RAM PL curves in the following environments under consideration:

1. Track A, SEIF transect in winter.
2. Track B, SEIF transect in summer, downslope propagation direction only.
3. Track C, upslope/downslope enhancement transect.
4. Track D, Faeroes-Shetland Channel transect.
5. Track E, Anton Dohrn Seamount transect in winter and in the downslope propagation direction in summer.

The perceived reasons for the HODGSON model producing realistic results for these transects either are as a result of range independent, reflective

geoacoustic parameters (1 and 3 listed above) or the loss at range from both models being outside operationally significant levels (2, 4 and 5 in the above list). The regions where correction is necessary and an explanation/analysis for their need is described in the following paragraphs.

(1) Track B, SEIF transect in summer, upslope propagation path. Geoacoustic parameters for the HODGSON model in this scenario are those associated with deep water, i.e., a mud and ooze mix. This sediment type is highly absorptive and constitutes high attenuation of acoustic energy. As the transect shoals onto the Iceland-Faeroes Rise, the sediment type changes to a sand-silt-clay mix and becomes more reflective. The attenuation to acoustic energy is reduced in the shallower region of this environment. Figure 38(a) shows the difference between the HODGSON, absorptive sediment, and RAM, absorptive-becoming-reflective sediment, PL curves. The discrepancy from 2-16 km is a result of the vertical beam width in the HODGSON model being limited to $\pm 15^\circ$ as required for LFAS assessment. In this instance the HODGSON model is more accurate because it adequately accounts for the vertical beam pattern. RAM, on the other hand, is overly optimistic in the same region, as vertical beam pattern is not taken into account. HODGSON appears optimistic in the 35-40 km region. This is a consequence of convergence zone propagation differences between RAM and HODGSON described in Section III.B.2(b). The region of primary concern begins at approximately 55 km, where the HODGSON geoacoustic parameters being absorptive result in too great a loss, whilst the RAM parameters are reflective and more realistic. A correction to the HODGSON curve must be applied in this region.

A characteristic of acoustic propagation in the ocean is that the predominant source of acoustic energy at large ranges is from ray paths that emanate from the source at shallow angles from the horizontal plane. In a scenario where the water depth is shoaling this results in acoustic interaction with the seabed at relatively shallow grazing angles. In this particular case, in the upslope region HODGSON continues to apply high levels of seabed loss associated with the absorptive deeper water sediment. In reality, with a more reflective seabed, less loss should be applied. The difference between respective seabed loss levels is shown in Figure 39. At shallow grazing angles ($< 20^\circ$) the difference in loss is ~ 5 -13 dB/reflection. It is evident from the

HODGSON PL curve that there are four instances of reduced transmission loss, labeled 1-4. These regions are associated with zones of energy convergence separated by the bottom-reflected skip distance. The difference in propagation loss between region 1 and region 4 on the HODGSON PL curve is ~42 dB, i.e., 14 dB between successive low transmission loss peaks. At the grazing angle associated with a 14 dB loss in the mud/ooze seabed loss curve (Figure 39), the loss associated with sand-silt-clay is ~2 dB. Therefore, a 12 dB per reflection correction must be applied throughout the HODGSON PL curve from ~55 km, i.e., at 55 km the correction is 12 dB, at point 4 the loss correction is 48 dB (4 x 12 dB). The correction is cumulative throughout the range from ~55 km and is given by;

$$\text{Correction at range } R = 12 + [(R - 55) \times (48-12)/(90-55)] \quad 3.1$$

in this instance. The correction is subtracted from the calculated propagation loss. As a more general formula for upslope propagation loss changes such as this;

$$\text{Correction at range } R = L_d + [(R - R_{b1}) \times dL/dR] \quad 3.2$$

$$L_d = PL_{b1} - PL_{b2} - L_r \quad 3.3$$

where,

L_d = difference between original seabed loss applied and seabed loss that should be applied at the range of upslope enhancement. (dB)

PL_{b1} = propagation loss at first bounce. (dB)

PL_{b2} = propagation loss at second bounce. (dB)

L_r = required seabed loss, the reflection per bounce from the sediment type that should be applied in the region of interest. This is acquired by relating the angle where the original applied seabed loss ($PL_{b1} - PL_{b2}$) to the more realistic loss curve, points A and B in Figure 39.

R = range in PL plot. (km)

R_{b1} = range of where loss correction is to be applied from (< R). (km)

dL/dR = gradient correction to loss over required region. (dB/km)

It is recommended that the gradient is calculated over the maximum range possible, $dL = (\text{number of bottom bounce regions} - 1) \times L_d$

$$dR = R_{BL} - R_{bl}, R_{BL} = \text{range of last bottom bounce region.}$$

This method is designed specifically for upslope propagation where the sediment is changing from absorptive to reflective. It is anticipated that in most cases of upslope environmental transects the sediment type will alter from absorptive/refractive in deep water to reflective in shallow water. This method has been developed for this specific case but may be applied in similar cases of upslope enhancement in the NWAPPS in summer. An additional note is that the degree of upslope enhancement is dependent upon the water column sound speed and the proximity of the source to the slope. This method requires knowledge of the sediment types along a transect and the ability to utilise the sediment parameters and seabed loss curves within HODGSON to their full potential. This is a training issue.

The amended HODGSON PL curve is shown in Figure 38(b) and exhibits strong correlation with the RAM PL curve.

(2) Track E, Anton Dohrn Seamount transect in summer, upslope propagation direction. The HODGSON PL curve for this environment was corrected by application of equations 3.2 and 3.3 in conjunction with appropriate BLUG loss vs. grazing angle curves.

Although the correction method proves robust for the cases outlined, the method requires rigorous testing. This will not be attempted in this thesis. The correction method detailed is applied in the LFAS performance assessment phase of this research if considered operationally significant. However, the potential exists for the method not to be applied due to increased transmission loss as a result of the inclusion of sea surface loss and absorption loss in this phase. Although relatively small for the frequencies of interest these contributors to acoustic attenuation are significant.

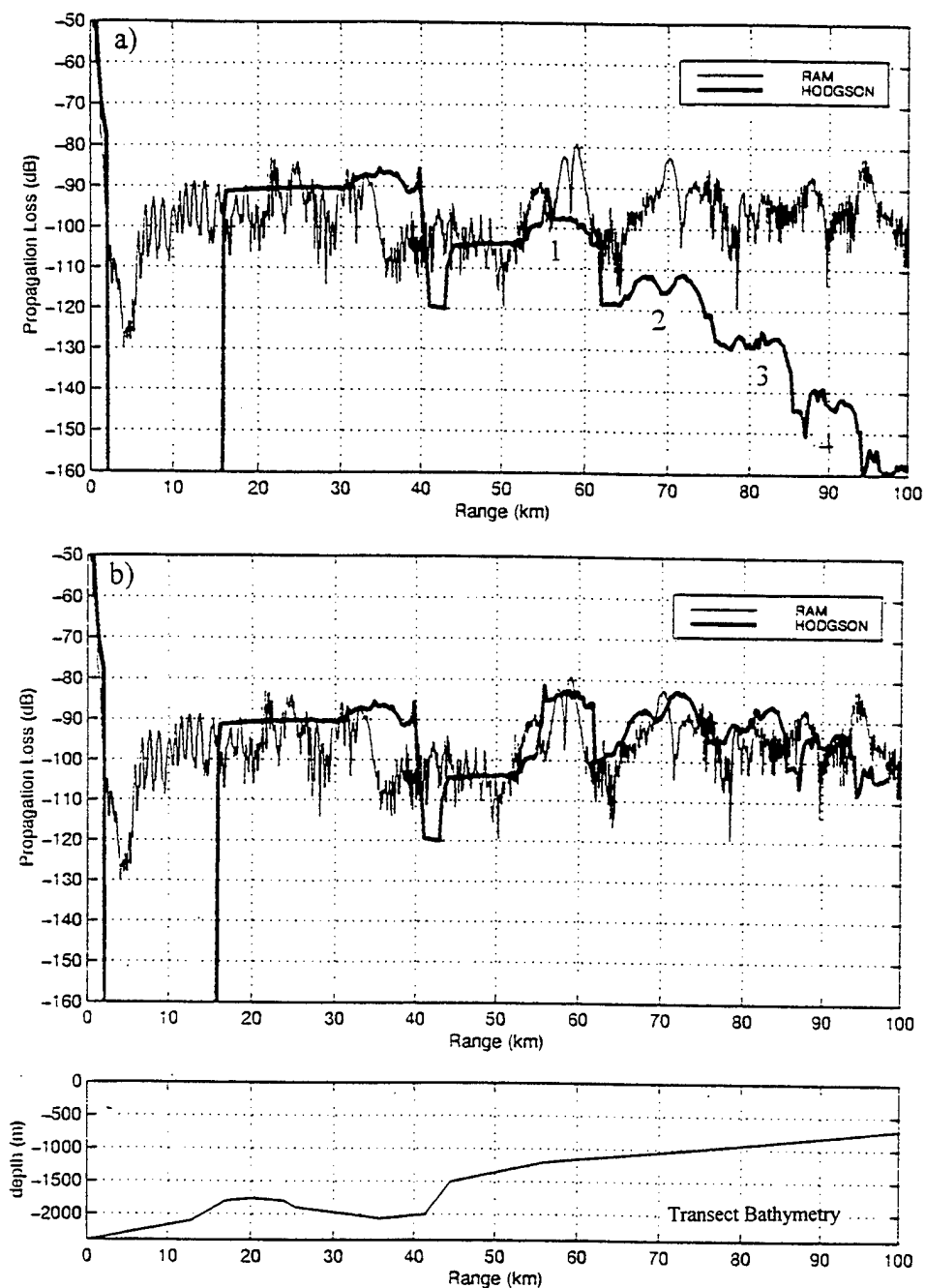


Figure 38. Comparison of propagation loss curves at 400 Hz from RAM, range dependent acoustic parameters, (thin line) and HODGSON, range independent geoacoustic parameters, (thick line) upslope through the SEIF in summer. a) PL comparison prior to amendment of HODGSON output, the shallow water has an inherently reflective sand-silt-clay sediment type, this produces relatively lower loss in the RAM PL curve. Labels 1 through 4 refer to the number of bottom reflection paths that lead to relatively low transmission loss. b) PL curves after application of correction method to HODGSON output.

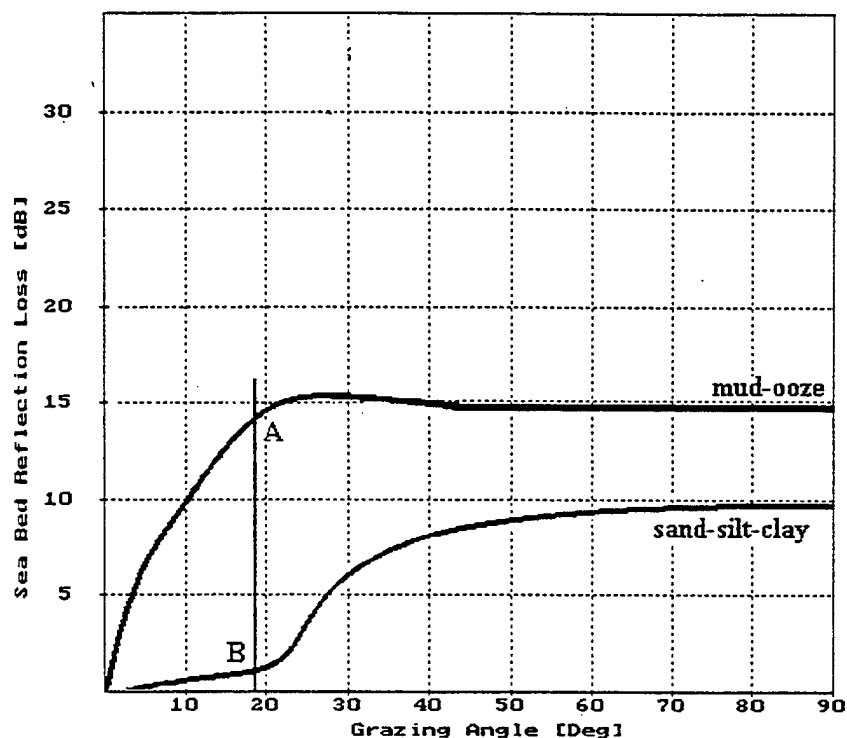


Figure 39. Seabed loss (dB/reflection) associated with mud-ooze mix and sand-silt-clay mix sediment types. The sediment types are representative of the transect through the South East Icelandic Front and are used to adjust the HODGSON acoustic model propagation loss curve to give a more representative range dependent geoacoustic propagation loss curve as applicable for Low Frequency Active Sonar performance assessment. Point A corresponds to the mud-ooze mix seabed loss applied by the HODGSON model throughout transect B. Point B corresponds to the sand-silt-clay seabed loss that should be applied in the shallow region as a result of a change in sediment type. The difference between the loss/reflection at A and B is used in correcting the HODGSON propagation loss curve for this environment.

C. LOW FREQUENCY ACTIVE SONAR PERFORMANCE ASSESSMENT

The relatively recent development of LFAS systems is in response to quieter submarine source levels that have effectively negated the use of conventional passive towed array sonar systems. Operational assessments of LFAS performance must now be made. Such assessments should include prediction of both initial detection ranges and reverberation limited ranges. The intention of this study is to review the facets involved in making accurate predictions.

This section outlines the methods applied and predicted sonar ranges achieved in making the LFAS performance assessment in the NWAPPS to the UK in a monostatic scenario.

1. Environmental Transects

The environmental transects are described fully in Sections III.B.3. and III.B.4. In addition to these standard environments, the cross-frontal transect summer is investigated in a similar manner to the methods employed by Carman and Robinson (1994). Acoustic propagation at 400 Hz and 800 Hz will be modeled and compared along the frontal transects in the following way: 1) a fully range dependent environment, and 2) a range dependent geoacoustics and bathymetry, range independent sound speed. This methodology is applied in order to investigate the effect of sound speed variation through the SEIF in summer at the frequencies of interest. The reason for this additional research is to ascertain the requirement for range dependent sound speed variation in sonar performance assessments. The summer cross-section is selected as this is likely to have greatest influence upon acoustic propagation variability.

2. Source/Target Depths

The active sonar source depth (also the receiver depth for this monostatic study) and target depth have a major influence on the propagation loss between the source and target. The Command decision for LFAS source depth is primarily based upon the most recent, in situ, SSP and an estimation of the likely target depth. In this study the target depth is chosen to exploit any negative sound speed gradients (which cause sound to refract downwards) that can be used for evasion tactics. If a deep surface layer exists, as in the winter months, the target is placed within the layer at an operationally acceptable

depth. In response to the target depth, the LFAS is towed at the same or similar depth as the target. This is in accordance with generic ASW Command guidance. Another consideration for the LFAS tow depth is mobility in which the LFAS towing ship generally employs a shallow deployment depth, typically less than 100 m. The LFAS source depths and submarine target depths for each environmental transect are both 60 m in winter and 50 m in summer. The exception to this is an additional target depth of 150 m in the SEIF winter transect; this depth is selected as it is within the negative thermocline.

3. Acoustic Propagation Loss Models

The HODGSON propagation loss model is used throughout the LFAS performance assessment phase. The model is operated in the two-way loss mode and reverberation is calculated.

In order to determine the effects of sound speed variation across the SEIF, RAM is used to model the acoustic energy propagation at 400 Hz across the summer frontal transect. This simulates one-way propagation path, i.e., a passive scenario.

4. Results of the Investigation of Range Dependent (RD) vs. Range Independent (RI) Propagation of Acoustic Energy for the South East Icelandic Front (SEIF) in summer

The acoustic propagation conditions are modeled using RAM with 1) a fully range dependent transect through the SEIF in summer as described in Section III.B.3, and 2) a range independent sound speed cross-section but range dependent bathymetry and geoacoustic parameters. The SSP applied for b) is that associated with the northern end of track B, to the north of the SEIF, shown in Figure 31(b). The propagation direction throughout is from deep to shallow water.

The aim of this phase of the research is to investigate the effects of the SEIF, in summer, on acoustic energy at the frequencies of interest, 400 Hz and 800 Hz. This is achieved by simulating a passive scenario with the source and receiver located at depths of operational significance. The source is placed at 50 m, within the negative sound speed gradient (downward refraction dominates the propagation path of the acoustic energy) to simulate a submarine evasion scenario, and 250 m, at the sound channel axis (the channel cut-off frequency is 191 Hz) to simulate potentially excellent propagation conditions. For

both source dispositions the receiver is placed at 50 m and 250 m depth. It should be noted that in the fully range dependent scenario the source depth of 250 m corresponds with the shallow sound channel axis at the beginning of the transect.

a. Source Depth 50 m

With both source and receiver at 50 m the relatively small difference between the transmission loss for the RD and RI scenarios is primarily a result of increased downward refraction in the frontal zone (Figure 40(a)). Once significant changes in the SSP occur, from ~20-30 km, and a strong waterborne propagation path is developed (convergence zone propagation), the differences are significant. Figure 40(a) clearly shows a convergence zone at 32-38 km in the RI transmission loss curve whilst it is not evident in the RD curve. This is a function of SSP changes in the frontal zone. In the case of RI convergence zone propagation acoustic energy will return to the same depth as the source with relatively low attenuation. Conversely, in the case of RD convergence zone propagation the negative sound speed gradient is more significant in the frontal zone and recurvature of the acoustic energy (upper turning point) occurs at deeper depths and less energy reaches the receiver at 50 m. A 2D contour plot of transmission loss (not shown) indicates that the depth of the upper turning point in the range dependent scenario is at ~100 m. Despite the considerable difference between the RD and RI transmission loss curves for convergence zone propagation when the incidence of seabed interaction is increased, the differences are relatively small.

When the receiver is at 250 m the difference between the PL curves is insignificant (Figure 40(b)). There is little discrepancy between the convergence zone region in the RD and RI PL curves as the receiver is at sufficient depth to be within the low transmission loss region associated with CZ propagation in both scenarios. From ~50 km the transmission loss is dominated by seabed interaction and, as stated above, there is little difference between the PL curves in such a region.

b. Source Depth 250 m

When the source is placed within the shallow sound channel and the receiver at 50 m (outside the boundaries of the shallow sound channel) the major difference between the propagation loss curves for the RD and RI scenarios is, once again, related to convergence zone like propagation (Figure 41(a)). Acoustic energy

leaving the source at angles greater than approximately 5° from the horizontal propagates outside the shallow sound channel. Consequently, the major influence upon the propagation path of this energy is, initially, the near-surface negative sound speed gradient, the positive sound speed gradient at depth refracts the energy back towards the surface resulting in CZ-like propagation as shown in plate 1. As stated in Section III.C.4.a., the difference between the PL curves in the CZ region is caused by greater downward propagation in the frontal zone. Once again, when considerable seabed interaction occurs the difference between the PL curves is insignificant.

With both source and receiver at 250 m the differences between the RD and RI scenarios are considerable, approaching 30-40 dB in some regions. Figure 41(b) and Plate 1 clearly show these different propagation loss levels and propagation paths. In the RI transect a considerable amount of energy is trapped within the sound channel and results in the modal shape to the PL curve with low transmission loss due to the cylindrical spreading associated with channeled propagation paths. In the RD scenario the shallow sound channel weakens and dissipates in/near the frontal zone. The acoustic energy becomes more directly coupled into the deep sound channel. This can be seen in Plate1(b) in the range 20-40 km and between depths of 250-1000 m. The changing SSP's within the frontal zone are the dominant factor in governing the propagation loss for this source/receiver disposition.

In summary, for the frontal transect in summer;

(1) If the source is shallow, within the negative thermocline:

- A range dependent transect is required if convergence zone propagation paths are possible. A range independent transect is likely to misrepresent the range to, strength and width of the convergence zone region.
- When seabed interaction is the dominant propagation path changes in SSP appear to have little effect. In this case the geoacoustic conditions must be accurately characterised.
- Comparison of the range dependent PL curves in Figure 41(a) and (b) indicate that, if the receiver is placed deep, the transmission loss is reduced. This is a function of the receiver being at sufficient depth to take

advantage of the convergence zone path (35-40 km) which, at deeper depths, is stronger and better defined as acoustic energy is refracted away from the near-surface strong negative sound speed gradient.

(2) If the source is deeper within the shallow sound channel:

- Inputting range-dependent SSP's to characterise the frontal zone is a necessity. Even in regions not associated with frontal zones, range-dependent SSP's are required because shallow sound channels are generally quite variable in their vertical, horizontal and temporal dimensions. The results shown in Figure 41(b) and Plate 1 suggest that accurate characterisation of shallow sound channel variability is important in enabling a USW Commander to tactically exploit the environment. This is particularly true where shallow sound channels pass through frontal features.

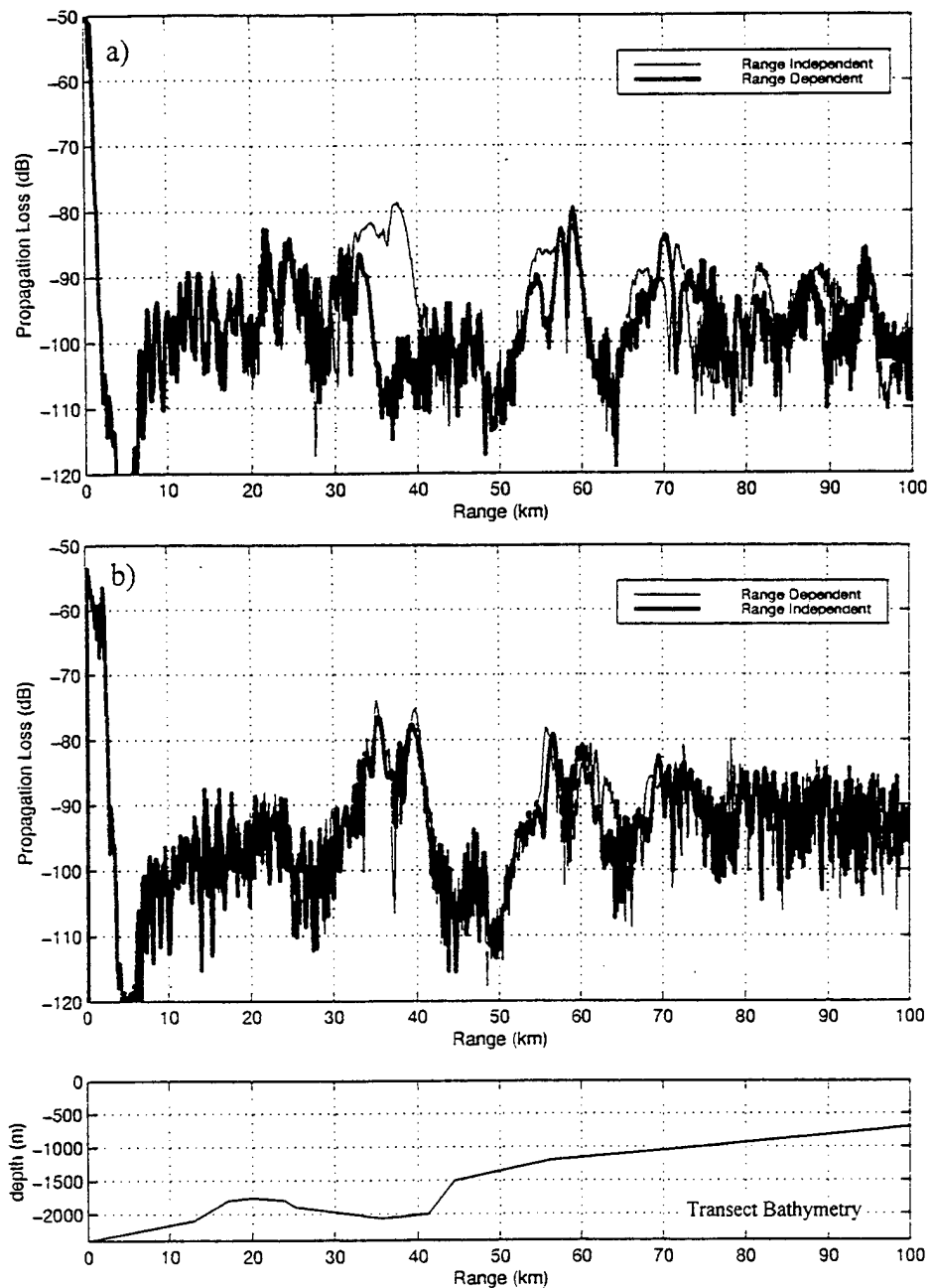


Figure 40. Propagation loss curves for a 400 Hz source and receiver in a range dependent and range independent transect of the South East Icelandic Front in summer. The propagation direction is from deep to shallow water. a) Source and receiver at 50 m depth. b) Source depth 50 m, receiver depth 250 m.

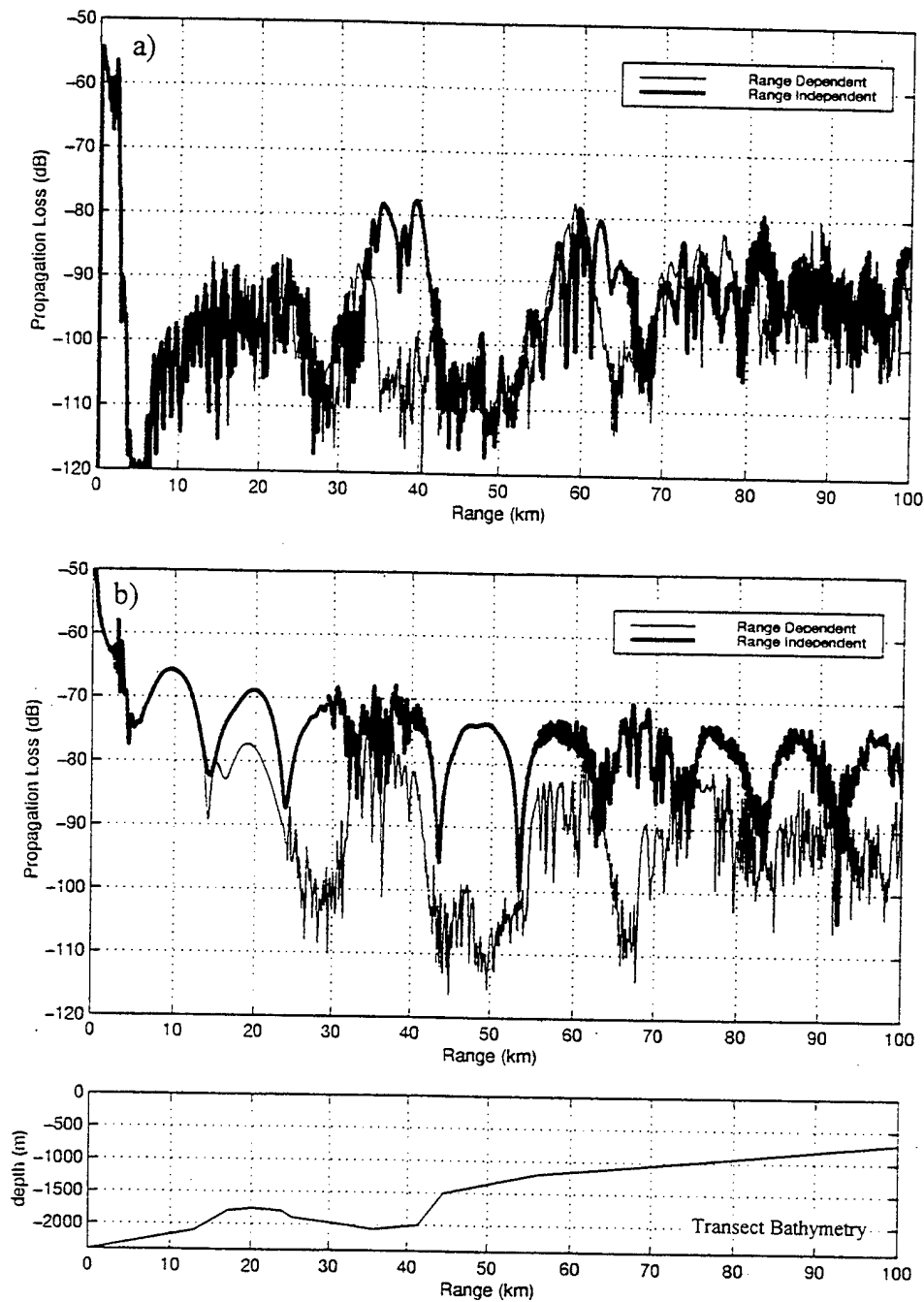


Figure 41. Propagation loss curves for a 400 Hz source and receiver in a range dependent and range independent transect of the South East Icelandic Front in summer. The propagation direction is from deep to shallow water. a) Source depth 250 m, receiver depth 50 m. b) Source and receiver at 250 m depth.

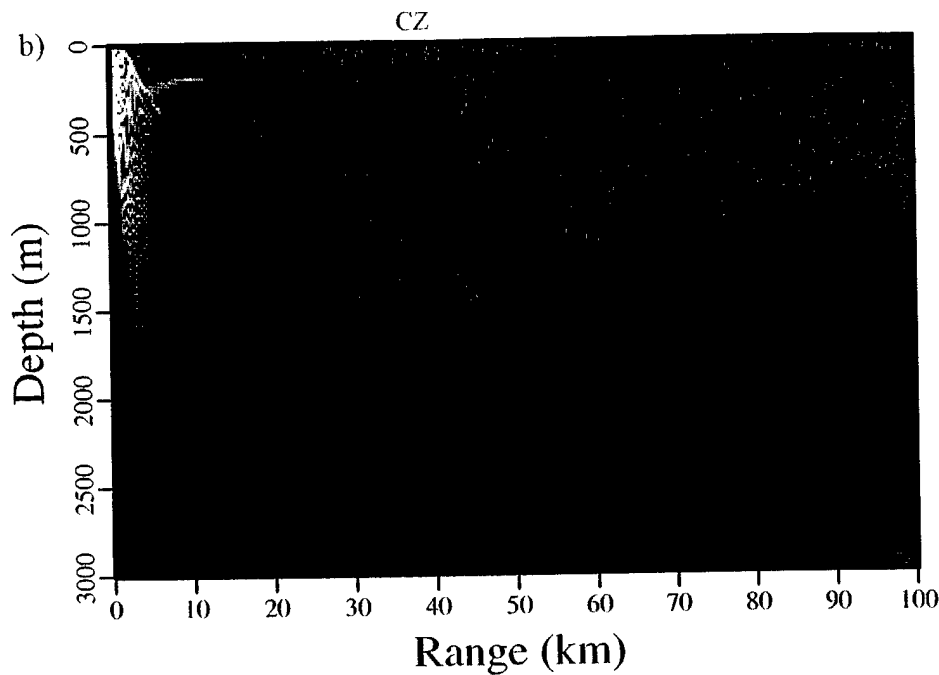
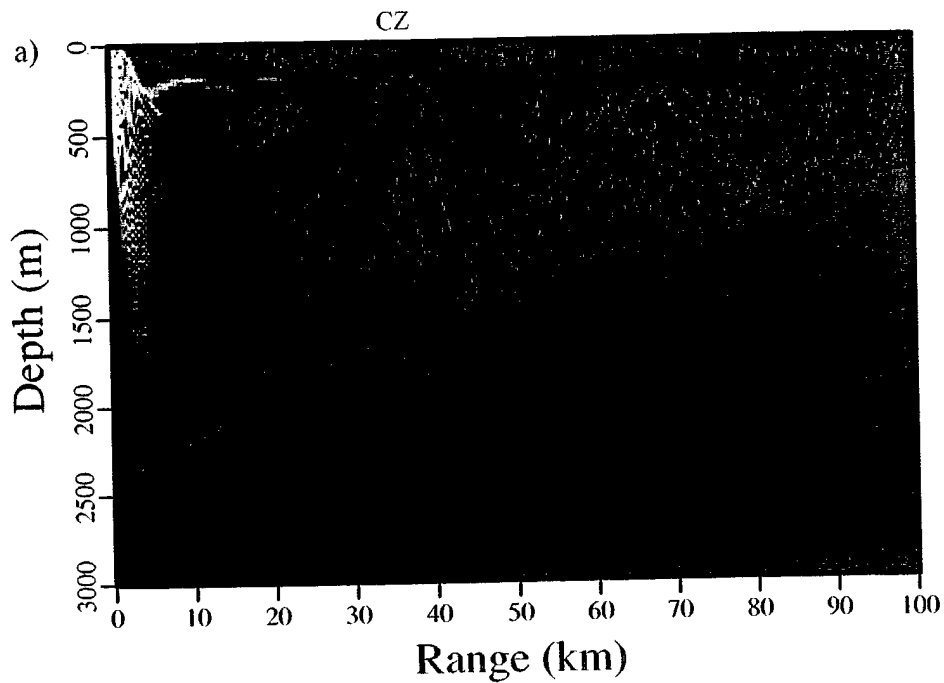


Plate 1. Two-dimensional contour plot of transmission loss from a 400 Hz source at 250 m depth. a) Summer sound speed profile from north of the South East Icelandic Front applied range independently along track B. The geoacoustic parameters and bathymetry are range dependent. b) Fully range dependent transect of the South East Icelandic Front in summer. The color scale equates to transmission loss levels as follows; orange <50 dB, yellow 50-60dB, lime green 60-70 dB, green 70-80 dB, blue 80-90 dB, dark blue 90-100 dB, purple >100 dB.

5. Active Figure of Merit (AFOM)

Sonar performance modeling of initial detection ranges is heavily dependent upon the probability of detection and application of the appropriate form of the sonar equation (Urick, 1983). In this study the probability of detection applied is 50 %, the range where the transmission loss (TL) is numerically equal to the active figure of merit (AFOM) and signal excess (SE) = 0. The AFOM is essentially the ratio between the signal at the sonar display and the noise or reverberation level (whichever is dominant) for a specific sonar setup. In this study a sigma FOM of 5 dB is applied; this may be interpreted in a number of ways. In this research the sigma FOM refers to the confidence level of the parameters within the sonar equation; as such, on application to a transmission loss curve, the variation in initial detection range between the limits of the sigma FOM gives the variability of the IDR for the 50th percentile.

a. Active Sonar Equation

Assuming reciprocity, i.e., the TL of the acoustic energy from the source at the target is the same as the TL from the target to the receiver, the active sonar equation is:

$$\text{AFOM}_{\text{NL}} = 2\text{TL} + 2\text{ESL} = \text{SL} + \text{TS} - (\text{BN} - \text{AG}) - \text{DT} \quad (\text{noise limited}) \quad 3-4$$

$$\text{AFOM}_{\text{RL}} = 2\text{TL} + 2\text{ESL} = \text{SL} + \text{TS} - \text{RL} - \text{DT} \quad (\text{reverberation limited}) \quad 3-5$$

where, TL = transmission loss (dB)

SL = source level (dB)

ESL = energy spreading loss (dB)

TS = target strength (dB)

RL = reverberation level (dB)

BN = background noise (sum of ambient noise and self noise) (dB)

AG = Array Gain (dB)

DT = detection threshold (dB)

AFOM_{NL} = active figure of merit, noise limited (dB)

AFOM_{RL} = active figure of merit, reverberation limited (dB)

A precise estimate of all terms in the active sonar equation for LFAS in the NWAPPS to the UK will not be attempted in this research. However, utilising representative estimates of these parameters typical AFOM values are calculated.

Ambient noise values are derived from the modified Wenz curves (NAVO, 1981) and the typical 50 Hz ambient noise values given in Section I.A.5. for area D. The values shown in Table 16 have been assessed for; 1) the winter scenario with a mean wind speed of 20 kts, with and without moderate rain, and 2) the summer scenario with a mean wind speed of 12kts and no precipitation.

Frequency (Hz)	Ambient Noise Level (dB)		
	Winter (wind 20 kts)		Summer (wind 12 kts)
	No rain	Moderate rain	
400	70	77	66
800	69	78	65

Table 16. Ambient noise level used in LFAS active figure of merit calculations.
(Adapted from NAVO, 1992 and modified Wenz curves (NAVO, 1981).

Energy spreading loss (ESL) is a consideration when operating active sonar systems in shallow water. It is qualitatively defined as the reduction in peak power level due to the time stretching of the original transmitted acoustic pulse due to multipath propagation from seabed interactions. The time stretched energy does reach the receiver array but is an energy loss because matched filters or signal replica correlators used in current operational active sonar systems are matched to the transmitted pulse, not the propagated pulse (Adams, 1997). In general, this source of loss is not a problem in deep water situations. Adams (1997) highlights that pulse lengths in excess of 2 sec in intermediate depth water only appear to be susceptible to low loss levels associated with ESL (<2 dB). The majority of the transects in this study are in water depths that can be classified as intermediate or deep (>600 m), hence ESL is not considered in this thesis.

The target strength (TS) of a target is highly dependent on size, shape and aspect of the target in addition to surface coating and typically varies from 0-30 dB for a submarine (Urlick, 1983). In this study, a generic target strength of 10 dB is used to represent a random aspect target.

AFOM_{NL} values applied for the LFAS performance assessment phase of this study are given in Table 17.

Frequency (Hz)	Noise Limited Active Figure of Merit (AFOM) (dB)		
	Winter (wind 20 kts)		Summer (wind 12 kts)
	No rain	Moderate rain	
400	167	160	171
800	168	159	170

Table 17. Active Figures of Merit used in LFAS performance assessment.

b. Reverberation

The conventional method of reverberation assessment in the United States Navy (USN) is to calculate a reverberation-limited figure of merit by application of equation 3.5. This gives an AFOM that varies with range (unlike the noise limited AFOM) that is applied in the same manner as the noise limited AFOM. However, the HODGSON model does not use this method, indeed neither does the Royal Navy (RN). The HODGSON model calculates reverberation loss. Target strength is applied to the reverberation loss and this sum is displayed on the same axes as the transmission loss, allowing direct comparison between the two curves. If the reverberation loss is less than the transmission loss then the assessment is that detection ranges are likely to be reverberation limited. If reverberation loss is greater than the transmission loss, the detection ranges are noise limited.

Reverberation from a surface is given by Urick (1983) as;

$$RL_s = SL - 40 \log r + S_s + 10 \log A$$

Where RL_s = surface reverberation

SL = source level

r = range of scatterer from the source

S_s = scattering strength for surface reverberation

A = area of the surface of scattering strength S_s

The area A is directly proportional to the pulse length of the active transmission. Therefore, for long pulse lengths, A is relatively large and reverberation levels increase. The pulse length applied in this study is generic and selected as 2 seconds (adapted from Taylor (1993)); as such the reverberation levels are expected to be

relatively high. In the display format used this equates to a relatively low reverberation loss.

6. Low Frequency Active Sonar Performance Assessment Results

As a consequence of the generic approach applied in this research for system parameters, variables such as advanced signal processing and display techniques and operator competence are omitted. The factors available for contrast and discussion are environmentally driven and include season, operating area (topography and sound speed variation) and reverberation. As will be outlined the reverberation levels are high associated with the long pulse length. It is anticipated that the LFAS system in use by the UK has a signal processing method that suppresses reverberation. Therefore, only background noise limited ranges are considered in this performance assessment, however, reverberation levels will be discussed, as necessary, in order to highlight features of note.

a. Track A, South East Icelandic Front Transect in Winter

As a consequence of the surface layer having a depth in the order 80-100 m and the $\pm 15^\circ$ vertical beam width of the LFAS being considered, a substantial amount of acoustic energy is able to propagate out of the half channel. As a consequence of downward refraction, much of this acoustic energy interacts with the seabed. Because the energy reflected from the seabed will contribute to the transmission loss, it is likely that the PL curves associated with upslope and downslope propagation paths will be different, even for source and target depths that are within the surface layer. As both the surface layer and the negative thermocline are exploitable by the submariner, this phase of the study considers a target operating within the surface layer (60 m) and below the layer (150 m). IDR's for this transect are given in Table 18.

(1) Upslope propagation. Upward refracting, half channel propagation dominates the PL curve to approximately 40 km. Thereafter, acoustic energy that has undergone seabed interaction (mostly reflection in this case as the sediment type is a sand-silt-clay mix) influences the PL curve and, consequently, detection ranges and opportunities (Figure 42(a)). When the target is below the surface-mixed layer, acoustic energy from the LFAS undergoes cycles of downward refraction and reflection back towards the surface. The regions of low transmission loss (Figure 42(b)) occur where these bottom reflected paths intercept the target. The peaks in the TL curve are the

principal means of detection . In-layer IDR's at 400 Hz are continuous to 32-47 km. Cross-layer detection ranges are associated with specific regions of low loss at 30-37 km, 50-53 km and lower SE detection areas at 65-68 km and 75-78 km (Figure 42(b)). Closer to the source, cross-layer ranges are 0-4 km and 11-37 km. The near field region of no detection from 4-11 km is due to the shadow zone created by the $\pm 15^\circ$ vertical beam width of the active sonar.

The bottom reflected-refracted skip distance is a function of water depth and seabed slope. If the source is moved upslope into shallower water depths, the seabed reflected detection ranges would alter in both range from the source and width of detection opportunity because of the seabed and sea surface acting as an ever-shrinking wave-guide. It is noticeable from the predicted ranges given in Table 18 that the presence of moderate rain (ambient noise level increase of 7-9 dB depending upon frequency) can degrade detection ranges by the order of ~25%.

UPSLOPE			Frequency (Hz)/Initial Detection Range (km)			
Source Depth (m)	Target Depth (m)		400		800	
			IDR	1σ Band	IDR	1σ Band
60	60	NR	40	37-47	32	26-40
		R	32	26-39	22	17-27
	150	NR	4, 11-37, 50-53.	4-5, 11-37, 50-53.	4, 11-24, 31-37, 49-53	4-5, 11-37, 49-53
		R	4, 11-13, 31-35	4-5, 11-19, 31-56	4, 31-35	4-5, 11-16, 31-36
DOWNSLOPE			Frequency (Hz)/Initial Detection Range (km)			
Source Depth (m)	Target Depth (m)		400		800	
			IDR	1σ Band	IDR	1σ Band
60	60	NR	29	28-29	28	27-29
		R	28	18-29	19	15-27
	150	NR	32	22-33	23	22-32
		R	22	14-23	18	13-22

Table 18. Initial Detection Ranges and sigma-IDR's for the winter transect through the South East Icelandic Front, Track A. NR – no rain, R – moderate rain.

(2) Downslope propagation. The most striking feature of the predicted IDR's is the relative insensitivity to target depth (Table 18). This is a consequence of high seabed reflection and the relatively shallow water column acting as

a wave-guide to effectively ensonify the whole water column in the shallow water region (Figure 43(b)). If the LFAS is moved in to deeper water, the wave-guide effect of the shallower water is reduced and detection ranges become more dependent upon target depth.

Considering propagation paths within the surface layer, the IDR's for both upslope and downslope scenarios might be expected to be similar as a consequence of half channel propagation dominating the shape of the transmission loss curve. However, a marked difference is noted, primarily due to the range-dependent nature of the SSP. Detection ranges are better for upslope propagation (32-47 km with no rain) when the LFAS is positioned on the cold, deep-water side of the front (to the northeast) than the warm, shallow-water side (the southwest) where ranges are 28-29 km. The reason for this can be explained by observing the sound speed cross-section shown in Figure 28. The positive sound speed gradient to the southwest of the front is distinctly weaker than that to the northeast. As a result, to the southeast of the front acoustic energy within the surface layer is subject to less upward refraction and more energy is able to penetrate through the surface layer. Because less energy remains in the layer, the transmission loss in the layer is increased and IDR's are reduced.

(3) Reverberation. Clearly indicated in Figures 42 and 43, reverberation loss is distinctly less than transmission loss over almost the whole prediction range. At all ranges a target signal is likely to be severely masked by reverberation. This is primarily a function of the long pulse length of the LFAS transmissions.

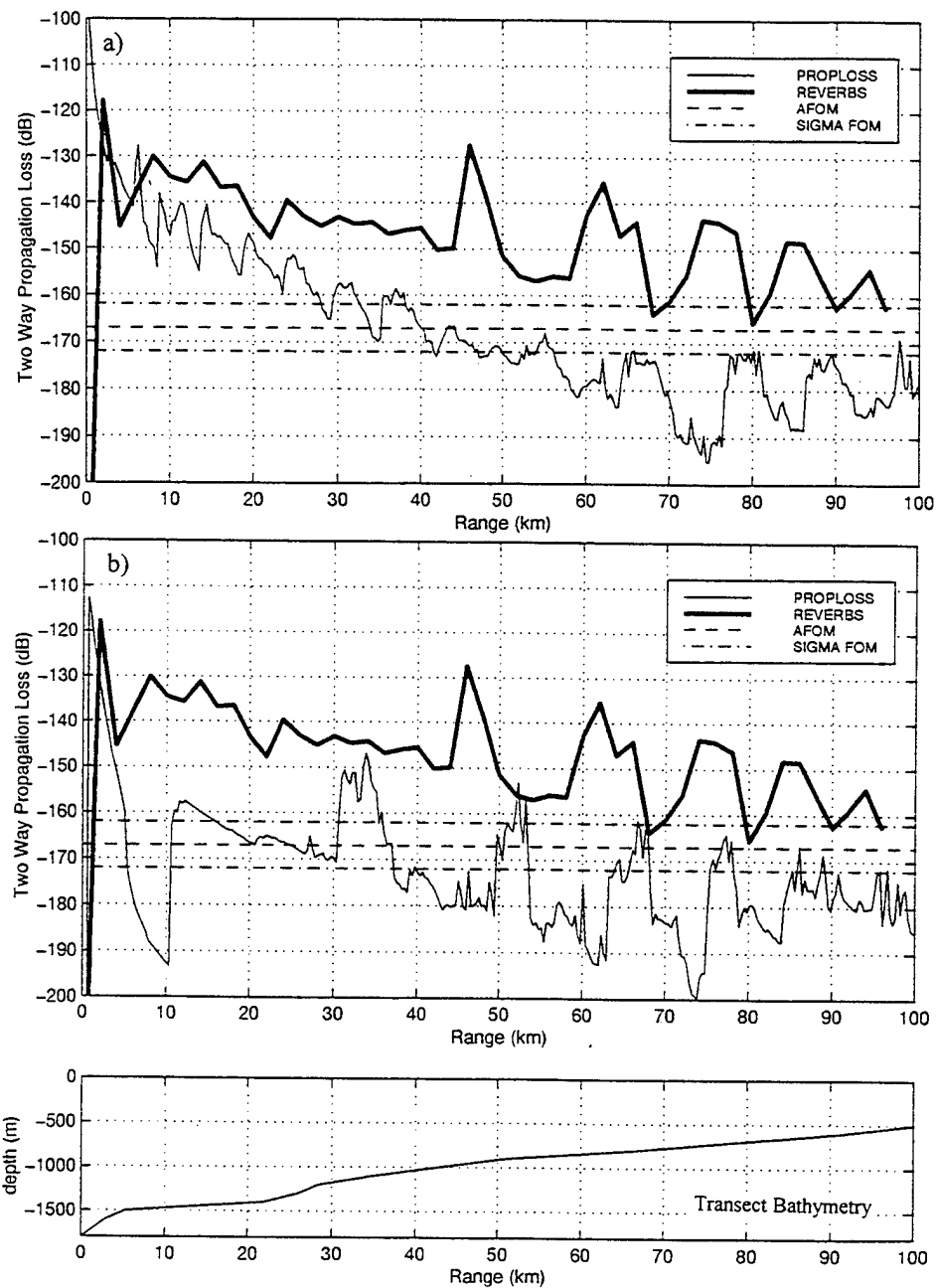


Figure 42. Propagation loss and reverberation loss curves for the winter South East Icelandic Front transect, propagation direction is upslope. a) 400 Hz, source and target depth 60 m, active figure of merit 167 dB, no rain. This PL curve is representative of in-layer propagation through the frontal zone. b) 400 Hz, source depth 60 m, target depth 150 m, active figure of merit 167 dB, no rain. The regions of upslope enhancement are clearly visible at 30-35 km, 50-53 km, 63-68 km and 75-78 km.

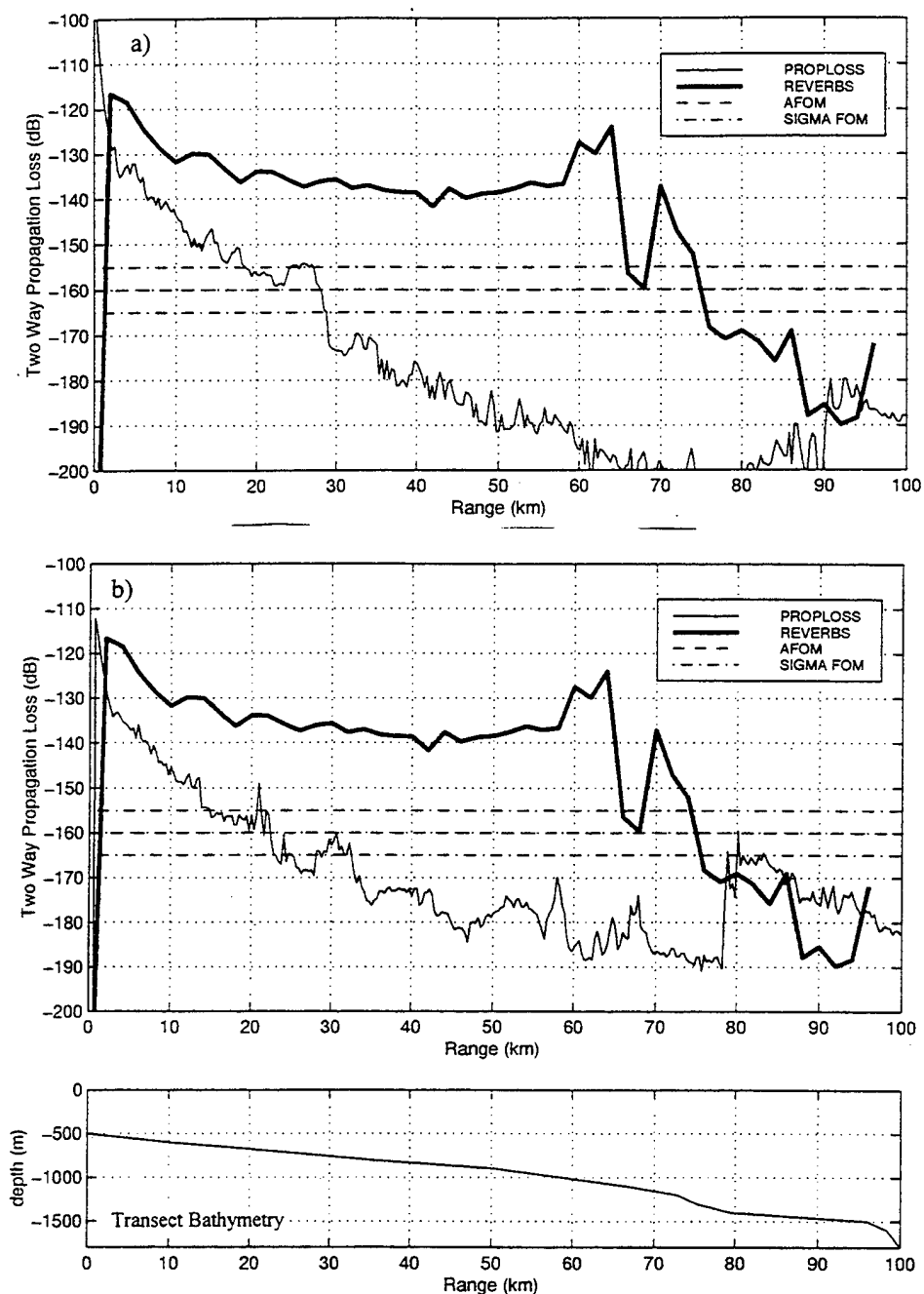


Figure 43. Propagation loss and reverberation loss curves for the winter South East Icelandic Front transect, propagation direction is downslope. a) 400 Hz, source and target depth 60 m, active figure of merit 160 dB, moderate rain. This PL curve is representative of in-layer propagation through the frontal zone. b) 400 Hz, source depth 60 m, target depth 150 m, active figure of merit 160 dB, moderate rain. There is little difference between the propagation loss curves as a consequence of the reflective seabed and the shallow water acting as a wave-guide for the acoustic energy.

a. Track B, South East Icelandic Front Transect in Summer

The SEIF in summer occasions strong downward refraction of acoustic energy (Figure 29). As a result, the propagation paths for both the upslope and downslope scenarios are dependent upon seabed interaction. Because of this constraint to the propagation path of acoustic energy, LFAS performance is dominated by the geoacoustic properties of the sediment. Table 19 gives the IDR's for this transect scenario.

(1) Upslope propagation. In deep water detection opportunities are limited to direct path propagation. The near-field IDR is 3 km and convergence zone propagation gives a possible region of detection at 39-41 km. This is a function of high attenuation of acoustic energy by the absorptive sediment type (mud-ooze mix) in deep water regions and the large shadow zone from 3-17 km due to the vertical beam pattern of the LFAS. As acoustic energy propagates upslope, the seabed becomes more reflective as the sediment type changes (sand-silt-clay mix). As a consequence, the transmission loss is reduced and upslope enhancement detection opportunities become available. Figure 44(a) shows intermittent detection opportunities from 55-85 km in bands approximately 5-7 km wide.

(2) Downslope propagation. The PL curve associated with downslope propagation is markedly different from that of upslope (Figure 44(b)). In shallower water the seabed and sea surface act as a wave-guide, acoustic energy is reflected from the seabed and provides for nearly continuous detection ranges to 23-33 km, at 400 Hz. As a function of the vertical beam pattern of the active sonar, a region of no detection is observed in the near-field from 3-5 km.

(3) Reverberation. As in the winter frontal scenario reverberation is a major limiting factor to LFAS performance. Figure 44(a) suggests that reverberation is not a problem in the regions of upslope propagation in the range 65-93 km; this is anomalous. The PL curve has been corrected as outlined in Section III.B.4.d.(1), however, the reverberation loss curve has not. As such, it is likely that reverberation will be a limiting factor in this region. In the downslope propagation direction reverberation loss fluctuates significantly. Indeed, in the range 27-32 km reverberation loss is significantly higher than the propagation loss (Figure 44(b)) and any detection's are likely to not be affected by reverberation.

UPSLOPE		Frequency (Hz)/Initial Detection Range (km)			
Source Depth (m)	Target Depth (m)	400		800	
		IDR	1 σ Band	IDR	1 σ Band
50	50	3, 39-41, 55-62, 70-74, 81-85	3, 39-41, 55-63, 66-75, 78-85	3, 38-40	3, 38-40
DOWNSLOPE		Frequency (Hz)/Initial Detection Range (km)			
Source Depth (m)	Target Depth (m)	400		800	
		IDR	1 σ Band	IDR	1 σ Band
50	50	3, from 5-24	3, from 5 to 23-33	3, 5-23	3, from 5 to 23-32

Table 19. Initial Detection Ranges and sigma-IDR's for the summer transect through the South East Icelandic Front, Track B.

In summary, in order to contrast the propagation conditions between the summer and winter scenarios of propagation through the SEIF:

1. Sound speed profiles. In winter, propagation paths are primarily upward refracting in a well-defined duct.

In summer, propagation paths are primarily downward refracting.

2. Downslope propagation. Little seasonal variation in IDR's, however, a strong surface duct in winter favours this season. The reason for little seasonality is the overall bottom-surface reflected nature of the propagation path in shallow water acting as a wave-guide in summer and thus overcoming any refractive effects.

3. Upslope propagation. In this case the SSP shape dominates propagation. The surface duct in winter traps energy, reducing high loss bottom interaction. The converse is true in summer.

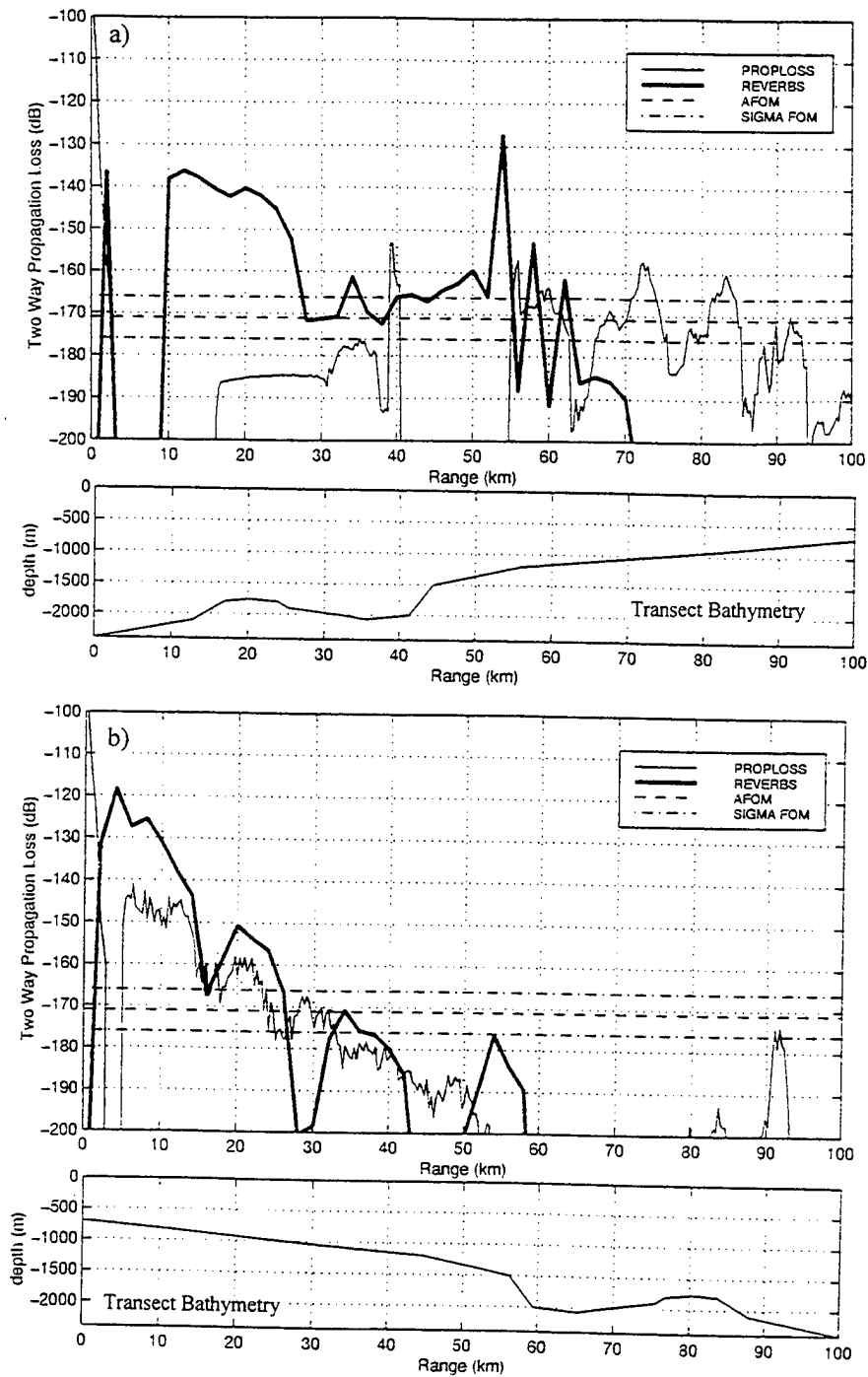


Figure 44. Propagation loss and reverberation loss curves for the summer South East Icelandic Front transect. a) Upslope propagation through the front, 400 Hz, source and target depth 50 m, active figure of merit 171 dB. In deep water the detection opportunities are scarce whilst the occurrence of upslope propagation allows for detection at long ranges, 55-85 km. b) Downslope propagation through the front, 400 Hz, source and target depth 50 m, active figure of merit 171 dB. The reflective seabed and shallow water act as a wave-guide for acoustic energy allowing detection opportunities at ranges to 23-33 km.

c. Track C, Upslope/Downslope Propagation Comparison

The effects of upslope or downslope propagation can play a major role in submarine detection opportunities. This phase of the research broaches the question as to which propagation direction provides the greatest tactical advantage. This transect is chosen to characterise a typical seabed slope that may be encountered when operating in the NWAPPS to the UK. The IDR's for the winter and summer scenarios are listed in Tables 20(a) and Table 20(b), respectively.

(1) Upslope/downslope propagation in winter. As shown in Table 20(a), IDR's associated with the upslope propagation paths are only marginally better than the downslope propagation direction despite upward refracting, half-channel propagation being the dominant path for upslope acoustic energy. When the propagation direction is downslope, the initially shallow water acts as a wave-guide. However, this is a dominant effect relatively close to the sonar and becomes of little tactical significance in comparison to the acoustic energy from in-layer propagation. Reflective acoustic properties of the seabed have greater influence on the PL curve for upslope propagation as a consequence of acoustic energy from the reflected path combining with that of in-layer propagation. Transmission loss is slightly less upslope than that of downslope at range and IDR's are improved (Figure 45).

UPSLOPE			Frequency (Hz)/Initial Detection Range (km)			
Source Depth (m)	Target Depth (m)		400		800	
			IDR	1σ Band	IDR	1σ Band
60	60	NR	46	36-55	36	28-45
		R	35	26-45	26	22-28
DOWNSLOPE						
60	60	NR	42	33-51	35	28-41
		R	30	23-39	28	21-30

Table 20(a). Initial Detection Ranges and sigma-IDR's for the winter upslope/downslope propagation transect, Track C. NR – no rain, R – moderate rain.

(2) Upslope/downslope propagation in summer. The presence of a strong negative thermocline causes propagation paths in summer to be dominated by seabed interaction. At 400 Hz, downslope ranges are nearly continuous to 20-22 km, whilst upslope ranges are intermittent between 28-61 km (Table 20(b)). Shoaling of the

water depth in the upslope propagation direction acts as a wave-guide for acoustic energy and provides for less transmission loss and better IDR's in this direction. In contrast, the predominant propagation paths downslope are into the deep sound channel (axis is at ~500 m) (Figure 47(b)). Therefore, IDR's in the downslope propagation direction for a shallow target are somewhat poorer relative to the upslope scenario.

UPSLOPE		Frequency (Hz)/Initial Detection Range (km)			
Source Depth (m)	Target Depth (m)	400		800	
		IDR	1 σ Band	IDR	1 σ Band
50	50	4, 9-45	4, from 9 to 28-61	4, from 9-30, 36-46	4, from 9 to 27-56
DOWNSLOPE					
50	50	22	20-22	22	19-22

Table 20(b). Initial Detection Ranges and sigma-IDR's for the summer upslope/downslope propagation transect, Track C.

(3) Reverberation. The sediment type along track C is sand. Although highly reflective and, thus, exploitable for up/downslope propagation, sand also has a relatively high back-scattering effect. Hence, the reverberation levels associated with this scenario are high and severely hamper detection opportunities. Despite this severe limitation, Figures 45(a) and 46(a) show some interesting features of reverberation loss in this scenario.

Referring to Figure 45(a), the reverberation loss increases (reverberation level weakens) markedly in the range 50-70 km. Both sea surface reverberation and seabed reverberation contribute to reverberation loss. As the dominant path of acoustic energy in winter is within the surface mixed-layer, sea surface contributions to reverberation will contribute throughout the propagation range. This is not the case for seabed reverberation. Figure 47(a) shows a raytrace for the winter downslope scenario. The vertical beam width is $\pm 15^\circ$ (as required for LFAS) although the number of rays, sea surface and seabed reflections have been limited. For ranges greater than ~50 km there are no seabed interacting rays. Remembering that the seabed is effectively a 'target' when reverberation algorithms are applied and that reciprocity is assumed, the contribution of seabed reverberations to the total reverberation loss ceases from approximately this range due to the acoustic energy being coupled into the deep

sound channel rather than continuing to interact with the seabed. The term 'approximately' is applied in this instance as not all rays that interact with the seabed are depicted in Figure 47(a).

Many of the transmission and reverberation loss curves produced in this research indicate that the two curves are, in general, almost parallel to each other. An exception to this is shown in Figure 46(a) where low reverberation loss (strong reverberation level) is maintained throughout the range of the plot whilst the transmission loss increases rapidly with range. The scenario is that of downslope propagation in summer. This effect is caused by a similar principle to that described above, however, in this instance the strongly downward refracting negative sound speed gradient near the surface allows for the majority of the acoustic energy from the LFAS to interact with the seabed. This raytrace clearly indicates that the acoustic energy interacts with the seabed throughout the range of the transect, although beyond 60 km much of the energy becomes waterborne. Therefore, seabed reverberation is the dominant source of reverberation in this scenario and it contributes throughout the range of the plot.

Both of the cases outlined above indicate that downslope propagation of acoustic energy from an active sonar system with a relatively high back-scattering sediment type, particularly in summer, can be severely detrimental to the sonar detection capability. Although reverberation levels associated with upslope propagation paths are also relatively high, they are considerably less than the downslope direction.

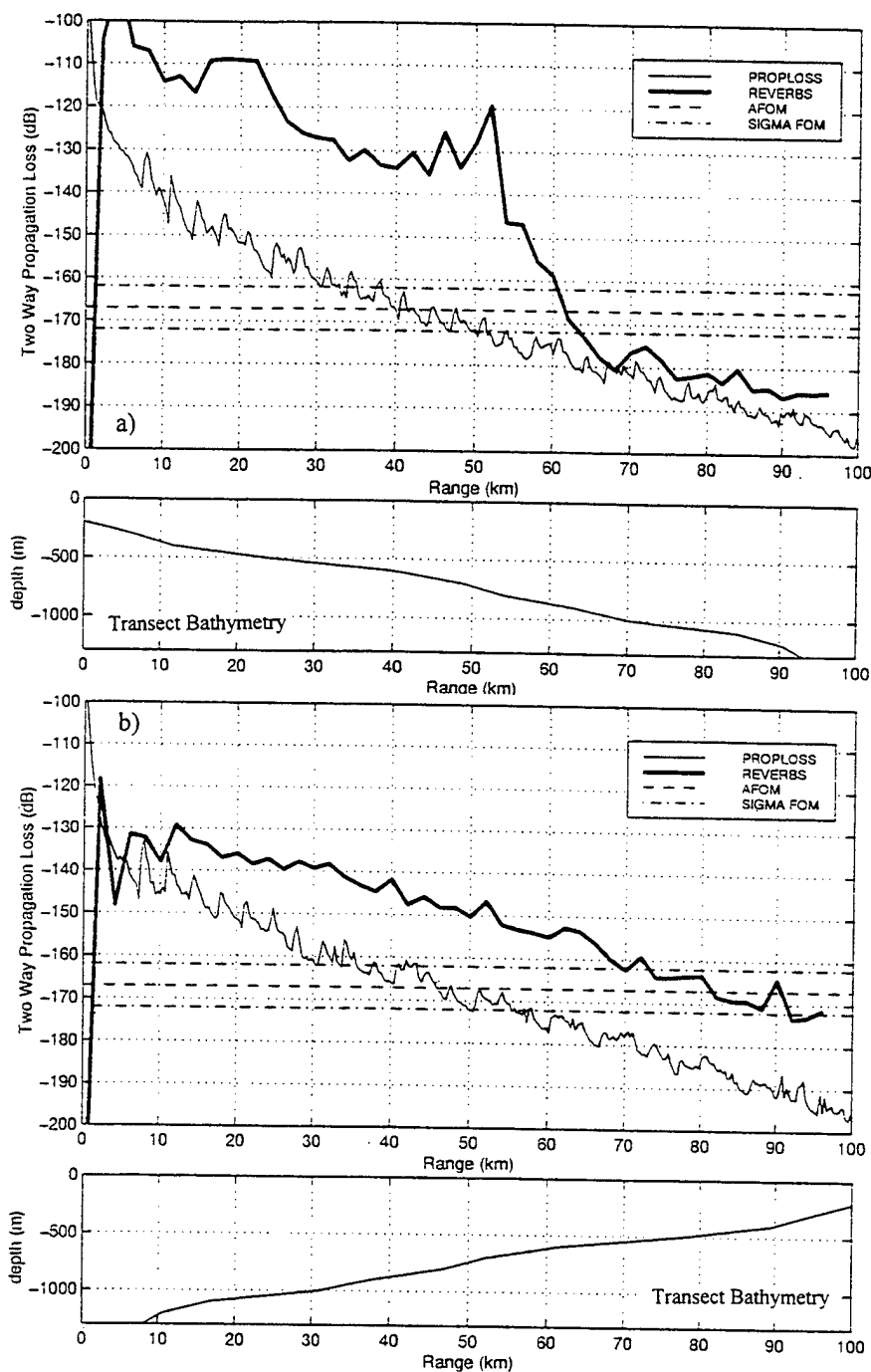


Figure 45. Propagation loss and reverberation loss curves for the upslope/downslope propagation transect in winter, Track C. a) Downslope propagation, 400 Hz, source and target depth 60 m, active figure of merit 167 dB. Propagation of acoustic energy within the surface layer affords excellent acoustic conditions with IDR's of 33-51 km. b) Upslope propagation, 400 Hz, source and target depth 60 m, active figure of merit 167 dB. Despite the predominant path for acoustic propagation being within the surface layer upslope propagation of acoustic energy from the reflective (sand) seabed improves detection ranges over downslope propagation to 36-55 km.

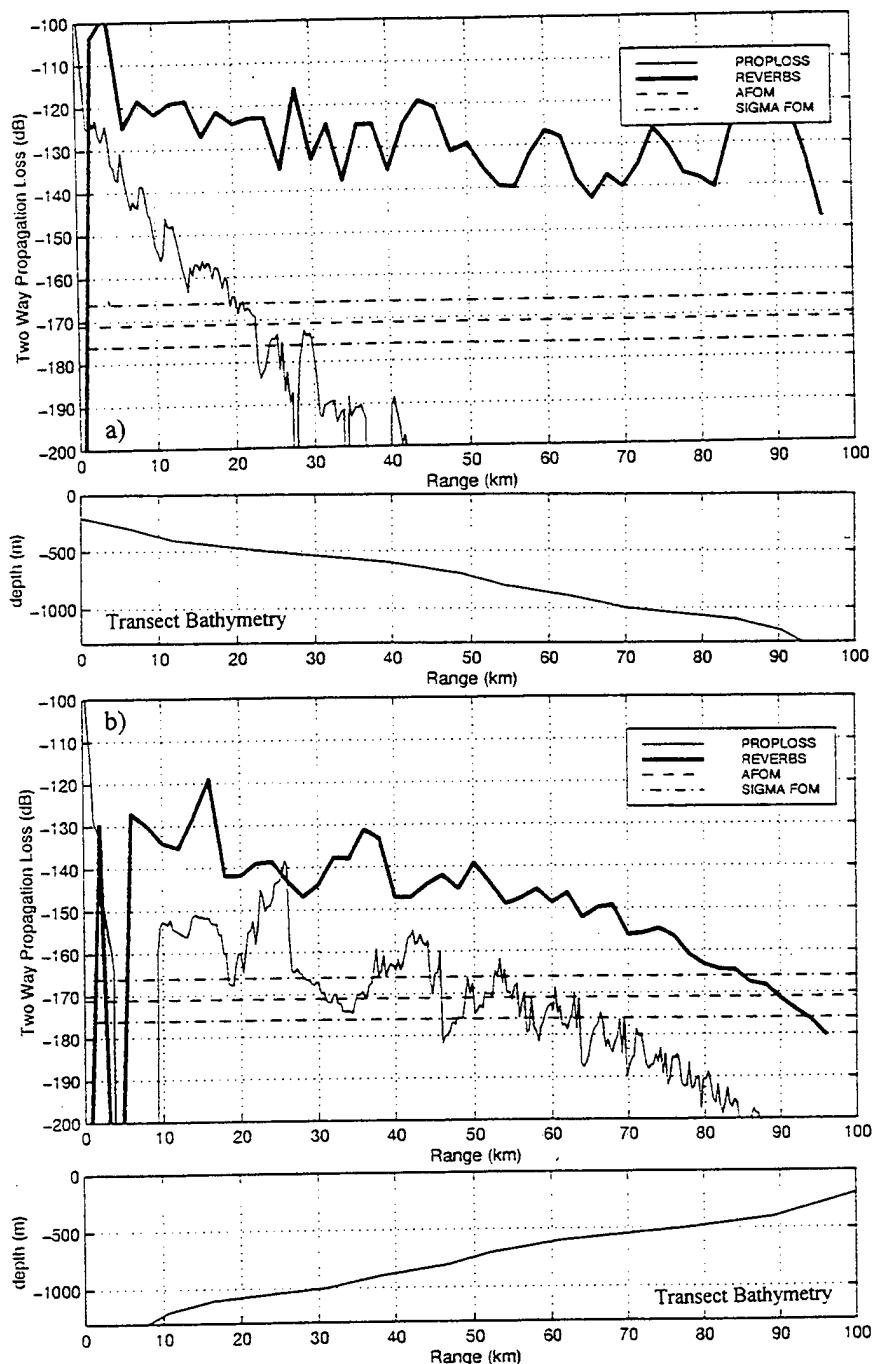


Figure 46. Propagation loss and reverberation loss curves for the upslope/downslope propagation transect in summer, Track C. a) Downslope propagation, 400 Hz, source and target depth 50 m, active figure of merit 171 dB. In this scenario, target detection is predominantly due to seabed reflection, IDR's are 20-22 km. Reverberation loss does not vary greatly with range. b) Upslope propagation, 400 Hz, source and target depth 50 m, active figure of merit 171 dB. As water depth decreases with range the sea surface and seabed act more as a wave-guide for acoustic energy propagating upslope. Target detection is heavily reliant upon seabed reflection.

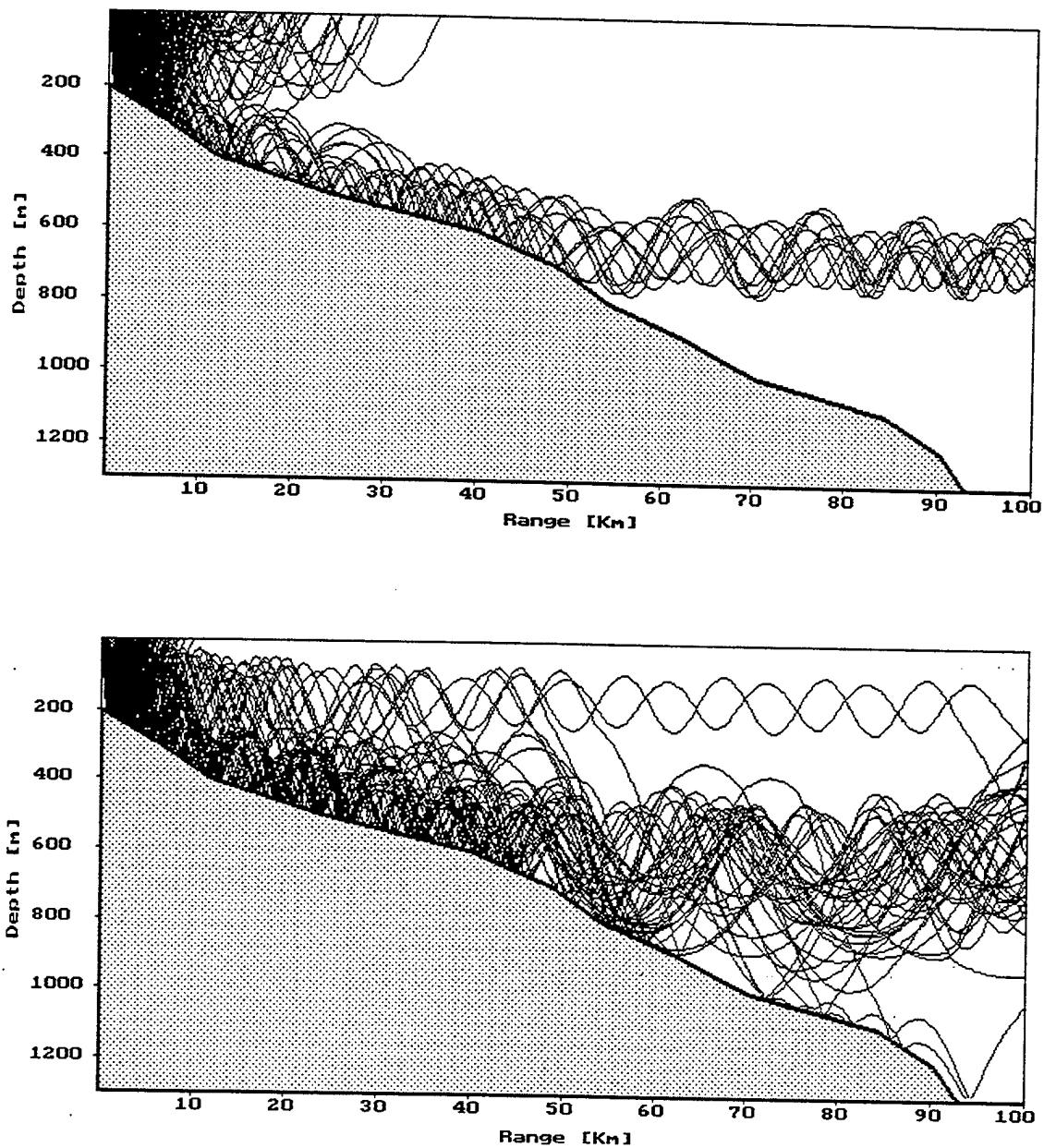


Figure 47. Raytrace of the propagation paths of acoustic energy in the downslope propagation direction for track C in a) winter with a source depth of 60 m, and b) summer, source depth 50 m. The vertical beam width is $\pm 15^\circ$, number of rays plotted, sea surface reflections and seabed reflections have been limited in order to reduce clutter.

d. Track D, Faeroe-Shetland Channel

The Faeroe-Shetland Channel is a feature of tactical interest for LFAS operations. The only propagation direction considered for this scenario is upslope; the reason for this is explained in the paragraphs that follow. Initial detection ranges for the region in winter and summer are shown in Table 21.

(1) Winter. Propagation of acoustic energy is dominated by a deep, upward refracting surface-layer, i.e., good propagation conditions. Despite the reduction of IDR's by approximately 25% in moderate rain, a relatively common occurrence at this time of year, the detection ranges are inherently good at 34-46 km (24-37 km in moderate rain) at 400 Hz.

(2) Summer. Downward refraction ensures that acoustic energy from the LFAS will interact with the seabed (the maximum depth along the transect is 1300 m). As the predominant seabed type is relatively reflective (sand-silt-clay mix), detection opportunities from seabed reflected paths are available, typical IDR's are 33-42 km at 400 Hz. Due to the vertical beam width of the LFAS a near-field region of no detection from 4-7 km is encountered. It can be anticipated that detection ranges will improve if the source is moved upslope into shallower water. Shallow water will act as a wave-guide for the acoustic energy.

WINTER			Frequency (Hz)/Initial Detection Range (km)			
Source Depth (m)	Target Depth (m)		400		800	
			IDR	1 σ Band	IDR	1 σ Band
60	60	NR	40	34-46	34	27-40
		R	31	24-37	24	21-28
SUMMER						
50	50		4, from 7-37	3-4, from 4 to 33-42	4, from 7-36	3-4, from 7 to 33-37

Table 21. Initial Detection Ranges and sigma-IDR's for the Faeroe-Shetland Channel in winter and summer, Track D.

(3) Reverberation. As in the previous scenarios, reverberation loss is considerably lower than transmission loss (typically 10-20 dB). As stated in Section (2) above, if the LFAS is moved into shallow water, initial detection ranges are likely to improve. However, a limitation of LFAS operation in the shallower water regions of this transect is the extremely high reverberation levels encountered. This is associated with

high levels of backscattering from the gravel seabed type. As such, target masking by reverberation is likely to be a major inhibiting factor to detection opportunities. This is the reasoning applied in considering upslope propagation only.

e. Track E, Anton Dohrn Seamount

As with the Faeroe-Shetland Channel, Anton Dohrn Seamount is a feature of tactical interest. The initial detection ranges for this transect in winter and summer are given in Table 22.

(1) Winter. The sound speed profile in winter is characterised by a very deep surface mixed-layer, typically to 900 m. Thus, acoustic propagation conditions are excellent. Initial detection ranges are typically 42-58 km at 400 Hz, no rain (Figure 48(a)). This is irrespective of whether the propagation direction is upslope or downslope because the shallowest depth, on top of the seamount, is 560 m and seabed reflection has little influence upon the transmission loss at the source and receiver depths under consideration in this research.

(2) Summer. There is considerable difference between the PL curves associated with upslope and downslope propagation. In deep water the sediment type is a mud-ooze mix and is therefore highly absorptive. Detection opportunities are limited to a convergence zone at 58-64 km, which gradually merges with upslope propagation as the acoustic energy interacts with the steep-sided Anton Dohrn Seamount. It can be anticipated that as the source moves towards Anton Dohrn, from deep water to shallow water, upslope detection opportunities will occur, although they are likely to be intermittent. In the downslope propagation direction ranges are typically 33-42 km associated with the highly reflective gravel sediment type on top of the sea mount (Figure 48(b)).

(3) Reverberation. The reverberation loss is, once again, very low. As such, target signals are likely to be masked by reverberation. However, in winter, when the propagation direction is upslope, the effect of seabed reverberation is reduced due to the sediment type being absorptive in deep water and acoustic energy that has interacted with the seabed not returning to near the surface until ranges of approximately 9 km. As a result, detection's are not reverberation limited at ranges between 2-9 km. Also note the high increase in reverberation loss (decrease in reverberation level) in

Figure 48(b) [downslope summer] due to the sudden shift from shallow water to deep water. Similarly, in the upslope propagation direction there is a decrease in the reverberation loss (higher reverberation level) associated with the sudden shift from deep to shallow water.

WINTER (independent of propagation direction)			Frequency (Hz)/Initial Detection Range (km)			
Source Depth (m)	Target Depth (m)		400		800	
			IDR	1σ Band	IDR	1σ Band
60	60	NR	48	42-62	47	33-51
		R	36	28-47	29	22-37
SUMMER (downslope)						
50	50		4, from 5 to 38	3-4, from 5 to 33-42	4, from 5 to 34	3-4, from 5 to 32-38
SUMMER (upslope)						
50	50		3, 58-60 (cz)	3, 58-64 (cz)	3	3, 58-61 (cz)

Table 22. Initial Detection Ranges and sigma-IDR's for the Anton Dohrn Seamount transect in winter and summer, Track E.

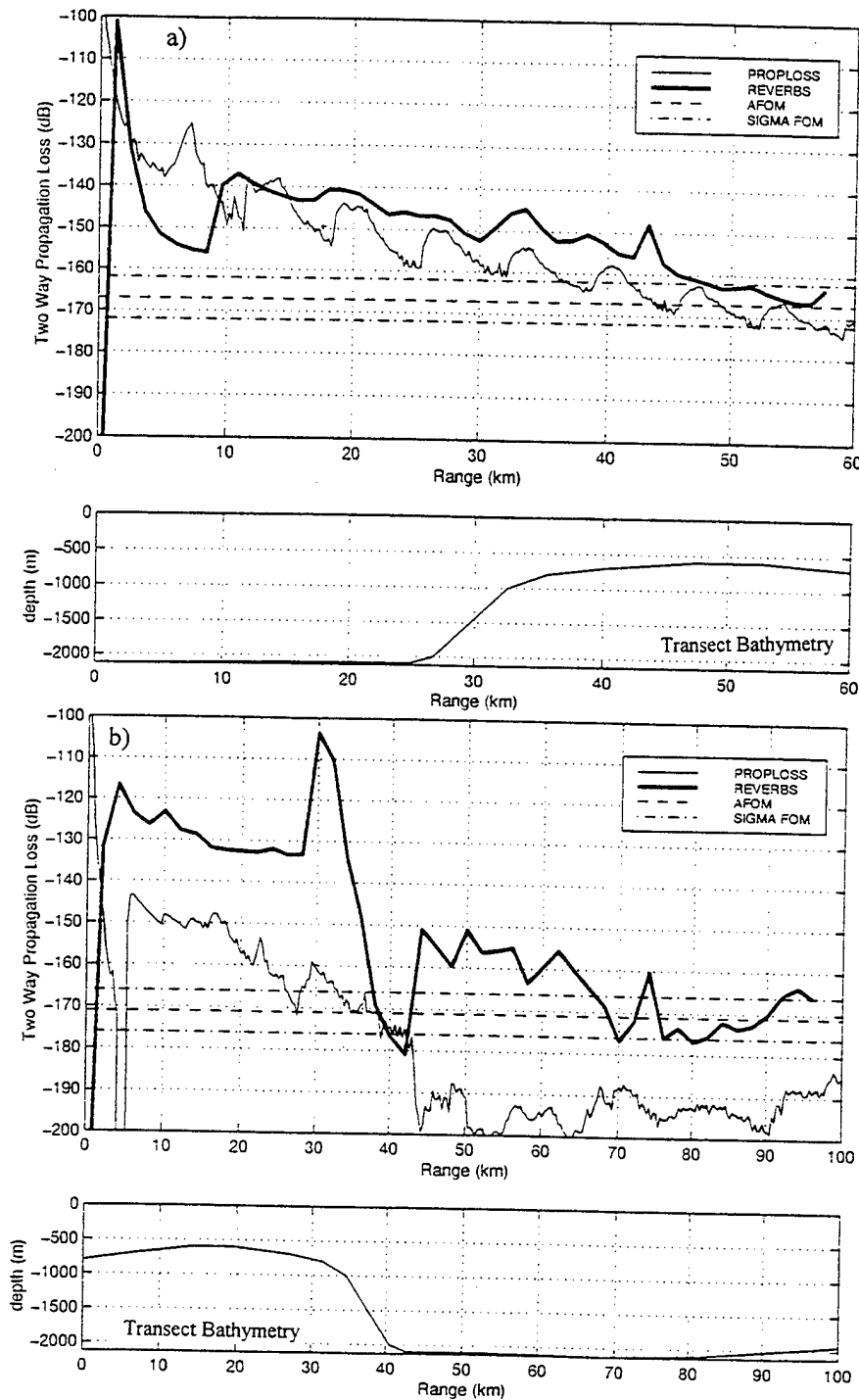


Figure 48. Propagation loss and reverberation loss curves for the Anton Dohrn Seamount transect, Track E. a) Winter scenario, 400 Hz, source and target depth 60 m. The transmission loss is irrespective of whether the propagation direction is upslope or downslope (upslope in this instance). Note that reverberation loss is greater than transmission loss in the range 2-9 km. b) Summer scenario, 400 Hz, source and target depth 50 m, downslope propagation direction. In summer downslope propagation off Anton Dohrn gives better detection opportunities than upslope propagation.

D. ADVANCED SIGNAL PROCESSING TECHNIQUES

The aim of this area of the study is to highlight the improvements in predicted sonar performance that can be attained by advanced signal processing techniques. The techniques concentrated upon in this study are Adaptive Beamforming (ABF), Matched Field Processing (MFP) and Inverse Beamforming (IBF). The basic concepts behind each technique are described, improvement in sonar gain and thus sonar performance, as applicable to the NWAPPS to the UK, are stated and improvements for reverberation suppression are discussed.

IV. ADVANCED SIGNAL PROCESSING TECHNIQUES

For operational sonar systems, signal processing consists of operations performed upon received acoustic waveforms at the hydrophone that improve the sonar operator's ability to detect, classify and track a desired target (DiLoreto, 1998). Three possible ways to apply signal processing techniques in order to improve signal excess (SE) and, therefore, improve IDR's, are 1) enhance the array gain (AG), 2) suppress the reverberation level (RL) and 3) improve the detection threshold (DT). All three of these parameters are dependent upon the processing technique employed and the acoustic environment, (DiLoreto, 1998). This is particularly true for shallow water where environmental variability can dominate sonar performance.

Most operational sonar arrays are time or phase delayed and based upon the plane wave assumption. Such sonars use signal processing algorithms that incorporate conventional beamforming (CBF) methods and other algorithms that only perform well (near the theoretical AG) if the ocean environment consists of a single plane wave arrival immersed in spatially incoherent noise. These beamforming methods suffer significant performance degradation in shallow water as a result of the acoustic propagation paths being dominated by normal modes, not plane waves (Wilson and Veenhuis, 1997). Ultimately, particularly in shallow water, the wave front received at the array is curved, not a plane.

Applying advanced signal processing algorithms that can sense and process critical environmental and target-related parameters, in order to increase the efficiency of signal processing operations, can significantly enhance sonar performance (DiLoreto, 1998).

The purpose of this Chapter is to provide an overview of three recently developed advanced signal processing techniques 1) adaptive beamforming (ABF), 2) inverse beamforming (IBF), and 3) matched field processing (MFP). The basic criterion of these techniques is to overcome performance degradation associated with conventional plane wave beamformers.

A. ADAPTIVE BEAMFORMING

The goal of adaptive beamforming (ABF) is the rejection of interference received in the array sidelobes, be it noise or reverberation. Early passive acoustic methods focussed on cancellation of continuous interference. This requires long time constants for interference data collection that are a function of environmental fluctuations and the rate of motion of the interference. For application in active sonar systems, where the time between individual transmission pings is on the order of seconds, long time constants are not applicable. In addition, reverberation returns that are transient and non-stationary must be cancelled. Beam-based and element-based ABF algorithms were developed to address this issue. (Raff, 1996)

1. Beam-based ABF Algorithm

The beam-based ABF algorithm makes use of a partially adaptive sidelobe canceler. Sidelobe leakage from a conventional beamformer is suppressed by comparison with a set of reference beams, hence the interference is estimated (Raff, 1996). This method provides some gain in reverberation-limited environments, provided the environment is highly anisotropic. Unfortunately, the nature of noise and reverberation, particularly in shallow water environments, demonstrates a tendency toward spatially homogeneous and isotropic conditions. Hence, ABF becomes less applicable for active sonar AG enhancement. (DiLoreto, 1998 and Raff, 1996)

2 Element-based ABF Algorithm

This approach is a family of algorithms that are aimed at adapting the beamforming over short time periods, thus enabling the more transient and isotropic acoustical environment, associated with active sonar application, to be sampled. It is achieved by applying a matched filter prior to beamforming; the time-bandwidth product is reduced and a narrowband beamforming approach is applied. Results highlighted from Critical Sea Test (CST) trials show significant gains over CBF in resolution and in providing gain whilst maintaining background noise at a manageable level. (Raff, 1996)

Both approaches to ABF have been investigated. Results suggest that, as the environment becomes more homogeneous and isotropic, more degrees of freedom are required to provide any worthwhile reduction in reverberation levels (Raff, 1996). Raff

(1996) intimates that it is too early to recommend a robust algorithm that provides interference rejection without introducing unknown target signal reduction.

Using present ABF algorithms, in order to achieve significant improvements in active sonar performance, a coherent signal must dominate the acoustic field. In shallow water environments, as previously stated, propagation of acoustic energy is dominated by normal modes, resulting in non-coherent echo returns and AG from ABF is likely to be insignificant. (DiLoreto, 1998)

B. INVERSE BEAMFORMING

1. IBF Algorithms

IBF is comprised of three algorithms, the Fourier integral method (FIM) beamformer (Nuttall and Wilson, 1990), a data threshold technique called the eight nearest neighbour peak picker (ENNPP) and a sophisticated three-dimensional M of N tracker (Wilson, 1995). The FIM contains 3 dB less area within its beam pattern than CBF and thus provides 3 dB more array gain than CBF for a line array. The ENNPP identifies relative peaks in the matched field processor correlation surface as correlation coefficients are generated. A peak is defined as a correlation coefficient greater than that of all eight cells around a particular range/depth cell. The M of N tracker is a three-dimensional tracker which operates in conjunction with ENNPP to track persistent peaks on the range/azimuth (RAZ) surface for active sonar systems, frequency/azimuth (FRAZ) surface for passive sonars or on the range/depth surface for MFP. The M of N tracker reduces false target detections that do not satisfy the M of N criteria. Combined, the ENNPP and the M of N tracker provide enhanced performance when used in frequency/azimuth space as a plane wave post-processing algorithm or in range/depth space for MFP.

2. The IBF Performance Advantage

IBF has been shown (Wilson, 1995) to produce a 3 dB array noise gain (ANG) or reverberation level gain (RLG) advantage over CBF under ideal conditions. Such gains increase relative to CBF as the conditions depart from the ideal. IBF results in a narrower beamwidth and the 3 dB ANG/RLG relates to less area under the beam pattern curve when compared to CBF. This means there is less reverberation in the echo to

reverberation ratio or noise in the signal to noise ratio. The 3 dB ANG/RLG advantage leads to significant (>10 dB) minimum detectable level (MDL) performance gains using IBF (Fabre and Wilson, 1995).

CBF is the optimum detector for the ideal acoustic field. Unfortunately, such conditions rarely exist. IBF has been successful in detecting echoes and signals of very low levels in measured ocean data and during real-time, at-sea, experiments (Wilson and Veenhuis, 1997). The passive IBF algorithms resulted in 10-15 dB detection gain over the performance of the submarine sonar system. Additionally, IBF provided high bearing resolution tracking solutions at very low frequencies where the towed array aperture was of the order of one wavelength. Therefore, the IBF approach to MFP is expected to greatly out-perform the well-known conventional MFP algorithm as discussed in the next Section.

C. MATCHED FIELD PROCESSING

1. Passive Sonar MFP with IBF

MFP is a beamforming technique that allows for the detection and localisation of an acoustic source in range and depth using passive sonar arrays (Wilson and Veenhuis, 1997). MFP enhances or augments the performance of plane wave beamforming in situations where the acoustic arrival is not approximated well by a single plane wave, e.g., shallow water. Such situations occur when vertical arrays are used in deep water or when either horizontal or vertical arrays are used in shallow water where multipath arrivals or normal modes dominate the arrival structure. (Wilson, Pers. Comm.)

MFP supplements the passive plane wave beamformer detection and tracking capability by not requiring a change of course or speed to arrive at a tracking solution for a horizontal line array. MFP makes use of the multipath acoustic arrivals in the shallow water environment to estimate target bearing, range and depth. It utilises steering vectors generated by a propagation model with the source located at a specified range and depth. FIM, the IBF beamformer, is used to spatially weight the measured data instead of using the CBF weights. This is the method that provides the 3 dB AG advantage achieved by IBF over CBF. In plane wave beamforming the source is at infinite range. As no change of course is required for MFP to estimate the three-dimensional location of the target, it is a promising solution to the passive sonar problem. In addition, this computationally

intensive method is more easily implemented as a function of recent computer hardware and software improvements. (Wilson, Pers. Comm.)

2. Active Sonar MFP

For active sonars, such as LFAS, MFP (and IBF) is used differently than for the passive sonar case. As the MFP and IBF methods are complementary, they are now considered simultaneously in this Section.

A known waveform is transmitted, therefore, the two propagation paths (from the sonar to the target and from the target to the sonar) and the target reflection must be modeled accurately in the time domain prior to beamforming. The local ocean environment for each FIM beam must be partitioned into range/depth cells based upon the propagation pulse changing little between neighbouring cells. MFP with FIM beamforming is then run using an accurate time-domain acoustic model for each range/depth cell of interest in each beam. The correlation of the model and the sonar data for each transmitted pulse is calculated and displayed for each range/depth cell and each beam by the MFP algorithm. Peaks and relative maxima are detected by a twenty six nearest neighbour peak picker (TSNNPP) (beam level vs. azimuth, range and depth). A ping to ping M of N tracker is run over several surfaces (a time series of correlation peaks from ping to ping) to detect tracks that could represent a submarine. (Wilson, Pers. Comm.)

Performance of MFP is significantly degraded by mismatch, i.e., the difference in the actual (represented by received data) and modeled (assumed) environments along the propagation paths between the transmit array and the target and between the target and the receive array. Mismatch can be significantly reduced by using Inversion Techniques (IT's) (Wilson, Rajan and Null, 1996) on each ping to estimate the actual three-dimensional sound speed distribution and the spatial distribution of sediments along the propagation path. With mismatch minimised the performance of MFP with IBF will be significantly enhanced.

D. TACTICAL DECISIONS

Recent simulation results (Nuttall and Wilson, 1998) comparing ABF with CBF and IBF for short averaging times indicate superior performance for IBF over the highly non-linear ABF algorithms. The ABF algorithms require an estimation of the spatial

coherence between all hydrophone pairs. Additionally, the true coherence over short averaging times is not known exactly. The simulations performed by Nuttall and Wilson (1998) indicate that small errors in the estimate of the array spatial coherence results in large errors in the highly non-linear ABF output. The results also show that the element based ABF algorithms, such as the Minimum Variance Distortionless Response (MVDR), are significantly degraded in performance for short averaging times; once again this is due to the highly non-linear ABF algorithms. For these reasons the remainder of this Section considers the application of MFP with IBF. Note, Nuttall and Wilson are currently investigating and developing a linear adaptive IBF algorithm (AIBF) to apply in non-time stationary environments.

A critical question is when and on which beams should LFAS use MFP with IBF and when should plane wave IBF be applied. The LFAS receive array is the key to the answer to this question. Whether the propagated, beamformed active transmission pulse is plane wave or not depends upon the ocean environment. MFP requires that the propagated pulse at the receive array is not a plane wave to perform well. If the acoustic model predicts a single plane wave returning to the receiver, then do not use MFP with IBF, i.e., use IBF as a plane wave beamformer. If the received pulse is predicted to be non-plane wave, then use MFP with IBF. (Wilson, Pers. Comm.)

E. SUPPRESSION OF REVERBERATION USING NEURAL NETS AND HIGHER ORDER STATISTICS

Inversion Techniques (IT's) must be applied to every transmitted pulse in order to design Feature Vectors (FV's) for an environmentally adaptive LFAS processor. In the past, the higher order statistics (HOS) of reverberation and target echoes have been significantly different and neural nets (NN's) have been successfully trained to extract echo features in the received pulse in high reverberation environments, e.g., DISTANT THUNDER. However, there are many more environmentally related features that may be input into (NN's) and FV's in order to exploit the differences in the echo and reverberation time series. This is an area of continuing research, but offers considerable potential gain for LFAS systems. (Wilson, Pers. Comm.)

V. OPERATIONAL ISSUES, CONCLUSIONS AND RECOMMENDATIONS

A. OPERATIONAL ISSUES

Many of the results from this research have potential as a tactical consideration when operating LFAS. Indeed, some of the results have application in many facets of ASW operations. The aim of this Section is to raise the operationally significant issues borne from the results of this study in order to increase awareness of the effects of the environment on ASW and LFAS operations.

1. The HODGSON Propagation Loss Model

Historically, ray model transmission loss calculations have not compared well with the transmission loss calculated by acoustic models that are exact solutions to the wave equation (Bourke and Wilson, Pers. Comm.). Results indicate that in the frequency range 400 to 800 Hz (it is reasonable to assume that the same is true for higher frequencies) the HODGSON model provides an accurate solution provided the sediment type remains range independent. In many ASW scenarios range dependent sedimentary parameters are not available due to a sparsity of data or little change in sediment type exists within the area of interest. Therefore, this limitation is not considered severe in most scenarios. The HODGSON model is an operational propagation loss model used by the Royal Navy. These results suggest that operator confidence in the model output should be high. However, operators should also be aware that in certain situations where sediment changes are commonplace (e.g., most shallow water areas), particularly from a highly absorptive (mud, silt) sediment to highly reflective (sand, gravel), the HODGSON model is likely to misrepresent the acoustic energy within the water column. This depends upon the bottom loss selected by the operator.

It should be noted that the RAM system was used as the control in the model comparison whereas measured transmission loss would have been more applicable, if available. However, RAM provides a realistic, high resolution, accurate solution to the wave equation, so one can anticipate the conclusions drawn from this study are realistic.

2. Range Dependent SSP/Geoacoustic Data

The aim in considering the effects of the SEIF in summer upon propagation of acoustic energy at 400 Hz was to highlight whether accurate and finely-spaced SSP data

through a frontal zone is required for acoustic transmission loss modeling in the operational theatre. The simple answer is clearly yes.

Results clearly indicate that if seabed interaction is the dominant propagation path of acoustic energy, then detailed knowledge of the spatial distribution of geoacoustic parameters is more important than accounting for SSP variability. However, for direct path propagation through a frontal zone finely-spaced SSP's are required in order to avoid misrepresentation of propagation paths and transmission loss and, therefore, IDR's. Additional to propagation of acoustic energy across a front, the results suggest that spatial and temporal variability of features such as shallow sound channels are an important consideration in any ASW theatre. Climatological data generally provides insufficient resolution to accurately characterise frontal zones and small scale spatial and temporal variability. In order for representative IDR assessment, ASW Commanders should consider oceanographic data collection and dissemination an integral part of ASW operations and consider utilisation of all data gathering assets at their disposal. The underlying thought should be 'mechanically and electronically efficient weapons and sensors are only as efficient as the environment allows'.

3. LFAS Performance

The aim of this Section is to highlight the important considerations and modeled capability of a generic UK LFAS system.

a. Initial Detection Range Summary

Somewhat surprisingly, the variation in IDR's over the five transects that were selected to represent differing propagation directions and time of year is relatively small and may even be considered of little tactical significance. In generating a summary of the IDR's calculated in this research the range bracket is determined from the shortest range to the longest range for all scenarios. The IDR's can be summarised as follows:

1. IDR's in winter are typically 28-62 km at 400 Hz and 26-51 km at 800 Hz. Ranges are reduced by ~20-25% in moderate rain.
2. IDR's in summer for upslope propagation are highly dependent upon proximity to and the gradient of the slope. However, in general, when the water depth is shallower than 2000 m, typical IDR's are 28-61 km at 400 Hz and 27-56 km at 800 Hz (surprisingly similar to the winter IDR's above). It should be noted

that a shadow zone is inherently present from ~3-16 km depending upon the depth of water; this is a function of the LFAS vertical beam width. If the water depth is greater than ~2000 m, then convergence zone detection's are possible (38-41 km and 58-60 km in the examples experienced) and seabed reflected ranges provide for intermittent detection opportunities.

3. IDR's in summer for downslope propagation appear to exhibit less variability than upslope, typical ranges are 23-42 km at 400 Hz and 23-38 km at 800 Hz. If any shadow zone exists, it is generally in the range 3-5 km.

b. Frequency

A characteristic of many active sonar systems is the ability to select the frequency of operation. Results of this study, as summarised above, suggest that 400Hz allows for slightly greater detection ranges than 800 Hz. This is a function of reduced transmission loss, due to sea surface reflection and absorption losses, and reduced ambient noise levels, particularly in rain, at 400 Hz.

Results suggest that as frequency increases, reverberation level increases primarily as a consequence of sea surface backscatter; this is also supported by Urick (1983). Therefore, ASW Commanders should consider operating at low frequency settings particularly in high sea states.

c. Seasonal Variability

The SSP's of the NWAPPS to the UK are characterised by relatively large seasonal variability. Somewhat surprisingly, however, the IDR's assessed in this study exhibit little seasonal variability unless the depth of water is greater than ~2000 m. This is a function of the relatively shallow water acting as a wave-guide for the acoustic energy and much of the area having a sediment type of sand-silt-clay mixes, which is relatively reflective.

In generalising, detection ranges from each individual scenario suggest that winter is likely to give longer IDR's, but these, in reality, are subject to high variability due to the weather.

d. Upslope/Downslope Propagation

Both upslope and downslope propagation are a function of many variables including source and receiver disposition, SSP, sediment type and depth of water. Results

of this study suggest that upslope propagation of acoustic energy provides for the longest detection ranges. However, detections are likely to be intermittent. In the downslope direction, IDR's are shorter, approximately 80-90% that of upslope IDR's, but give a continuous detection opportunity. The question of whether upslope propagation is better than downslope depends upon the aim of the operation. If initial detection is the aim, then upslope propagation towards the target is likely to give longer initial detection ranges. If target tracking is the aim, then downslope propagation is likely to give more continuous target contact. It is assumed that the theatre of operation is in water depths less than ~2000 m.

A disadvantage associated with reliance upon detection from acoustic energy that has interacted with the seabed is the possibility of range and bearing errors. Depending upon the environment and topography this may be alleviated by application of matched field processing (MFP) with inverse beamforming (IBF), which relies upon differing propagation paths in calculating target location.

e. Reverberation

Long pulse lengths inherently result in high reverberation levels. It is anticipated that a method of reverberation suppression is present in the existing UK LFAS system, although the benefits of adopting MFP and IBF have been highlighted.

The HODGSON Propagation Loss Model incorporates reverberation algorithms. Similar to the application of geoacoustic parameters in a range dependent manner, the seabed type for entry within the reverberation algorithms is also range independent. Whilst this is not a severe limiting factor, for many environmental considerations operators should be aware that in areas of high sediment type variability, particularly from a muddy sediment to a sandy sediment, the reverberation loss curves given by HODGSON are likely to misrepresent seabed reverberation.

B. CONCLUSIONS

The goal of this research was to make a performance assessment for a generic UK Low Frequency Active Sonar (LFAS) operating in the tactically significant area of the northwest approaches to the United Kingdom. Five diverse and operationally significant sound speed and geoacoustic transects of the region in winter and summer were

considered. The intention was to use an operational, ray theory based, acoustic propagation loss model to assess performance at 400 Hz and 800 Hz for typical source and receiver depths.

Prior to the assessment phase the HODGSON PL Model was compared with a finite element primitive equation based model (RAM) in order to validate the propagation loss output of the ray model and to investigate the limitations of the HODGSON model, if any, as a consequence of its treatment of the geoacoustic parameters as range independent. HODGSON and RAM compared well in all scenarios except where the water column sound speed profile was strongly downward refracting, causing a high incidence of seabed interaction of acoustic energy in a range dependent geoacoustic environment. This only occurred to an operationally significant level on one occasion, the South East Icelandic Front (SEIF) transect in summer. A correction method to overcome this shortcoming was devised that performed well for this scenario, however, it requires more robust testing to be applicable in other scenarios.

As a purely passive acoustic propagation study, RAM was used to model the propagation of acoustic energy at 400 Hz through the SEIF in summer in order to investigate the requirement for range dependent SSP's across the frontal zone. Results indicated that when seabed interaction is the dominant propagation path of acoustic energy, the need for accurate geoacoustic parameters along the acoustic path exert greater importance than finely-spaced sound speed profiles. When the propagation path is inherently direct path (convergence zone and sound channel propagation), then high resolution SSP's must be accurately characterised to avoid misrepresentation of transmission loss and, therefore, initial detection ranges (IDR's). In conclusion, results suggest that, at 400 Hz, both SSP and geoacoustic spatial variability must be accurately known in order to provide accurate IDR predictions.

In the LFAS performance assessment phase generic sonar parameters were applied to calculate typical active figure's of merit and initialise the HODGSON propagation loss model. The sound speed environments were generated using climatological SSP data and measured survey data in the frontal zones. The geoacoustic parameters were adapted from typical values suggested by Hamilton and Bachman (1982). The IDR's associated with 400 Hz were consistently better than at 800 Hz,

typically ranges at 800 Hz are 5-15 % less than at 400 Hz. This is a function of 400 Hz being less subject to transmission loss from sea surface scatter and absorption, and also, to some extent, by having lower ambient noise levels.

In winter initial detection ranges exhibit little spatial variability, i.e., similar values were attained in all transects, and were in the range 28-62 km (the values are taken at the one-sigma level extremes of the confidence limits of the 50 % probability of detection). However, results suggest that these IDR's are likely to be heavily dependent upon the weather conditions, which can be highly variable in this season. Whether the propagation direction is upslope or downslope appears to have little significant effect on IDR's, a consequence of the SSP for all transects in winter being inherently upward refracting.

In summer ranges associated with upslope and downslope propagation are considerably different. Upslope propagation allows for longer initial detection ranges (28-61 km) than downslope propagation (23-42 km). However, there are large areas of no detection opportunities as a consequence of the vertical beam width of the active sonar and due to strong downward refraction. Although downslope propagation constitutes shorter ranges, detection probability is continuous, or near-continuous, throughout the detection range.

Reverberation loss was low, relative to propagation loss, for all scenarios (there were some small regions of where PL was less than reverberation loss in some scenarios). This is primarily a function of the long pulse length applied, 2 seconds (typical for LFAS systems). The advantage of a long pulse length is that energy spreading loss (ESL), particularly in shallow water, is significantly reduced. However, a long pulse length results in high reverberation levels and a large blank-out range (2 seconds constitutes a blank-out range of approximately $(2s \times 1500m/s) = 3$ km from the source).

As a consequence of the high reverberation levels experienced during this study, a brief description of signal processing techniques available to improve detection opportunities, in particular reverberation suppression, were considered. Preliminary indications are that adaptive beamforming (ABF) algorithms, are not capable of fully characterising reverberation in order to improve detection and localisation. However, recent developments in the application of inverse beamforming (IBF) algorithms, in

conjunction with matched field processing (MFP), offers potential improvements, not only to IDR's in a noise-limited environment, but in a reverberation limited environment.

C. RECOMMENDATIONS

The following recommendations arise from this study;

1. It is apparent that a potentially severe limitation of the HODGSON PL model in some complex ocean environments is the inability to include range dependent geoacoustic parameters. In addition, seabed reverberation algorithms are similarly applied range-independently. It is recommended that these algorithms be developed further to incorporate range dependency.
2. A limitation of the Range dependent Acoustic Model (RAM) is the stepped application of environmental range dependence. It is recommended that a smoothing function be incorporated in the model to merge between consecutively defined environmental inputs.
3. High-resolution climatological environmental data of operationally significant frontal zones are not readily available for operational use. It is recommended that sound speed climatological databases be improved by including high resolution frontal sections from measured data to allow users to properly simulate the spatial resolution of the rapidly varying SSP's and more realistically model acoustic propagation in these tactically important areas.
4. In many areas, particularly shallow water, sonar performance is heavily dependent upon the seabed type and its spatial variation. A major limitation of modeling propagation loss of acoustic energy in the operational theatre is the lack of accurate high-resolution geoacoustic data. It is recommended that investigations be made into improving geoacoustic database resolution and the inclusion of backscatter data for reverberation assessments. This may be achieved by employing inverse techniques. Therefore, it is recommended that if inverse techniques are used, investigations should be made into the application of data acquired from military sonars for post-processing. This would also allow parameterisation of the seabed at the frequencies of particular interest.
5. Reverberations are a major limiting factor for any active sonar operation. Therefore, a method of suppressing reverberations is a much-needed requirement.

It is recommended that further investigations are carried out into the applicability of matched field processing with inverse beamforming algorithms and neural-net processing techniques for reverberation suppression.

6. An obvious problem highlighted by this research is that the ocean environment is complex and diverse. ASW Commanders must make tactical decisions based upon information that is highly temporally and spatially variable. It is recommended that high resolution environmental databases, advanced ocean modeling systems and accurate, possibly three-dimensional, acoustic propagation loss modeling systems be incorporated into tactical decision aids (TDA's) to assist the Command as completely and accurately as possible.

7. It is recommended that investigation be made into LFAS best operating depths in diverse environmental situations at a variety of target depths.

LIST OF REFERENCES

- Adams, B. S. An analysis of the effects of ESL and TL on LFAS operations in shallow water, Masters Thesis, Naval Postgraduate School, Monterey, 1997.
- Alekseev, A. P. and B. V. Istoshin, Scheme of constant currents in the Norwegian and Greenland Seas, *Trudy Poliarnyi Nauchno-Issledovatel'skii Institut Morskogo Rybnogo Khoziaistva I Okeanografii*, 9, 62-68, 1956.
- Bachman, R. T., A 3D geoacoustic model for the Catalina Basin, Aug 1994. (Retrieved from Internet at www.guppy.nosc.mil/services/sti/publications/pubs/tr/1669).
- Beckmann, P. and A. Spizzichino, Scattering of electromagnetic waves from rough surfaces, p.93, The MacMillan Company, New York, 1963.
- Bourke, R. H., Personal Communications, 1997-98.
- Carman, J. C. and A. R. Robinson, Oceanographic-topographic interactions in acoustic propagation in the Iceland-Faeroes Front region, *J. Acoust. Soc. Am.*, 95, 1882-1894, 1994.
- Chen, C. and F. J. Millero, Speed of sound in seawater at high pressures, *J. Acoust. Soc. Am.*, 62, 1129-1135, 1977.
- Chin-Bing, S. A., D. B. King, J. A. Davis, R. B. Evans, PE Workshops 11, Proceedings of the 2nd parabolic equation workshop (edited), NRL/BE/7181-93-0001, NRL, Stennis Space Centre, MS, 1993.
- Collins, M. D., User guide for RAM versions 1.0 and 1.0p, unpublished notes, undated.
- Collins, M. D., FEPE User's Guide, NORDA Technical Note TN-365, Naval Ocean Research and Development Activity, Stennis Space Centre, 1988.
- Collins, M. D. and E. K. Westwood, A higher-order energy-conserving parabolic equation for range-dependent ocean depth, sound speed, and density, *J. Acoust. Soc. Am.*, 89, 1068-1075, 1991.
- Collins, M. D., A split-step Padé solution for parabolic equation method, *J. Acoust. Soc. Am.*, 93, 1736-1742, 1993a.
- Collins, M. D., An energy-conserving parabolic equation for elastic media, *J. Acoust. Soc. Am.*, 94, 975-982, 1993b.
- Collins, M. D., Generalization of the split-step Padé solution, *J. Acoust. Soc. Am.*, 96, 382-385, 1993c.

- Crouch, J. A. M., Towed array performance in the littoral waters of N. Australia, Masters Thesis, Naval Postgraduate School, Monterey, 1997.
- Dickson, R. R., Variability in continuity within the Atlantic Current of the Norwegian Sea, Rapport et Procès-Verbaux des Réunions, Conseil International pour l'exploration de la Mer, 162,167-183, 1972.
- DiLoreto, A., Current signal processing, Appendix B. in: Environmentally Adaptive Sonar Technology (EAST), Technical Steering Group, Study report, volume II, Office of Naval Research, Virginia, Jan 1998.
- Fabre, J. P., Personal Communications, 1997-98.
- Fabre, J. P., RAM user's guide, unpublished, Dec. 1997.
- Francois, R. E. and G. R. Garrison, Sound absorption based on ocean measurements: Part II. Boric acid contribution and equation for total absorption, J. Acoust. Soc. Am., 72, 1879-1899, 1982.
- Gathman, S. G., Climatology, in: The Nordic Seas, edited by B. G. Hurdle, New York, NY, Springer-Verlag, New York, 1-18, 1986.
- Hamilton, E. L. and R. T. Bachman, Sound velocity and related properties of marine sediments, J. Acoust. Soc. Am., 72, 1891-1904, 1982.
- Hodgson, J. M. and D. S. Hodgson, HODGSON information sheet, Ocean Acoustic Developments Ltd., Bude, UK, 1997.
- Hodgson, J. M. and D. S. Hodgson, WADER Global Ocean Information System: User manual, Ocean Acoustic Developments Ltd., Bude, UK, March 1998a.
- Hodgson, J. M. and D. S. Hodgson, Reverberation Revisited, Ocean Acoustic Developments Ltd., OAD Report WIN/10/98, July 1998b.
- Hodgson, J. M. and D. S. Hodgson, Personal Communications, 1997-98.
- Hopkins, T. S., The GIN Sea – Review of physical oceanography and literature from 1972, SACLANTCEN Report SR-124, July 1988.
- Hydrographic Office UK, Environmental Data for the GIN Sea and South West Approaches, Physical Oceanography Branch (compiled and produced for Lt Cdr C J Hunt RN), UK Hydrographic Office, Taunton, UK, Dec 1997.
- Jensen, F. B., G. Dreini and M. Prior, Acoustic effects of the Iceland-Faeroe Front, in: Ocean Variability and Acoustic Propagation, edited by J. R. Porter and A. Warn-Varnas, Kluwer Academic, Dordrecht, The Netherlands, 1991.

Johannessen, O. M., Brief overview of physical oceanography, in: The Nordic Seas, edited by B. G. Hurdle, New York, NY, Springer-Verlag, New York, 103-127, 1986.

Kislyakov, A. G., Fluctuations in the regime of the Spitzbergen current, in: Soviet Fisheries Investigations in the Northern European Seas. Moscow, The Polar Research Institute of Marine Fisheries and Oceanography (PINRO), 39-49, 1960.

McKinney, C. M. and C. D. Anderson, Measurements of backscattering of sound from the ocean bottom, J. Acoust. Soc. Am., 36(1), 1964.

Millero, F. J. and Xu Li, Comments on: On equations for the speed of sound in seawater, J. Acoust. Soc. Am., 95, 2757-2759, 1994.

Milne, A. R. and J. H. Ganton, Ambient noise under Arctic sea ice, J. Acoust. Soc. Am., 36, 855, 1964.

Monrad, P. D. and D. R. Jackson, A model/data comparison for low frequency bottom backscatter, J. Acoust. Soc. Am., 94, 344-358, 1993.

Naval Oceanography Office, Stennis Space Centre, Environmental Guide, North Atlantic area NA5(U), SP3160-NA5, 1986 – unclassified entry.

Naval Oceanography Office, Stennis Space Centre, Data base description for low frequency bottom loss, MS-39522-5001, June 1990.

Naval Oceanography Office, Stennis Space Centre, Environmental Guide, Norwegian and Greenland Sea, SP3160-3, June 1992 – unclassified entry.

Nekritz, R., Oceanographic atlas of the North Atlantic Ocean, Pub. 700, section V, Marine geology, Naval Oceanography Office, Stennis Space Centre, 1975.

Nuttall, A. H. and Wilson, J. H., Limitations of adaptive beamforming (ABF) for tactical sonar applications at short averaging times and at very low frequencies (VLF), submitted to J. Acoust. Soc. Am., 1998.

Saelen, O. H., Studies in the Norwegian Atlantic current: Part II. Investigations during the years of 1954-1959 in an area west of Stad, Geophysica Norwegica, 23(6), 1-82, 1963.

Raff, B. E., Key signal and information processing products, in: Critical Sea Test Final Report 1996, USN Space and Naval Warfare Command (PMW 182), 1996.

Schulkin, M., Surface coupled losses in surface sound channels, J. Acoust. Soc. Am., 44, 1152, 1968.

Tanaka, A., An analysis of ESL associated with tactical active sonar performance in a shallow water environment, Masters Thesis, Naval Postgraduate School, Monterey, 1996.

Taylor, B., Location accuracy of LFAS, DRA Report 328054, 1993.

Trangeled, S., Oceanography of the Norwegian and Greenland seas and adjacent areas, Volume II – Survey of 1870-1970 literature, SACLANT ASW Res. Centre Memorandum, SM-74, Italy, 1974.

Urick, R. J., Principles of Underwater Sound, 3rd Edition, McGraw-Hill NY, 1983.

Vogt, P. R., Seafloor topography, sediments and paleoenvironments, in: The Nordic Seas, edited by B. G. Hurdle, Springer-Verlag, New York, 237-410, 1986.

Weston, D. E. and K. C. Focke, Caustics in range averaged sound channels, J. Acoust. Soc. Am., 77(5), 1985.

Wilson, J. H. and R. S. Veenhuis, Shallow water beamforming with small aperture horizontal towed arrays, J. Acoust. Soc. Am., 101, 384-394, 1997.

Wilson, J.H., S.D. Rajan and J.M. Null, editors, Special issue on inversion techniques and the variability of sound propagation in shallow water, IEEE J. Oceanic Eng., 21(4), 1996.

Wilson, J. H., Application of inverse beamforming theory, J. Acoust. Soc. Am., 98, 3250-3261, 1995.

Wilson, J. H., Personal communications, 1997-98.

INITIAL DISTRIBUTION LIST

		No. of copies
1.	Defense Technical Information Centre 8725 John J. Kingman Rd., STE 0944 Ft. Belvoir, VA 22060-6218	2
2.	Dudley Knox Library Naval Postgraduate School 411 Dyer Rd. Monterey, CA 93943-5101	2
3.	Commanding Officer Naval Underwater Center Division 1176 Howell St. Newport, RI 02841-1708 Attn: Mr. Edmond P Jensen (Code 3111)	1
4.	Prof. Robert H. Bourke (Code OC/BF) Department of Oceanography Naval Postgraduate School Monterey, CA 93943-5000	1
5.	Dr. James H. Wilson Neptune Sciences, Inc. 3834 Vista Azul San Clemente, CA 92674	2
6.	Director of Naval Surveying, Oceanography and Meteorology DNSOM/M Room 2384 Ministry of Defence Main Building Whitehall LONDON SW1A 2HW United Kingdom	1
7.	Cdr R Pegg RN Cdr USW British Naval Staff British Embassy 3100 Massachusetts Ave., NW Washington, DC 20008	1

8. Naval Space and Warfare Command 1
PD18
153560 Hull St.
San Diego, CA 92152-5002
Attn: Capt. G. Nifontoff

9. Flag Officer Submarines 1
HMS WARRIOR
Northwood
Middlesex
LONDON
United Kingdom
Attn: Cdr R Smith RN

10. Hydrographic Office 1
Physical Oceanography Branch
Admiralty Way
TAUNTON
Somerset
TA1 2DN
United Kingdom

11. Mr. John M. Hodgson 1
Ocean Acoustic Developments Ltd.
Pendower
Leverlake Rd.
Widemouth Bay
BUDE
Cornwall
EX23 0AF
United Kingdom

12. Lt Cdr C J Hunt RN 1
272 Via Del Rey
Monterey, CA 93940-2356